MARMARA UNIVERSITY

INSTITUTE FOR GRADUATE STUDIES IN PURE AND APPLIED SCIENCES

MODELLING AND PERFORMANCE ANALYSIS OF A REFRIGERATION SYSTEM FOR DIFFERENT REFRIGERANTS AND CONFIGURATIONS

TUTKU MUTLU

MASTER THESIS

Department of Chemical Engineering

THESIS SUPERVISOR

Prof. Dr. Sibel TİTİZ SARGUT

THESIS CO-SUPERVISOR

Assoc. Prof. Dr. Ebru MANÇUHAN

ISTANBUL, 2018

MARMARA UNIVERSITY

INSTITUTE FOR GRADUATE STUDIES IN PURE AND APPLIED SCIENCES

MODELLING AND PERFORMANCE ANALYSIS OF A REFRIGERATION SYSTEM FOR DIFFERENT REFRIGERANTS AND CONFIGURATIONS

TUTKU MUTLU

524515001

MASTER THESIS

Department of Chemical Engineering

THESIS SUPERVISOR

Prof. Dr. Sibel TİTİZ SARGUT

THESIS CO-SUPERVISOR

Assoc. Prof. Dr. Ebru MANÇUHAN

ISTANBUL, 2018

MARMARA UNIVERSITY
INSTITUTE FOR GRADUATE STUDIES IN PURE AND APPLIED SCIENCES

Tutku MUTLU, a Master of Science student of Marmara University Institute for Graduate Studies in Pure and Applied Sciences, defended her thesis entitled **"Modelling and Performance Analysis of a Refrigerator System for Different Refrigerants and Configurations"**, on July 09, 2018 and has been found to be satisfactory by the jury members.

Jury Members

Prof.Dr. Sibel TİTİZ SARGUT (Advisor)
Marmara University .....(SIGN).....

Dr. Barış YILMAZ (Jury Member)
Marmara University .....(SIGN).....

Prof. Dr. Düriye BİLGE (Jury Member)
Yıldız Technical University.....(SIGN).....

APPROVAL

Marmara University Institute for Graduate Studies in Pure and Applied Sciences Executive Committee approves that Tutku MUTLU be granted the degree of Master of Science in Department of Chemical engineering, on July 09, 2018. (Resolution no: 2018/16-05).

Director of the Institute
Prof. Dr. Bülent EKİCİ

ACKNOWLEDGEMENTS

For this study, it would not be possible and easy to complete successfully without guidance, contribution and help of many people.

First of all, I would like to express my sincere thanks to my supervisors Prof. Sibel TITIZ SARGUT and my co-supervisor Assoc. Prof. Dr. Ebru MANÇUHAN for their endless support and helping.

This research was promoted by Commission of Scientific Research Project (BAPKO). The project number is FEN-C-YLP-110117-0023.

Also, i would like to thank my family, for being helpful and supportive all my life.

2018 **Tutku MUTLU**

TABLE OF CONTENTS

ACKNOWLEDMENTS ..... **i**

TABLE OF CONTENTS ..... **ii**

ÖZET ..... **v**

ABSTRACT ..... **vi**

LIST OF SYMBOLS ..... **vii**

LIST OF FIGURES ..... **x**

LIST OF TABLES ..... **xiii**

1. INTRODUCTION **1**

1.1. Objective of the Thesis 1

1.2. Refrigeration Cycles 2

1.2.1. The ideal vapor compression refrigeration cycle 3

1.2.2. The actual vapor compression refrigeration cycle 4

1.3. Innovative Vapor Compression Refrigeration Systems 4

1.3.1. Secondary loop refrigeration systems 5

1.3.2. Cascade refrigeration system 5

1.4. Refrigerants 6

1.4.1. Environmental concerns and restrictions 7

1.4.2. Future refrigerants 8

1.5. Primary Refrigerants 9

1.5.1. Halocarbons (Freon's) 9

1.5.2. Inorganic compounds 10

1.5.3. Hydrocarbons 10

1.5.4. Azeotropes 10

1.5.5. Unsaturated organic compounds 10

1.6. Thermal Energy Storage with PCMs: Materials, Techniques and Applications . 11
1.6.1. Phase change materials 11
1.6.2. Techniques 12
1.6.3. Applications 14
1.6.4. Selection of PCM for thermal energy storage applications 15
1.6.5. Heat transfer enhancement 15
1.7. Literature Review 17
2. MATERIALS AND METHODS 20
2.1. System Description: Vapor compression refrigeration system 20
2.1.1. The ideal vapor compression refrigeration cycle 20
2.1.2. The actual vapor compression refrigeration cycle 22
2.2. Mathematical Modeling of the Refrigeration System 23
2.2.1. Evaporator model 25
2.2.2. Compressor model 29
2.2.3. Condenser model 30
2.2.4. Expansion valve model 34
2.2.5. Overall cycle model 34
2.3. Engineering Equation Solver (EES) Software 35
2.4. Thermo Physical Properties of Refrigerants Used in the Model 36
3. RESULTS AND DISCUSSION 37
3.1. Evaporator Simulation Results 38
3.1.1. Mathematical modeling results related with mass flux-heat transfer coefficient for different refrigerants 41
3.1.2. Mathematical modeling results related with mass flux-heat transfer coefficient for various surface types 42
3.1.3. Mathematical modeling results related with vapor quality-mass flux for different refrigerants and surface types 45

3.2. Condenser Simulation Results 48

3.2.1. Mathematical modeling results related with vapor quality- mass flux for different refrigerants and surface types 50

3.2.2. Mathematical modeling results related with air velocity-fan power for various surface types 54

3.2.3. Mathematical modeling results related with air velocity-COP for different refrigerants and surface types 55

3.3. Refrigeration System Simulation Results 59

4. CONCLUSION 60

REFERENCES…….....61

APPENDIX…….....65

ÖZET

BİR SOĞUTMA SİSTEMİNİN FARKLI SOĞUTUCU AKIŞKANLAR VE KONFİGÜRASYONLAR İÇİN MODELLENMESİ VE PERFORMANS ANALİZİ

Bu çalışmada, dört farklı soğutucu akışkan (R134a, R404a, R410A ve R290) ve iki farklı yüzey tipi (8.03/8T ve CF-7.0-5/8J) kullanılan bir soğutma sisteminin performansını (COP) simüle etmek için, küçük ölçekli bir soğutma sistemi bileşenlerini (kondenser ve evaporatör) detaylı inceleyen bir matematiksel model sunulmuştur. Ayrıca, seçilen soğutucu akışkanların soğutma sistem performansı ve çevreye olan etkileri karşılaştırılarak değerlendirilmiştir.

İncelenen soğutucu akışkanlar için farklı çalışma parametreleri (kütlesel debi, sıcaklık, basınç) model girdisi olarak kullanıldı. Farklı akışkan ve yüzey tiplerinin COP'ye etkisini incelemek amacıyla buhar sıkıştırmalı soğutma sistemini tanımlayan bir matematiksel model Engineering Equation Solver (EES) yazılımı kullanılarak geliştirildi. Model ayrıca evaporatörün iki bölgesi (buharlaşma ve kızgın gaz) için giriş-çıkış havası sıcaklıklarını ($T_{air,evap,in}$, $T_{air,evap,out}$), kondenserin üç bölgesi (kızgın gaz, yoğuşma ve aşırı soğuma) için giriş-çıkış hava sıcaklıklarını tahmin edebilir ($T_{air,cond.,in}$, $T_{air,cond.,out}$). Model kullanılarak, evaporatör ve kondenserdeki farklı bölgeler için ısı taşınım katsayıları ve toplam ısı geçişini tahmin edilebilmektedir. Kondenser hava tarafı (ΔP_{air}) basınç düşümü, 8.03/8T ve CF-7.0-5/8J yüzey tipleri için hesaplanmıştır. Hesaplanan basınç düşümü kullanılarak kondenser fanında tüketilen güç ($\dot{W}$) belirlenmiştir. En yüksek toplam COP değeri, her iki yüzey tipi 8.03/8T ve CF-7.0-5/8J için de R410a sentetik soğutucu akışkanı için bulunmuştur. Diğer yandan, en düşük COP değeri ise doğal soğutucu R290 için hesaplanmıştır. Yüzey tipleri karşılaştırıldığında CF-7.0-5/8J tipi tüm soğutucu akışkanlar için daha yüksek toplam COP değerine sahiptir. Yüzey tipi 8.0-3/8T olan kondenserin, CF-7.0-5/8J yüzey tipindeki kondansere göre daha yüksek fan gücü tüketimine sebep olduğu bulunmuştur. Simülasyon sonuçları, sistem COP değerini arttırmak için evaporatör ve kondenserde, CF-7.0-5/8J yüzey tipinin kullanımını önermektedir.

Anahtar Kelimeler: Doğal ve Sentetik Akışkanlar, COP, Kompakt Isı Değiştiriciler

2018 **Tutku MUTLU**

ABSTRACT

MODELLING AND PERFORMANCE ANALYSIS OF A REFRIGERATION SYSTEM FOR DIFFERENT REFRIGERANTS AND CONFIGURATIONS

This study presented a mathematical model for a small scale refrigeration system components such as condenser, evaporator based upon different empirical correlations of heat transfer coefficients in order to simulate the performance of system using four different refrigerants (R134a, R404a, R410A and R290) and two different surface types (8.03/8T and CF-7.0-5/8J). In addition, the selected refrigerants are evaluated in a refrigeration system in respect of energy efficiency and environmental matters.

The improved model has been applied at variable operation parameters (mass flow rate, temperature, pressure) for investigated refrigerants. The numerical model defined a vapor compression refrigeration system is performed in EES to examine the effect of different refrigerants and surface types of condenser and evaporator on COP. The model is also capable of predicting the inlet and outlet air temperatures of evaporator for two regions ($T_{air,evap,in}$, $T_{air,evap,out}$), inlet and outlet air temperatures of condenser for three regions ($T_{air,cond.,in}$, $T_{air,cond.,out}$). According to the model, overall and convection heat transfer coefficients of different zones for evaporator and condenser are predicted. The pressure drop of the condenser air side (ΔP_{air}) is calculated for both surface types of 8.03/8T and CF-7.0-5/8J. Consumed power of condenser fan ($\dot{W}$) is determined by using calculated pressure drop.

The highest overall COP is calculated for the synthetic refrigerant (R410a) for both surface type 8.03/8T and CF-7.0-5/8J**.** On the contrary**,** the lowest COP is computed for the natural refrigerant (R290). In terms of surface type, type CF-7.0-5/8J has higher overall COP values than those of type 8.0-3/8T for all refrigerants. It is found that the condenser with a surface type of 8.0-3/8T has higher consumed fan power than that of surface type of CF-7.0-5/8J. Simulation results show that the utilizing type CF-7.0-5/8J is recommended to enhance system COP for both evaporator and condenser.

Keywords: Natural and Synthetic Refrigerants, COP, Compact Heat Exchangers

2018 **Tutku MUTLU**

LIST OF SYMBOLS

A	: Total surface area	m^2
A_f/A	: Fin area/total area	m^2/m^2
A_{fr}	: Frontal area	m^2
A/A_{fr}	: Total area/ Frontal area	m^2/m^2
C	: Mass flow factor	-
C_p	: Specific capacity	J/kg. K
D	: Diameter	m
D_o	: Outer diameter of tube	m
D_h	: Hydraulic diameter	m
f	: Friction factor	-
f_f	: Friction factor due to fins	-
f_t	: Friction factor due to tubes	-
F	: Fraction of heat exchanger	-
G	: Mass flux	kg/ m^2.s
h	: Convection coefficient/ enthalpy	W/ m^2.K, J/kg
H	: Height of heat exchanger	m
J	: Colburn factor	-
k	: Conductivity	W/ m.K
L	: Length of heat exchanger	m
$\dot{m}$	: Mass flow rate	kg/s
Nu	: Nusselt number	-
$N_{t,row}$	: Number of tube rows	-
$N_{t,col}$	: Number of tube coulomb	-
Pr	: Prandtl number	-
ΔP	: Pressure drop	N/ m^2
Q	: Heat transfer	W
Re	: Reynolds number	-
Re_D	: Reynolds number based on tube inside diameter	-
St	: Stanton number	-

$\mathbf{S_V}$	: Vertical separation distance between tubes	mm
$\mathbf{S_H}$	: Horizontal separation distance between tubes	mm
$\mathbf{S_F}$	: Fin spacing	fin/m
t	: Fin thickness	mm
T	: Temperature	°C, K
U	: Overall heat transfer coefficient	W/ m^2.K
υ	: Specific volume	m^3/kg
V	: Volume	m^3
$\dot{\mathbf{V}}$	: Volume flow rate	m^3/s
W	: Width of heat exchanger	m
$\dot{\mathbf{W}}$	: Work	W
x	: Quality	-

Δ	: Change	-
ρ	: Density	kg/m^3
σ	: Free flow area/ frontal area	m^2/ m^2
α	: Heat transfer area/total volume	m^2/ m^3
η	: Efficiency	-
μ	: Kinematic viscosity	m^2/s

air	: air
comp	: compressor
cond	: condensation region
evap	: evaporation region
in	: inlet
is	: isentropic
out	: outlet
R	: refrigerant
sc	:subcooling region
sh	: superheat region

tot : total

col : coulomb

row : row

f : fin

t : tube

e : expansion valve

LIST OF FIGURES

Figure 1.1.	Schematic view of a refrigerator	2
Figure 1.2.	Schematic of components and T-s diagram for ideal vapor compression refrigeration systems	4
Figure 1.3.	Schematic view the various components of a secondary loop refrigeration system.	5
Figure 1.4.	Schematic view of the cascade refrigeration system	6
Figure 1.5.	ODP and GWP values for Different Refrigerants	8
Figure 1.6.	Classification of PCM for thermal energy storage	12
Figure 2.1.	Schematic of components and T-s diagram for ideal vapor compression refrigeration systems	20
Figure 2.2.	Schematic of components and T-s diagram for actual vapor compression refrigeration systems	23
Figure 2.3.	Schematic representation of a fin heat exchanger	25
Figure 2.4.	Schematic view of an evaporator: divided into superheated and evaporation regions.	26
Figure 2.5.	Temperature distributions along the evaporator	28
Figure 2.6.	Schematic view of a condenser: divided into superheated, subcooling and condensation regions	31
Figure 2.7.	Temperature distribution simulation of refrigerant and air along the condenser	32

Figure 2.8.	Overview of relations in vapor compression refrigeration cycle	36
Figure 3.1.	Simulation results of evaporator for the inlet and outlet conditions of air and refrigerants	40
Figure 3.2.	Influence of mass flux on the convection coefficient for different refrigerants (Type: 8.0-3/8T)	41
Figure 3.3.	Influence of mass flux on the convection coefficient for different refrigerants (Type: CF-7.0-5/8J)	42
Figure 3.4	Effect of mass flux on the convection coefficient for R134a at different surface types	43
Figure 3.5.	Effect of mass flux on the convection coefficient for R290 at different surface types	43
Figure 3.6.	Effect of mass flux on the convection coefficient for R404a at different surface types	44
Figure 3.7.	Effect of mass flux on the convection coefficient for 410a at different surface types	44
Figure 3.8.	Influence of vapor quality on the mass flux for different refrigerants (Type: 8.0-3/8T)	46
Figure 3.9.	Influence of vapor quality on the mass flux for different refrigerants (Type: CF-7.0-5/8J)	46
Figure 3.10.	Influence of vapor quality on the mass flux for R290 at different surface types	47
Figure 3.11.	Influence of vapor quality on the mass flux for R134a at different surface types	47

Figure 3.12.	Simulation results of condenser for the inlet and outlet conditions of air and refrigerants	50
Figure 3.13.	Effect of vapor quality on mass flux for different refrigerants (Type: 8.0-3/8T)	51
Figure 3.14.	Effect of vapor quality on mass flux for different refrigerants (Type: CF-7.0-5/8J)	52
Figure 3.15.	Influence of vapor quality on the mass flux for R290 at different surface types	53
Figure 3.16.	Influence of vapor quality on the mass flux for R134a at different surface types	53
Figure 3.17.	Effect of air velocity on fan power for different surface types	54
Figure 3.18.	The effect of condenser air velocity on COP for different refrigerants (Type: 8.0-3/8T)	55
Figure 3.19.	Effect of condenser air velocity on COP for different refrigerants (Type: CF-7.0-5/8J)	56
Figure 3.20.	Effect of condenser air velocity on COP for different surface types a)R134a b)R290 c)R404a d)R410a	57
Appendix A.1.	Simulation results of type 8.03/8T for R134a	67
Appendix A.2.	Simulation results of type 8.03/8T for R290	68
Appendix A.3.	Simulation results of type 8.03/8T for R404a	69
Appendix A.4.	Simulation results of type 8.03/8T for R410a	70
Appendix A.5.	Simulation results of type CF-7.0-5/8J for R134a	71
Appendix A.6.	Simulation results of type CF-7.0-5/8J for R290	72

Appendix A.7. Simulation results of type CF-7.0-5/8J for R404a 73

Appendix A.8. Simulation results of type CF-7.0-5/8J for R410a 74

LIST OF TABLES

Table 2.1.	Design parameters of surface types for a circular tube-continuous fin compact heat exchanger: 8.0-3/8T and CF-7.0-5/8J	25
Table 2.2.	Correlations used in the condenser and evaporator model	27
Table 2.3.	Operating parameters used as input in the evaporator model	29
Table 2.4.	Operating parameters used as input in condenser design	34
Table 2.5.	Thermo-physical and environmental properties of refrigerants used in model	37
Table 3.1.	Evaporator model results for different surface types and refrigerants	39
Table 3.2.	Results of the condenser model for different surface types and refrigerants	49
Table 3.3.	Results of the simulated refrigeration system for different refrigerants and surface types	59

1. INTRODUCTION

1.1. Objective of the Thesis

Approximately 15% of the power consumption in the industrialized countries is connected to refrigeration applications nowadays. Therefore, improvement of the refrigeration system performances is a main issue in the current context of the rational using of energy. One of the largest application areas of energy usage is in supermarket refrigeration. Typical energy consumption for supermarket refrigeration is more than twice the energy consumed by a hotel or an office of the same size [1]. In consideration of the increase of lack of fossil energy sources and the still slow development of renewable technologies, optimal operation of refrigeration systems become a key solution to satisfy the cooling load demand.

Vapor compression based refrigeration systems are the leading technology over the world in cooling generation, including air conditioning, refrigeration and freezing. Power range of domestic, commercial and industrial refrigeration systems differs from less than 1 kW to above 1 MW.

In a conventional system, a single refrigerant is circulated throughout the system to cool off the air circulated in the display case. Furthermore, leakages can occur, so the refrigerant must be safe for contact with food and consumers. Synthetic refrigerants are commonly utilized in refrigeration applications. But, it is indicated that such refrigerants have unfavorable effects on the ozone layer of atmosphere. With regard to the increasing attention in environmental protection and conservation, there has been a recent resurgence in the interest of natural refrigerants. In recent years, natural refrigerants such as carbon dioxide, propane (R290) and different hydrocarbon compounds are suggested to substitute synthetic refrigerants in the industrial refrigeration systems. Propane (R290) is one of the most hope-inspiring and environment-friendly refrigerant solutions because of its thermo physical properties, low global warming potential and zero ozone depletion value.

The aim of this thesis is to put forth a mathematical model of operation conditions dependent on the alternative refrigerants and surface types of evaporator or condenser to improve the Coefficient of Performance (COP) of conventional refrigeration system.

To realize this aim a model for refrigeration system components such as condenser, evaporator to simulate the performance of system using four different refrigerants (R134a, R404a, R410A and R290) and various surface types (8.03/8T and CF-7.0-5/8J) is improved and evaluated.

1.2. Refrigeration Cycles

It is clear that heat flow is from high temperature environment to low temperature environment in the nature. Heat transfer in this direction occurs without any requiring devices in the nature. But reverse of this heat transfer process cannot happen by itself. For this reason, in order to heat from low temperature mediums to high temperature mediums, specific devices called refrigerating machines such as refrigerators and heat pumps are needed. The objective of the refrigerators is to keep it at low temperature by drawing heat from the refrigerated space. In Figure 1.1 shows that the schematic view of a refrigerator.

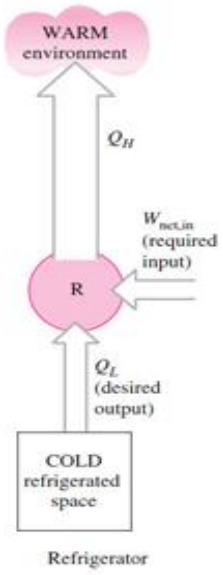

Figure 1.1. Schematic view of a Refrigerator [2].

The performance of refrigerators (COP) is expressed as shown below;

$$COP = \frac{Desired\ Output}{Required\ Input} \tag{1.1}$$

$$COP = \frac{Desired\ Output}{Required\ Input} = \frac{Cooling\ Effect}{Work\ Input} = \frac{Q_L}{W_{net,in}} \quad (1.2)$$

Q_L is positive value because it represents the thermal magnitude. On the other hand, $W_{net,in}$ indicates the amount of work that must be provided to the refrigerator. It can be seen from the correlation that COP value is bigger than 1. The refrigeration capacity of a refrigeration system is defined as the heat drawn from the refrigerated medium.

Refrigerating machines are based on cycle principle and the fluids utilized in the refrigeration systems are called refrigerants. Refrigeration systems consist of different components. Main components of refrigeration systems are evaporator, compressor, condenser and an expansion valve.

Compressor: The main purpose of the compressor is that it is to send refrigerant to the condenser at higher pressure. Since there is a great influence of efficiency of the compressor on the economy of the plant, different compressors have been developed according to the type and size of the refrigeration systems.

Condenser: This component condenses the superheated gas, which is compressed at the compressor, by cooling. In a refrigeration system, the heat drawn in the evaporator and the total heat given to the flow by the compressor are removed from the condenser.

Expansion valve: It is the component which enables to drop the pressure of the refrigerant at the high pressure to the desired evaporator pressure. It is assumed that enthalpy is constant during the process.

Evaporator: These are generally made of copper and steel depending upon the type of refrigerants [2].

1.2.1. The ideal vapor compression refrigeration cycle

A basic ideal vapor compression refrigeration cycle comprises of four fundamental components which are condenser, compressor, expansion valve and evaporator. This cycle comprises of four changes of state;

1-2 Isentropic compression in compressor

2-3 Heat rejection process at constant-pressure in a condenser

3-4 Throttling process

4-1 Heat absorption process at constant-pressure in an evaporator

Schematic of components and T-s diagram for ideal vapor compression refrigeration systems are indicated in Figure 1.2.

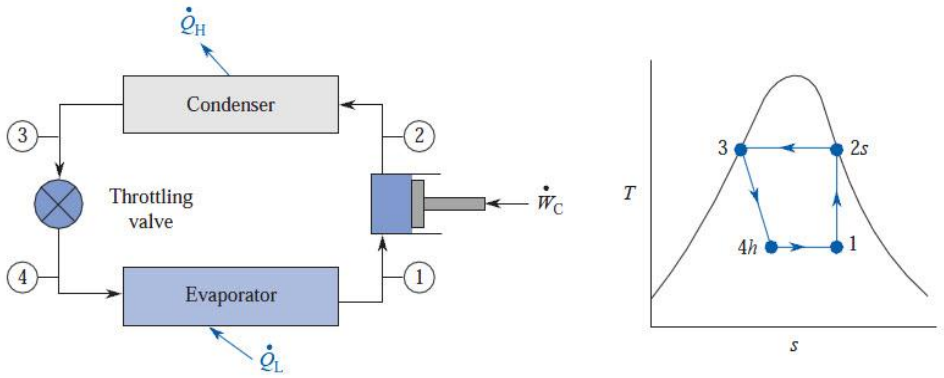

Figure 1.2. Schematic of components and T-s diagram for ideal vapor compression refrigeration systems [3].

1.2.2. The actual vapor compression refrigeration cycle

The actual vapor compression cycle differs a bit from ideal vapor compression systems. These differences are generally owing to irreversibility. Heat transfers between refrigerant and cold and warm regions are not reversible. Also, the friction of the fluid that causes the pressure drop is one of the irreversibility that takes place in the actual vapor compression refrigeration cycle. This topic can be found in detail Chapter 2.

1.3. Innovative Vapor Compression Refrigeration Systems

The simple refrigeration systems mentioned above are used in most refrigeration applications because of their low cost and simple. But these refrigeration systems are sometimes not sufficient and modified vapor compression systems are used in some large commercial applications.

Examples of innovative vapor compression refrigeration systems can be cascade refrigeration system and secondary loop vapor compression refrigeration systems.

1.3.1. Secondary loop refrigeration systems

A secondary loop refrigeration system is composed of two cycles, corresponding to low temperature and high temperature cycles. Second loop cycle (low temperature cycle) contains a heat exchanger which is employed as the air coil and a pump is used to circulate the secondary termofluid through the secondary loop. An open reservoir is located on the suction side of the pump. Also, it contains an intermediate heat exchanger which is an annular type heat exchanger between the secondary and primary loop. The annular type heat exchanger (tube in tube) is used to transfer energy from the secondary to primary loop. On the other hand, primary loop (or high temperature cycle) contains a compressor, a condenser, an expansion valve. A schematic of the secondary loop refrigeration system is shown in Figure 1.3.

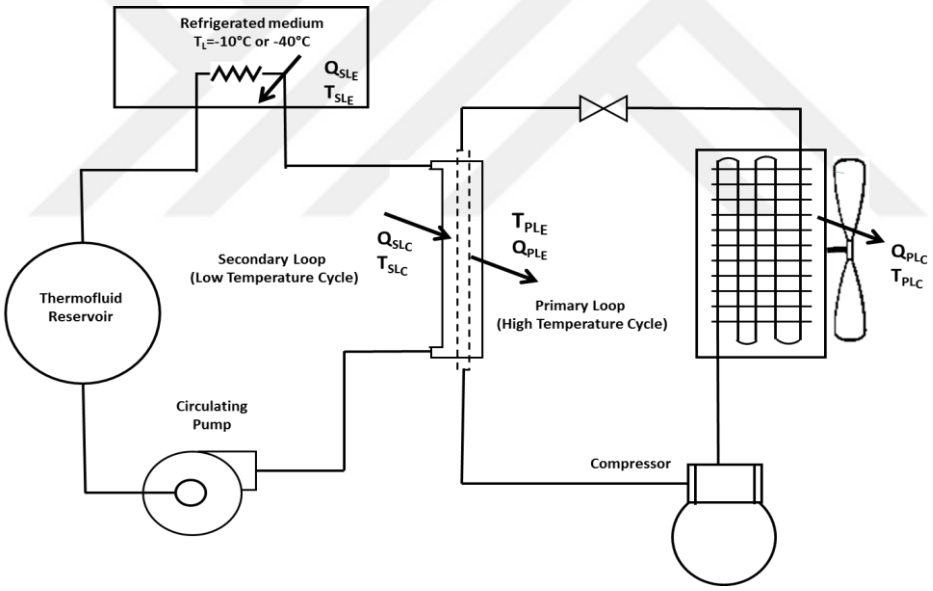

Figure 1.3. Schematic view the various components of a secondary loop refrigeration system.

1.3.2. Cascade refrigeration system

The cascade system is composed of the high temperature and low temperature cycles. Schematic diagram of the two-stage cascade refrigeration system is shown in Figure 1.4. High temperature cycle includes an expansion valve, an air-cooled condenser, a

compressor and a cascade condenser corresponding to evaporator of the cycle which is a heat exchanger. On the other hand, the low temperature cycle occur the same elements and as in high temperature cycle and a liquid receiver however the compressor and cascade condenser are replaced by an evaporator and compressor.

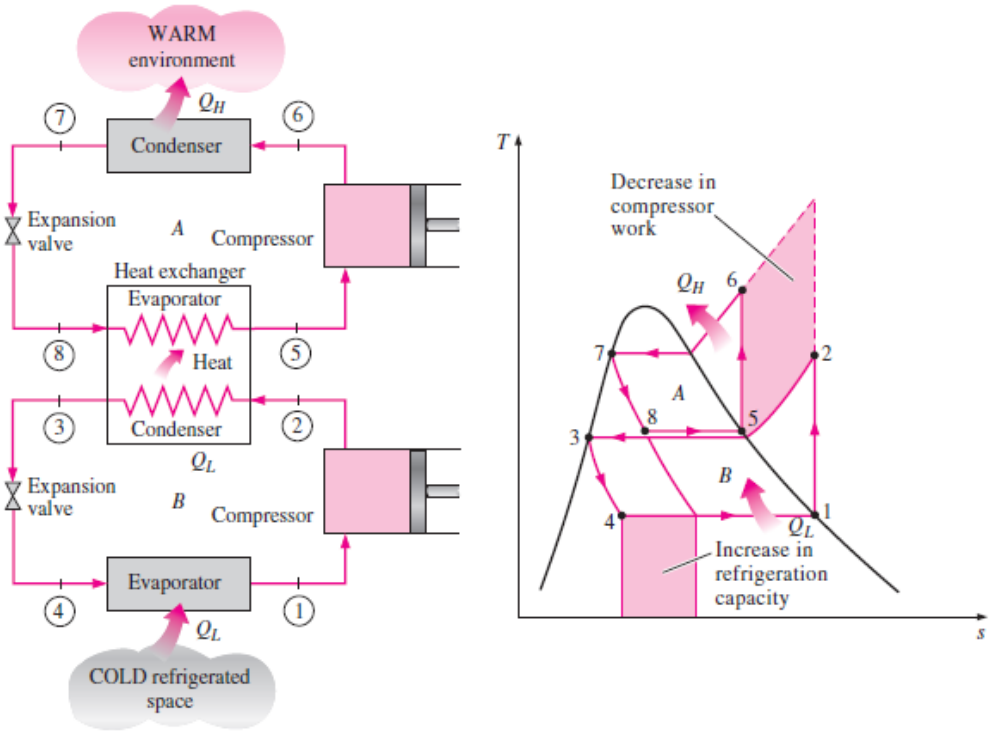

Figure 1.4. Schematic of the cascade refrigeration system [2].

1.4. Refrigerants

Refrigerants are the fluids used for heat transfer in a refrigerating system. Refrigerants release heat during condensation and absorb heat during evaporation at low and high temperature and pressure zones respectively. Refrigerants are classified under two main types as primary refrigerants and secondary refrigerants. Primary refrigerants are used in vapor compression refrigeration system and for the purpose of refrigeration. Main purpose of secondary refrigerants is cooling the primary refrigerants (brine, antifreeze etc.). Also there are both synthetic and natural refrigerants recently used in refrigeration systems. These refrigerants will be mentioned below.

1.4.1. Environmental concerns and restrictions

The ozone depletion potential (ODP) of a chemical compound is the relative amount of corruption to the ozone layer it can give rise to. ODP values are in the range of 0-1. R11 is the reference compound and it has an ODP of 1. Because Chlorofluorocarbons (CFCs) have three chlorine atoms in the molecule which are accused of extremely making contribution to the ozone depletion, they have the highest ozone depletion potential. Concerns about the environmental effect of discharging CFC refrigerants into the atmosphere led to the 1987 singing of the Montreal Protocol which is an international agreement designed to significantly decrease the manufacture and usage of ozone depleting substances [4]. The chlorinated hydrocarbon refrigerants will be phased out according to the Montreal Protocol by the year 2020 due to their ozone depletion potential [5].

The global warming potential (GWP) is the measure of how much greenhouse gases emitted into the atmosphere heat up. The amount of heat retained by a given mass of gas in question is compared to the amount of heat retained by an analogue mass of carbon dioxide. GWP values are computed over a particular time period, generally 500, 100 or 20 years. GWP is stated as a factor of carbon dioxide and GWP value of carbon dioxide is 1, is standardized to this value. To give an example, the 20 year GWP of methane is 86, in other words if the same mass of carbon dioxide and methane are let into the atmosphere, this methane is going to trap 86 times more heat compared to the carbon dioxide in the coming 20 years. Concentrations of the items to limitations under the Kyoto protocol are quickly going up in Earth's atmosphere.

Figure 1.5 shows schematically GWP and ODP values of some different refrigerants.

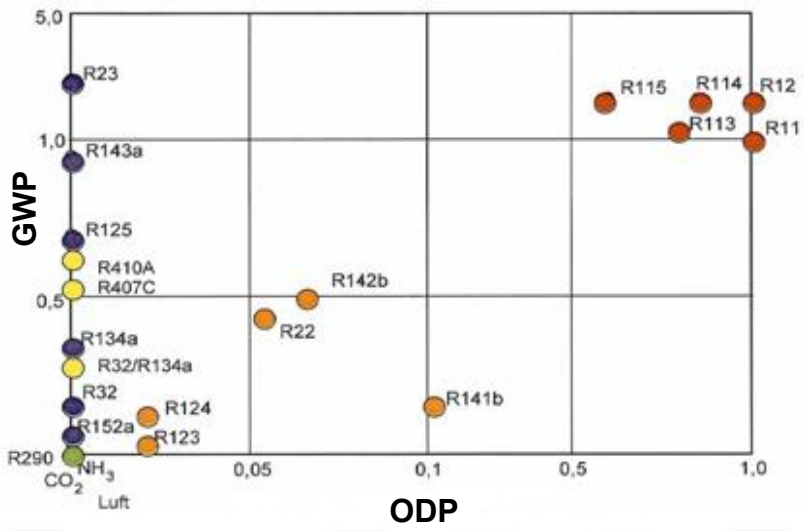

Figure 1.5. ODP and GWP values for Different Refrigerants [6].

Those below affect the GWP:

- the sucking of infrared radiation by a specific types
- the spectral site of its sucking wavelengths
- the atmospheric life of types [7].

1.4.2. Future refrigerants

Hydrofluorocarbon (HFC) refrigerants have some advantages; having zero ozone depletion potential, being non-toxic and being non-flammable. The only disadvantage of using HFC's is that they are in the category of greenhouse gases caused the global warming.

Presently, HFC refrigerants are not included in the scope of the Montreal Protocol and therefore, are not issue to phase out. However, because their global warming potentials are much more than that of carbon dioxide, it is not certain that these refrigerators will be used or not. In addition, state regulation of these refrigerants can remove them from future use.

When considering refrigerants presently used in refrigeration applications it is significant to regard the effect of refrigerants on humans or the environment. The following criteria's can characterize the influences of a refrigerant [8].

1. Toxicity for humans and animals, including:
    Acute toxicity
    Chronic toxicity, including genetic effects
2. Flammability and explosiveness
3. Influence on the ozone layer
4. Effect on global warming
    Direct effect from the molecule itself
    Indirect effect from CO_2 manufacture

1.5. Primary Refrigerants

Primary refrigerants can be divided into following categories according to their characteristics.

1.5.1. Halocarbons (Freon's)

Halocarbons have three different types; CFCs, HFCFs and HFCs.

Chlorofluorocarbons (CFCs) include Chlorine, Fluorine and Carbon and are synthetically produced. They were improved in the 1930's and were used in several areas such as automotive applications. CFCs are non-toxic and non-flammable. They don't also react with other chemical compounds. Because of these reasons CFCs are secure refrigerants. However, in 1973, it was found out that the Chlorine atom in the CFC's is a catalyst for ozone depletion Essentially the Cl atom separates the extra oxygen atom from the ozone compound. Since 1987 their usage has been being proscribed by the Montreal Protocol. Some important CFCs are;

- R11, R500, R13B1 , R113, R13, R114, R502, R12, R503

Hydrochlorofluorocarbons (HCFCs) include Chlorine, Fluorine, Hydrogen, and Carbon. They have approximately 10% of the ozone depleting potential as HCFCs. They are nontoxic, energy-efficiency and cost effective refrigerants. Some important HCFCs are;

- R123, R124, R416A, R22, R401B, R401A,R402A, R408A, R409A, R403B, R414B

Hydrofluorocarbons (HFCs) are refrigerants including Hydrogen, Fluorine, and Carbon. HFCs have zero ozone depleting potential and lower global warming potential. Unfortunately, they were targets of the Kyoto Protocol since they operate in a completely various greenhouse gas field. Some important HFCs are;

- R134a, R404A, R23,R407C, R417A, R508B, R422A, R410A, R422D, R507, R422B

1.5.2. Inorganic compounds

Inorganic compounds have been used in refrigeration systems for a long time. They are natural refrigerants used in the refrigeration systems. Due to its low Global Warming Potential, it is known as environmental friendly refrigerant. Some important inorganic compounds are;

- CO_2, H_2O, NH_3, Air,SO_2

1.5.3. Hydrocarbons

Hydrocarbons are organic compounds and comprise of the hydrogen and carbon. They are main components of natural gases and petroleum. Some important hydrocarbons are;

- Methane, Ethane, Propane

1.5.4. Azeotropes

Azeotropes are the mixtures of two or more various refrigerants. They behave as a compound so that; the components cannot be separated by distillation, pressure and temperature changes. Azeotrope refrigerants behave as single substance having properties that are different from those of either component [9]. For instance, R505 is an azeotrope which is a mixture of R12 (78%) and R31 (22%).

1.5.5. Unsaturated organic compounds

These are refrigerants from hydrocarbon group and have ethylene or propylene as in below.

- R1120 / Trichloro ethylene
- R1130 / Dichloro ethylene
- R1150 / Ethylene
- R1270 / Propylene

1.6. Thermal Energy Storage with PCMs: Materials, Techniques and Applications

1.6.1. Phase change materials

Phase Change Materials (PCMs) are materials that provide heat balance by changing the phase at a constant temperature by absorbing and spreading the heat in the environment and can minimize the ambient temperature fluctuations that degrade the quality of stored food when used in cooling. They store thermal energy in the shape of latent heat. The significant change in the internal energy of the heat storage material causes this material to undergo a phase change. At the optimum temperature limits, the latent heat generated by the phase change of the storage material can be stored. For the purpose of heat storage, materials which undergo phase changes at certain temperatures and whose latent heat values are high are used.

Phase change materials that are suitable for heat storage; solid-solid and solid-liquid. Liquid-vapor phase change is not suitable for heat storage owing to problems such as requiring storage of gas phase in pressure storage vessels. When a material in a solid state crystallizes to another solid phase (solid-solid exchange), heat is stored in the way that crystallization heat. When the material is converted to the solid phase in the first state, the heat stored during the phase change is also recovered. The amount of latent heat released during the solid-solid phase change is small. In solid-liquid phase change, less volume change occurs compared to other phase changes. Only solid-liquid or solid-solid phase changes with high heat of crystallization have practical precaution because of their high volumetric energy storage capacity in practice. PCMs can be applied in both heating and cooling systems [10].

There are three different phase change materials that are commonly used. These are organic, inorganic and eutectic phase change materials.

Organic PCMs are generally paraffinic and non-paraffinic carbon based compounds. As molecular weight or number of carbon atoms increase, the latent heat of fusion of the PCM increases. Organic PCMs have some advantages such as stable chemically, show

little or no extreme cooling, not being corrosive and toxic, high melting temperature and low vapor pressure, but they have also some disadvantages. For example; low thermal conductivity, large volume change during phase change.

Inorganic PCMs include hydrated salts. Low cost and good thermal conductivity of inorganic PCMs can be considered as the major advantages of inorganic PCMs, but it is corrosive in nature.

Eutectic PCMs are composition of two or more components to obtain the desired melting point. They melt and freeze comparably by forming a mixture of the component crystals during crystallization [11]. The melting point of the phase change material is one of the most important factors for choosing PCM for storage applications [12]. Eutectic PCMs can be classified as inorganic eutectic PCMs and organic eutectic PCMs.

PCMs are commercially available in market. Also these types of PCMs can also be utilized for most latent heat storage applications.

Figure 1.6 demonstrates the categorization of PCMs utilized for thermal energy storage.

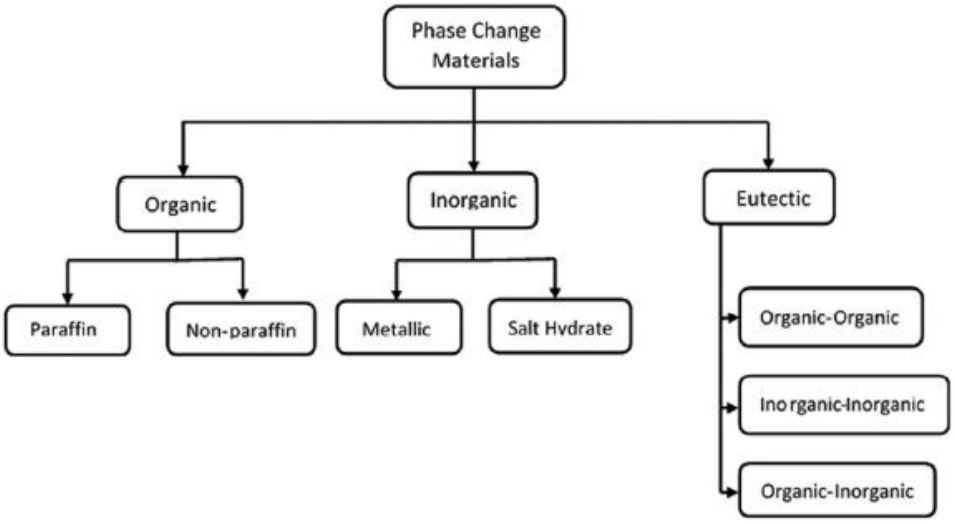

Figure 1.6. For thermal energy storage: Classification of PCM [13].

1.6.2. Techniques

Thermal energy storage systems enable direct cooling-heating without the need for chlorofluorocarbons (CFC), which damage the ozone layer. The need for electricity is diminished and overloading of the electric power can be avoided at times of greatest

need. Thus, it offers less polluting solutions by reducing the need for power plants and the use of fossil fuels.

Thermal energy storage is a method that includes adding cold thermal energy to an instrument and excerpting it when there is a need. The cold thermal energy can be deposited as a result of phase changing of the storage medium. It decreases the electricity peak load by depositing cold during off peak hours [14, 15] and also for seasonal storage [16].

The widely utilized thermal energy storage techniques are listed below;

Sensible Heat Storage: The energy storage capacity of this technique is based upon the temperature difference and specific heat capacity. There is no phase change in a sensible storage system. The amount of energy deposited in a sensible storage system is calculated by Equation (1.3).

$$Q = \int_{T_i}^{T_f} m\, C_p \Delta T \tag{1.3}$$

Latent Heat Storage: Latent heat storage is one of the favorite research interests with internal and industrial applications, such as energy recovery of air conditioning and under-floor electric heating by using PCM [17-19]. Latent heat energy storage draws more attention due to its high energy storage density of 5–14 times higher than sensible storage system [20, 21]. In this method, during energy storage and retrieval a phase change happens. The amount of energy deposited is depended upon the latent heat of fusion of the material. Phase change material is also utilized in order to enhance the energy storage capacity of a system [22]. The amount of energy deposited in a latent heat storage system is computed by Equation (1.4).

$$Q = \int_{T_i}^{T_m} m\, C_p \Delta T + m a_m H + \int_{T_m}^{T_f} m\, C_p \Delta T \tag{1.4}$$

Thermochemical Heat Storage: Thermochemical energy storage system relies upon the energy absorbed and released throughout a chemical reaction through breakage and reconstruction of molecular bonds. The chemical reaction must be totally reversible. The amount of reacting materials affect amount of energy stored.

1.6.3. Applications

Thermal energy storage by the phase change method has long attracted the attention of researchers and tried to find the most efficient method by using different materials in different fields. Today, studies on biomedical, construction, refrigeration and textile fields are very common.

In the field of textiles at the end of the 1970s and early 1980s, studies were started by NASA to increase the effectiveness of thermal protection in extreme changes of temperature caused by astronaut clothing in space. Today, the number of textile products produced by using PCM is increasing day by day with this study in textile field based on thermal protection. In many countries PCMs are used in the construction sector. The high proportion of residential energy consumption increased the saving efforts in this area.

Potential areas of usages of PCMs and locations where the efficiency of heat utilization can be increased with the help of these materials are listed as follows;

- Cooling: Installed power down
- Keeping food, diary and wine products in a cool place
- Space shuttle thermal applications
- Engine cooling: electric and internal combustion engine
- Hot water for heating
- Medical applications
- Keeping the temperature constant in living environment
- Thermal storage of solar energy
- Reduce the effect of exothermic peaks in chemical reactions
- Hot and cold climate clothes
- Thermal comfort in cars
- Passive heat storage in buildings
- Thermal protection of power tools

1.6.4. Selection of PCM for thermal energy storage applications

Selecting a correct PCM for a specific cold storage application is a significant criterion. The fact that a material has a high latent heat enthalpy and an appropriate phase change temperature is the two most important factors for an attractive PCM. These properties determine the basic thermo-physical properties of a material. However, other properties that a material other than these basic properties should have are listed below. These are;

Thermo-physical Properties:

- The melting temperature of the PCM ought to be between the ranges of operational temperature.
- High density.
- High thermal conductivity.
- High latent heat of fusion.
- Low volume change during phase change.
- Low degree of super cooling.

Kinetic Properties:

- There should be little or no over-cooling effect during freezing.

Chemical Properties:

- Less corrosive to the construction materials.
- Low degradation
- Chemically stable.
- Non-toxic and non-flammable.

Economic Properties:

- Easily available.
- Cost effective.

1.6.5. Heat transfer enhancement

When we want to use latent heat cold storage method, especially when using organic phase change materials, we encounter a problem that is low heat transfer rate. This will

lead to slow charging and discharging rates. To enhance the heat transfer rate, many studies have been performed to study heat transfer enhancement methods in phase change materials (PCMs). These are inclusion of nano-structures, shape stabilization of PCM and encapsulation.

- **Inclusion of Nanostructures**

In order to increase the heat transfer rate during phase change, nanostructures are inserted into the base PCM. There are some significant issues such as the size and shape of the nanostructures, because the surface to volume rate of nanostructure changes the thermo-physical properties of the PCM [23]. Commonly used nanostructures are metal and metal oxide. These make possible micro convection between pure PCM and nanostructures, and so the thermal conductivity also increased.

- **Encapsulation of PCM**

Encapsulation of PCM increases the heat transfer and it stays away PCM from mixing with the heat transfer fluid and it is an easy method. The PCM containment utilized for encapsulation has to some properties such as flexibility, strength, thermal stability and corrosion resistance [13]. Also, it must supply required surface area for heat transfer and structural stability.

There are two main means of encapsulation. These are microencapsulation which comprises the filling of PCM in micro scale capsules and macro encapsulation which includes the PCM filled in form of package such as tubes, panels, spherical capsules etc.

- **PCM Slurries**

Using micro encapsulated PCM slurries can enhance the heat transfer rate of heat transfer fluid and the thermal capacity.

- **Shape Stabilized PCM**

Shape stabilized phase change materials are special sort of PCMs. They comprises of supporting material and a working material. Even if phase change occurs in the working material, the supporting material stays in solid phase. Physical and chemical methods

are used to prepare the shape stabilized PCMs. The physical methods and the chemical methods include blending, adsorbing etc. and graft copolymerization, sol-gel method, respectively [24, 25].

1.7. Literature Review

There are various techniques in order to model a condenser or evaporator. An appropriate evaporator or condenser model need to understandable application of heat transfer coefficients. Many researchers have used different methods for this purpose [26-28].

Ge and Tassou developed a numerical modeling of supermarket refrigeration systems for design and energy prediction. In this study, the evaporator was separated to superheated and two-phase zones. In order to calculate for heat transfer coefficients for superheated region, they used Dittus-Boelter's correlation [26]. For the evaporation of refrigerants (two phase), proper correlations were attained from Chaddock and Noerager. Also McQuiston's correlations were utilized for air side heat transfer coefficient [27].

Horton improved a mathematical modeling of secondary loop refrigeration system for supermarket applications [4]. Evaporator for this system was modeled using a finite element method. While correlations from Chen were used for the single phase and two-phase refrigerant heat transfer coefficients, correlations from Kim et al were used for the air-side heat transfer coefficients [28].

H.M. Getu and P.K. Bansal performed the modeling and experimental analyses of the evaporators used in the supermarket. In this model, evaporator were divided into two different regions such as evaporation and superheated. Also, they were used different heat and mass empirical correlations of heat transfer coefficients and frost properties in a fin-tube heat exchanger to evaluate the effect of various operating conditions on the performance of evaporator. Finally, developed model was validated with the experimental results [26].

S. A. Tassou and R. K. Green developed a mathematical model to investigate the heat transfer performance of a shell and tube condenser. They were used the Effectiveness-Number of Transfer Units (ε-NTU) method to analyze the heat exchanger. Their outputs

such as heat transfer coefficients, total heat rejection and the exit fluid temperatures were determined by the improved model. Also they tested performance of the condenser at the same conditions to validate their model. And the results show that experimental and theoretical values are similar to each other [29].

Guillermo Bejarano and Jose A. Alfaya carried out the modeling and optimization of vapor compression refrigeration systems. Also in this study they examined how such systems are controlled. A simplified model was performed for controllability study and some difficulties and they laid emphasis on these difficulties using a model based on control strategy [30].

Ion Zabet, Vincent Lemort developed a numerical model for the evaporator (a fin and tube heat exchanger) using Engineering Equation Solver (EES) software which predict some parameters such as heat transfer coefficients, Reynolds number, friction factor, pressure drop etc. for this study. They used different refrigerants such as R152a, R404a, R407C, R410a and R744 and used air on the other side of evaporator in their model study. Also in order to validate the numerical model they carried out experimental studies in which they used R404a as a refrigerant. And consequently their measurements were compared with theoretical model results and the error was found around 2% [31].

Liu M. and Liang S. Y. improved a simulation model for the finned tube evaporators used in refrigeration systems in a humid environment. They modeled the flow characteristic of the refrigerant and distribution of air temperature in the evaporator. Also they investigated the influences of the some parameters such as evaporating temperature and relative humidity on the performance of the evaporator. It was observed that from the developed model the relative humidity is really important parameter in any refrigeration systems. As the humidity increases in the environment, cooling load increases [32].

Zhaoyi Zhuang and Yongjie Du developed a theoretical model which is applied to analyze the performance of some sewage condensers. Also they examined the influences of various tubes and pass arrangements on performance of condenser. The results indicated that when the sewage flux is kept constant, as the sewage condenser inlet temperature increases the condenser heat exchange increases. In addition, when the

sewage inlet temperature is fixed, as the condenser heat exchange and flow resistance increase, the sewage flux increases [33].

There are some studies done about the energy consumption of refrigerators in literature [13,23,34]. Latent heat storage using PCMs are more useful in applications such as buildings, solar energy, air conditioning etc.

S. Bakhshipour and M.S. Valipour developed a mathematical modeling of refrigeration system included in a PCM heat exchanger. For this purpose, both refrigeration systems with and without PCM were examined and compared with each other. They integrated PCM heat exchanger between the condenser and expansion valve. The PCM used in this study was n-octadecane. Matlab software is used for mathematical modeling in the present study and modeling results revealed that using PCM increased the performance coefficient of the refrigeration system by 9.58 percent [34].

2. MATERIALS AND METHODS

2.1. System Description: Vapor compression refrigeration system

2.1.1. The ideal vapor compression refrigeration cycle

Vapor compression refrigeration systems are mostly used in refrigerators, air conditioning systems and heat pumps. A basic ideal vapor compression refrigeration cycle comprises of four main components which are condenser, compressor, expansion valve and evaporator. This cycle consists of four changes of state;

1-2 Isentropic compression in compressor

2-3 Heat rejection process at constant-pressure in a condenser

3-4 Throttling process

4-1 Heat absorption process at constant-pressure in an evaporator

Schematic of components and T-s diagram for ideal vapor compression refrigeration systems are indicated in Figure 2.1.

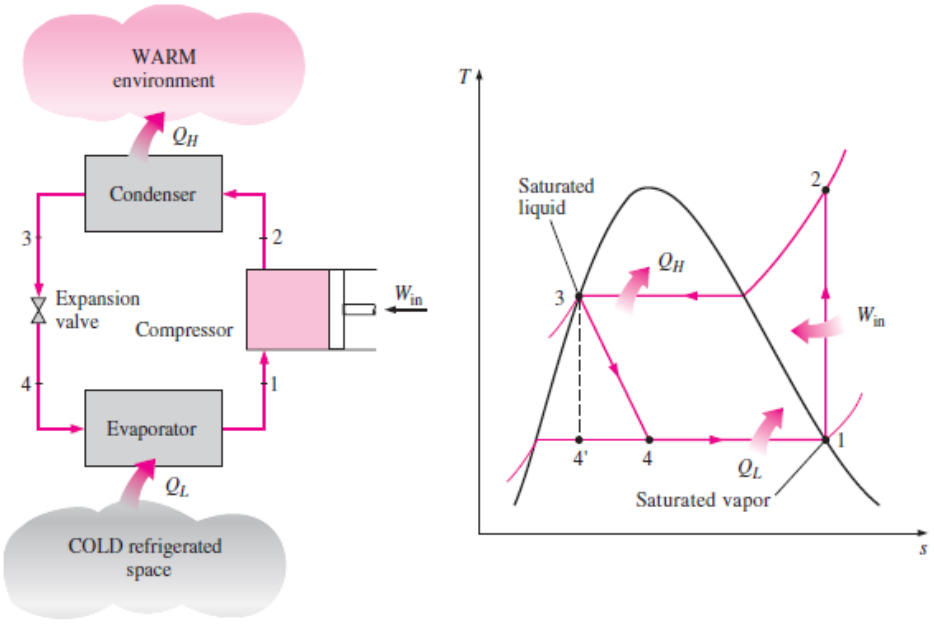

Figure 2.1. Schematic of components and T-s diagram for ideal vapor compression refrigeration systems [2].

In an ideal vapor compression refrigeration cycle, the refrigerant enters to the compressor as saturated vapor at state 1 and is pressed to condenser pressure isentropically. During this isentropic compression, the temperature of the refrigerant is higher than the temperature of the surrounding environment. Then, the refrigerant enters to the condenser as superheated vapor at state 2 and exits as saturated liquid at state 3. And then, this saturated liquid passes through the expansion valve. Here, the vapor is throttled down to a low pressure liquid and passed on to an evaporator at state 4 and refrigerant completely evaporates absorbing heat from the refrigerated environment. Refrigerant exited from evaporator completes the cycle by entering the compressor again.

The ideal vapor compression refrigeration cycle deals with a steady flow process, because all four components used in vapor compression refrigeration process is steady flow process. The kinetic and potential energy changes of the refrigerant can be neglected as they are generally small. Then the energy equation becomes:

$$(q_{in} - q_{out}) - (w_{in} - w_{out}) = h_{in} - h_{out} \tag{2.1}$$

$$COP_{R,ideal} = \frac{Q_L}{W_{net,in}} = \frac{h_1 - h_4}{h_2 - h_1} \tag{2.2}$$

When drawing a T-S chart in the ideal refrigeration cycle with steam compression, some assumptions are made. The accepted assumptions are as follows:

It is considered that there is no pressure drop between 1-2 and 3-4 points where the refrigerant passes through the evaporator and condenser and between 2-3 and 4-1 points, the compression in the compressor and the expansion in the expansion valve are isentropic and adiabatic, respectively.

It is considered that there is no heat loss and gain except evaporator and condenser during the cycle.

It is assumed that the pressure drop process in the expansion valve is performed on a constant enthalpy and there is no pressure loss in the pipes and fittings that provide the connection between the system components. In addition, it is considered that there is no heat transfer between the connection pipes and the environment.

It is assumed that the refrigerant at the evaporator outlet and the condenser outlet is saturated vapor and saturated liquid, respectively.

2.1.2. The actual vapor compression refrigeration cycle

Actual vapor compression systems are different from ideal vapor compression systems in some ways. This is usually due to the irreversibility in the various components such as condenser and evaporator. Two main sources of the irreversibility are the friction of the fluid that causes the pressure drop and heat transfer to the surrounding. Schematic of components and T-s diagram of actual vapor compression refrigeration systems are shown in Figure 2.2**.**

In the ideal cycle, the refrigerant exiting the evaporator enters the compressor as saturated vapor. But, in practical terms, it cannot be possible to check the refrigerant obviously. In place of this, it is much simpler to project the system so that the refrigerant has some superheated at the compressor inlet. As a result, it is ensured that the refrigerant completely evaporates at the compressor inlet. Also, the connection line between the evaporator and the compressor is generally long, so that the pressure drop caused by the fluid friction and the heat transfer to the surrounding refrigerant can be important. As a result of the heat at the evaporator outlet, the heat gain at the connection pipes, the pressure loss at the evaporator and connecting pipes, the specific volume increases. Since the steady flow work is proportional to the specific volume, the work to be given to the compressor also increases.

In the ideal cycle, because the compression process is internally reversible and adiabatic, as it is also isentropic. On the other hand, there is heat transfer increasing or decreasing entropy depending on the direction and the friction effect which increase the entropy in the actual compression process. As a result, the entropy of the refrigerant during actual compression process can be increased or decreased depending on which one is dominant. It may sometimes be desirable to comply with the state change rather than the isentropic state. In this case the specific volume of the refrigerant and so the work need are smaller. As a result, cooling of the refrigerant during compression process must be performed as long as it is feasible and economical.

It is presumed that refrigerant leaves the condenser as saturated liquid at compressor exit pressure in the ideal case. In the actual cycle, in the condenser, a small amount of pressure loss is inevitable in the pipes between the condenser and the compressor and the expansion valve. On the other hand, at the end of condensation, it is hard to complete the process with precision as the refrigerant is a saturated liquid. Also, it is not attractive that the refrigerant enters to the expansion valve before the refrigerant is totally condensed. For this reason, before the refrigerant enters the expansion valve, it is subcooled, so refrigerant enter the evaporator at lower enthalpy value, there is no problem with the process, as it will draw more heat from the refrigerated space. Pressure drop between the expansion valve and evaporator is small because of very close to each other.

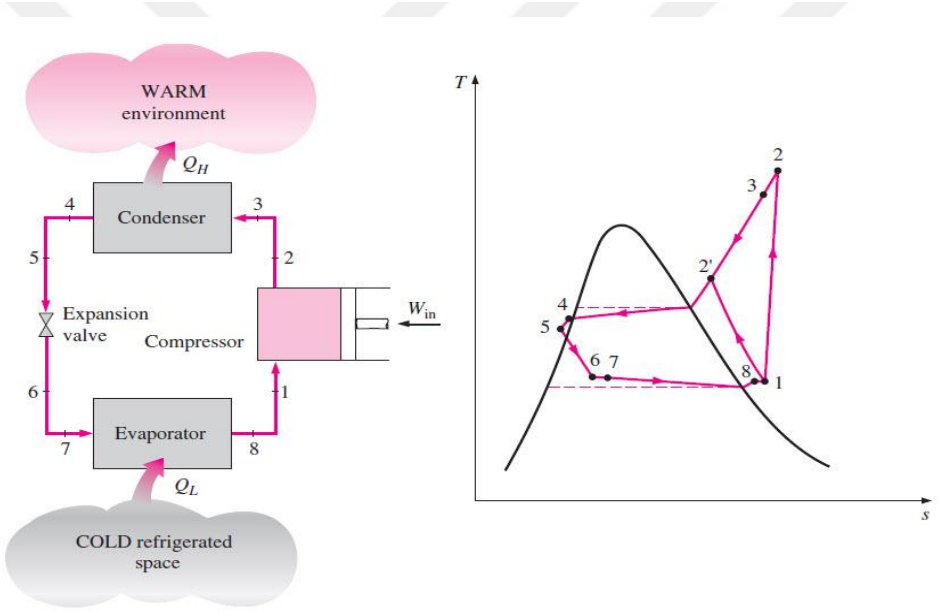

Figure 2.2. Schematic of components and T-s diagram for actual vapor compression refrigeration systems [2].

2.2. Mathematical Modeling of the Refrigeration System

The modeling of refrigeration systems is important in several respects. They are summarized below;

1) A well enhanced model can extensively decrease the time required to design a refrigeration system for a special application because the developed model can quickly adapt to new operating conditions,

2) The cost of developing system performance by reducing the number of experimental tests that must be performed can be significantly reduced with a model,

3) By modeling, the performance of different physical components can be quickly evaluated and the effects on the system can be examined [35].

In this section, definition of the vapor compression refrigeration system components and assumptions made for numerical modeling is performed for each component separately. System model was written using Engineering Equation Solver (EES) software which is more suitable to analyze a system thermodynamically. It has many physical and thermodynamic properties of various substance and refrigerants. The system comprise of four components: evaporator, compressor, condenser and expansion valve. In this study, compact heat exchangers are preferred for evaporator and condenser because they have a large heat transfer surface area per unit volume and at least one of the fluids is a gas. Many various plate and tubular configurations of compact heat exchangers have been designed in production. They have many differences due to fin design and arrangements [36].

The heat exchanger surface type to be modeled as a condenser or evaporator was selected as type 8.0-3/8T and CF-7.0-5/8J. Pipe material is copper, and pipe type is based on circular finned pipe. The width and height of the front surface area of the heat exchanger is W=0.25 m, H=0.30 m, respectively. Heat exchanger length in the direction of air flow is L = 0.06 m. The pipe rows number, $N_{t,row} = 10$, the pipe column numbers, $N_{t,col} = 2$, the copper pipe conduction coefficient, $k_{bakır} = 400 \frac{W}{mK}$ are selected. Schematic representation of a fin heat exchanger is given in Figure 2.3.

Design parameters of surface types used in modeling of evaporator and condenser are given in Table 2.1 in detail.

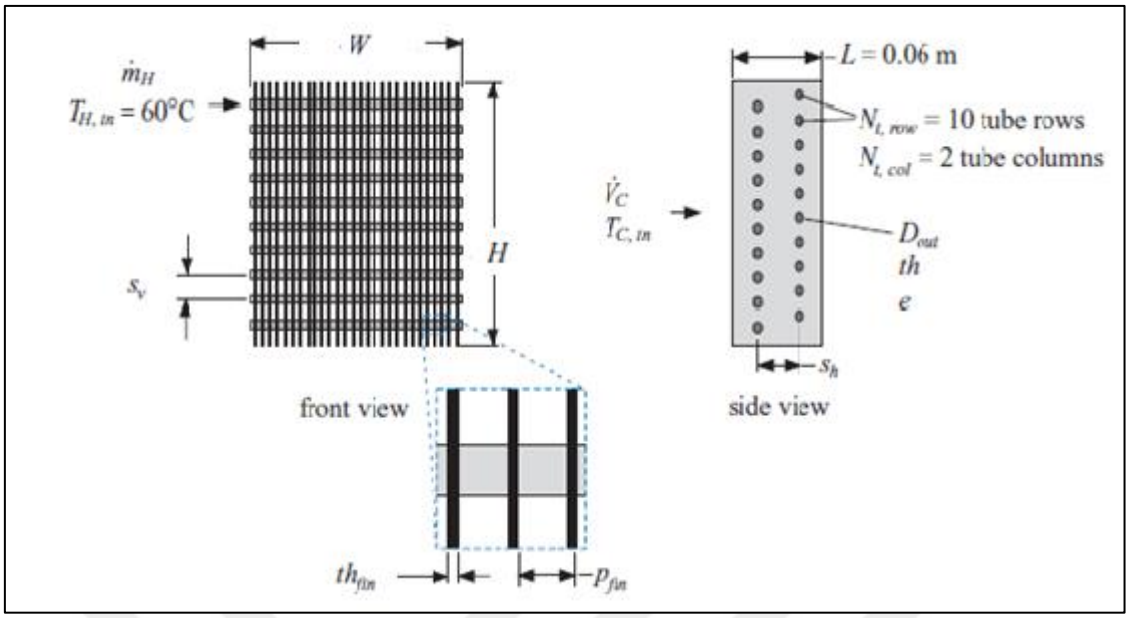

Figure 2.3. Schematic representation of a fin heat exchanger [37].

Table 2.1. Design parameters of surface types for a circular tube-continuous fin compact heat exchanger: 8.0-3/8T and CF-7.0-5/8J [38].

Surface Type	**8.0-3/8T**	**CF-7.0-5/8J**
Tube outside diameter, D_o (mm)	10.2	16.4
Tube wall thickness (mm)	0.9	0.9
Fin pitch (number/m)	315	275
Flow passage hydraulic diameter, D_h (mm)	3.63	6.68
Fin thickness, t (mm)	0.330	0.254
Free flow area/ frontal area, σ	0.534	0.449
Heat transfer area/total volume (m^2/m^3), α	587	269
Fin area/total area, A_f/A	0.913	0.83
Vertical gap between fins S_v (mm)	25.4	28.5
Horizontal gap between fins S_H (mm)	22.0	16.4
Fin efficiency η_f	0.89	0.89

2.2.1. Evaporator model

In this study, the evaporator is modeled as an air-cooled, counter-flow compact heat exchanger. The refrigerant in the evaporator is modeled as existing in two separate heat transfer regions: superheated and two-phase. The equations given in Table 2.2 utilized

into evaporator model to compute heat transfer rate between refrigerants and air. Average and an overall heat transfer coefficients are computed based upon the relevant area of the heat exchanger occupied by each region.

The following assumptions are used for modeling in the evaporator:

- Steady state operation.
- Flow is one dimensional.
- Air-side convective heat transfer coefficient is to be h_a= 100 W/m^{2}K [26].
- Negligible refrigerant pressure drops in the evaporator.
- Negligible heat loss from the evaporator.
- Constant the number of tubes and the length of the pipe
- State of refrigerant; superheated, two-phase.
- Constant fraction in each region; superheated (F=0.2), evaporation (F=0.8) [26].

The model is divided two different regions such as evaporation (two-phase) and superheated regions. Schematic view of these regions can be shown in Figure 2.4.

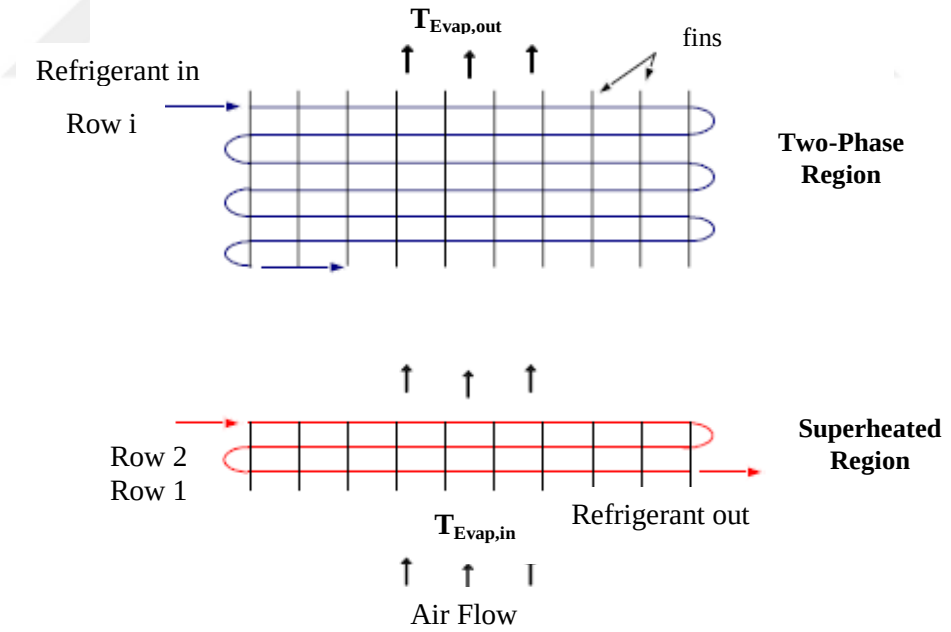

Figure 2.4. Schematic view of an evaporator: divided into superheated and evaporation regions.

The correlations used in modelling of refrigeration system are listed in Table 2.2.

The model outputs estimated by the mathematical model solution are as follows:

Calculations of the total heat transfer rate of evaporator:

$$\dot{Q_{tot,evap}} = \dot{Q}_{evap} + \dot{Q}_{evap,sh} \quad (2.3)$$

$$\dot{Q}_{evap} = \dot{m}_R \left(h_{R,evap,in} - h_{R,evap,out}\right) \quad (2.4)$$

$$\dot{Q}_{evap,sh} = \dot{m}_R \left(h_{R,evap,in} - h_{R,evap,out}\right) \quad (2.5)$$

Table 2.2. Correlations used in the condenser and evaporator model [26].

1) Refrigerant-side Heat Transfer Coefficient	
a) Superheated and Subcooling Region (one phase)	$Nu = 0{,}23 \times Re^{0.8} \times Pr^{0,3} \quad \bar{h}_{R,sc} = \frac{Nu \times k}{D_i}$ $h_{R,sat} = 0.023 \times [\frac{G_R \times (1-x) \times D_i}{\mu_F}]^{0.8} \times Pr^{0.4} \times (\frac{k_F}{D_i})$
b) Condensing Region (two-phase)	$\bar{h}_{R,two\ phase} = h_{R,sat} \times (0.55 + \frac{2.09}{Pr^{0.8}})$
2**) Refrigerant-side Heat Resistance**	
a) Superheated	$R_{R,sh} = \frac{1}{\bar{h}_{R,sh} \times \pi \times D_{in} \times L_{sh}}$
b) Two-phase	$R_{R,sat} = \frac{1}{\pi \times D_{in} \times L_{sat} \times \bar{h}_{R,sat}}$
c) Subcooling	$R_{R,sc} = \frac{1}{\bar{h}_{R,sc} \times \pi \times D_i \times L_{sc}}$
3) Air-side Heat Resistance	
a) Superheated	$R_{out,sh} = \frac{R_{out}}{F_{sh}}$
b) Two-phase	$R_{out,sat} = \frac{R_{out}}{F_{sat}}$
c) Subcooling	$R_{out,sc} = \frac{R_{out}}{F_{sc}}$
4) Refrigerant+Air-side Heat Resistance	
a) Superheated	$R_{sh} = R_{out,sh} + R_{R,sh}$
b) Two-phase	$R_{sat} = R_{out,sat} + R_{R,sat}$ $R_{sc} = R_{out,sc} + R_{R,sc}$
c) Subcooling	
5) Overall Heat Transfer Coefficient	
a) Superheated	$(U.A)_{sh} = \frac{1}{R_{sh}}$
b) Two-phase	$(U.A)_{sat} = \frac{1}{R_{sat}}$
c) Subcooling	$(U.A)_{sc} = \frac{1}{R_{sc}}$

Air outlet temperatures for two different regions of evaporator:

The outlet temperatures of air from two-phase regions and superheated of the evaporator can be computed using the mean logarithmic temperature difference method (LMTD) as in condenser.

$$T_{air,evap,out} = \frac{\dot{Q}_{evap}}{\dot{m}_{air} \times Cp_{air,evap} \times F_{evap}} + T_{air,evap,in} \quad (2.6)$$

$$T_{air,evap,out} = T_{air,evap,sh,out} \quad (2.7)$$

$$T_{air,evap,sh,out} = \frac{\dot{Q}_{evap,sh}}{\dot{m}_{air} \times Cp_{air,sh} \times F_{evap,sh}} + T_{air,sh,in,} \quad (2.8)$$

$$T_{air,evap,sh,out} = T_{air,evap,in} \quad (2.9)$$

Temperature distribution simulation along the evaporator can be seen in Figure 2.5.

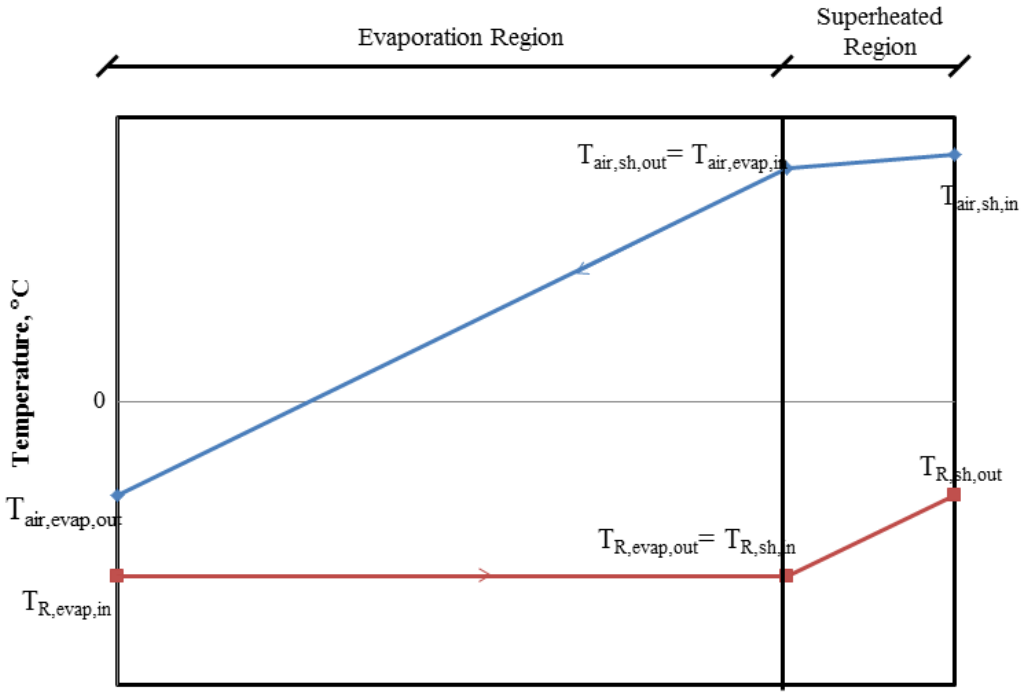

Figure 2.5. Temperature distributions along the evaporator

Operating parameters for different refrigerants and air side for the modelling of evaporator are given in Table 2.3. When evaporator capacity is kept constant at 1183 W, mass flow rate are calculated different for various refrigerants. When the refrigerant

inlet temperature of evaporator is kept constant at -18.8^{o}C, the refrigerant inlet pressures of evaporator are chosen 140 kPa for R134a, 320.5 kPa for R404A, 422.6 kPa for R410a, 258 kPa for R290 due to the physical properties of refrigerants. Air side inlet temperature, pressure and volume flow rate are determined 20^{o}C, 100 kPa and 0.01 m^3/s, respectively.

Table 2.3. Operating parameters used as input in the evaporator model

	Refrigerant-side				**Air-side**
	R134a	**R404a**	**R410a**	**R290**	
Inlet Temperature (^{o}C)	-18.8				20
Inlet Pressure (kPa)	140	320.5	422.6	258	100
Condensing Temperature (^{o}C)	~				
Mass Flow Rate (kg/s) $\dot{m}_{\mathbf{R}}$	0.0073	0.00854	0.00634	0.003875	-
Volume Flow rate (m^3/s) $\bar{V}_{air}$	-				0.01
Evaporator Capacity (W)	1183				

2.2.2. Compressor model

In this process, gas phase of the refrigerants is compressed by using the mechanical energy of a compressor and so pressure and temperature of the gas increases. Thus superheated vapor refrigerant at low pressure evaporator exit is compressed to the superheated vapor phase at high pressure and temperature at condenser inlet [34].

For the modelling of the compressor, following assumptions are considered [39].

- Constant volumetric and isentropic efficiencies.
- Negligible heat dissipation in compressor shell and refrigerant charge.
- It is assumed that the compression process is adiabatic.

Isentropic efficiency of the compressor is given as,

$$\eta_{is} = \frac{h_{2,is} - h_1}{h_2 - h_1} \tag{2.10}$$

Consumed compressor power is given as,

$$\dot{W} = \dot{m}_R (h_2 - h_1) \tag{2.11}$$

2.2.3. Condenser model

In this study, the condenser (compact heat exchanger) is modeled as an air-cooled, counter-flow heat exchanger like the evaporator model. In the proposed condenser model, there are three different heat transfer regions as superheated, condensing (two phase) and subcooling. The fractions of these regions and the temperature distribution vary depending on the flow and surface type of the fluids.

As the temperature of the refrigerant reduces to the saturation temperature at constant pressure, it condenses at the constant pressure and temperature in the condensation zone. The refrigerant leaves the subcooling zone at a lower temperature than the same pressure and condensing temperature.

To develop the mathematical model, assumptions can be listed as follows;

- Steady state operation.
- Flow is one dimensional.
- Air-side convective heat transfer coefficient is to be h_{air}= 100 W/m^{2}K.
- Negligible refrigerant pressure drops in the condenser.
- Negligible heat loss from the condenser.
- Constant the number of tubes and the length of the pipe
- State of refrigerant; superheated, two-phase and subcooling.
- Constant fraction in each region; superheated (F=0.2), condensing (F=0.7) and subcooling (F=0.1) The model is divided three different regions such as two-phase, subcooling and superheated regions. Schematic view of these regions can be shown in Figure 2.6.

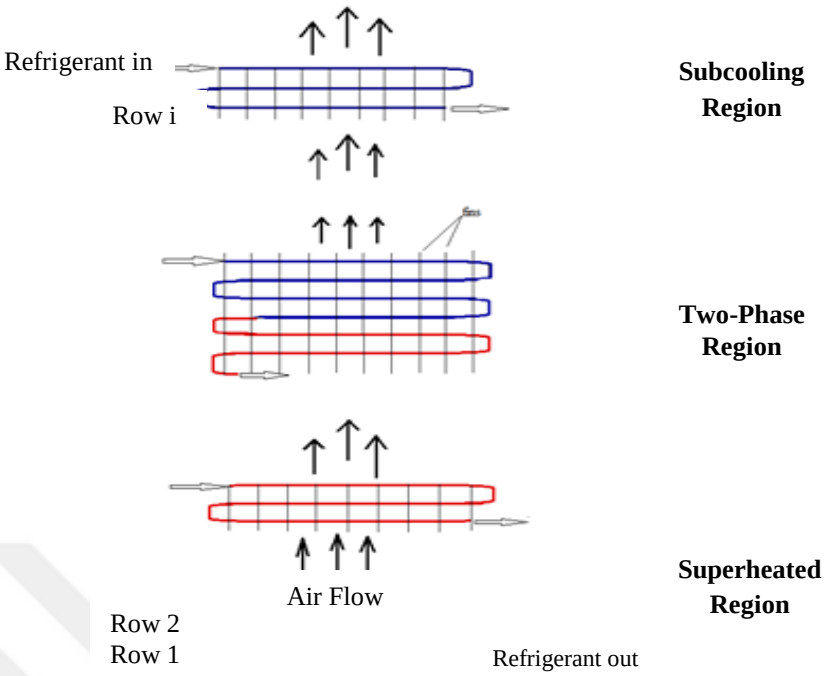

Figure 2.6. Schematic view of a condenser: divided into superheated, subcooling and condensation regions.

The model outputs for condenser estimated by the mathematical model solution are as follows:

Calculation of the total heat transfer rate:

Heat transfer from condenser to air in three different regions:

$$\dot{Q} = \dot{Q}_{cond,sh} + \dot{Q}_{cond} + \dot{Q}_{cond,sc} \quad (2.12)$$

$$\dot{Q}_{cond,sh} = \dot{m}_R \left(h_{R,cond,sh,in} - h_{R,cond,sh,out}\right) \quad (2.13)$$

$$\dot{Q}_{cond} = \dot{m}_R \left(h_{R,cond,out} - h_{R,cond,in}\right) \quad (2.14)$$

$$\dot{Q}_{cond,sc} = \dot{m}_R \times Cp_{R,sc} \times \left(T_{R,cond,sc,in} - T_{R,cond,sc,out}\right) \quad (2.15)$$

Air outlet temperature for three different regions of condenser:

The air outlet temperatures from subcooling, condensation (two phase) and superheated regions of the condenser can be computed using the mean logarithmic temperature

difference method (LMTD). Air outlet temperatures from condensation, superheated and subcooling regions are calculated by following equations;

$$T_{air,cond,sh,out} = \frac{\dot{Q}_{cond,sh}}{\dot{m}_{air} \times Cp_{air,sh} \times F_{cond,sh}} + T_{air,cond,sh,in} \quad (2.16)$$

$$T_{air,cond.,out} = T_{air,cond.,sh,in} \quad (2.17)$$

$$T_{air,cond.,out} = \frac{\dot{Q}_{cond.}}{\dot{m}_{air} \times Cp_{air,cond.} \times F_{cond.}} + T_{air,cond.,in} \quad (2.18)$$

$$T_{air,cond,sc,out} = T_{air,cond,in} \quad (2.19)$$

$$T_{air,cond,sc,out} = \frac{\dot{Q}_{cond,sc}}{\dot{m}_{air} \times Cp_{air,sc} \times F_{cond,sc}} + T_{air,cond,sc,in} \quad (2.20)$$

Temperature distribution simulation along the evaporator can be observed in Figure 2.7.

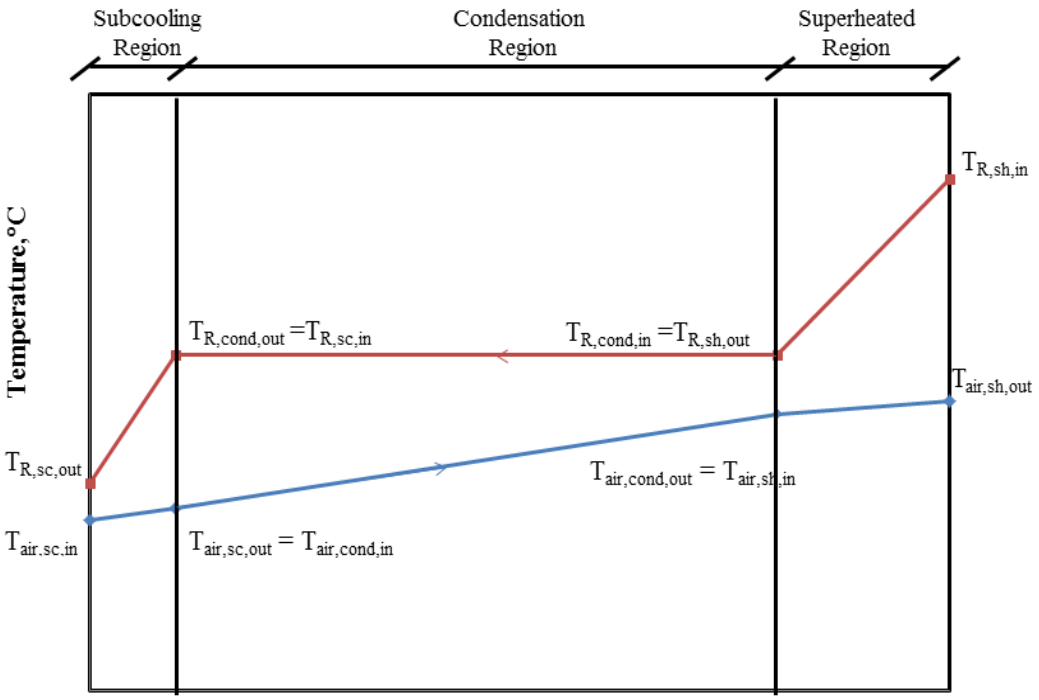

Figure 2.7. Temperature distribution simulation of refrigerant and air along the condenser

Air-side pressure drop of the condenser:

Condenser pressure drop of air-side (ΔP_{air}) is calculated using equation developed by Kays and London, where the overall friction coefficient (f) is used [38].

$$\Delta P_{air}=\frac{G_{max}^2}{2\rho_a}\left[(1+\sigma^2)\left(\frac{\rho_{a,i}}{\rho_{a,o}}-1\right)+f\frac{A_{total}}{A_f}\left(\frac{\rho_{a,i}}{\rho_{a,i}+\rho_{a,o}}\right)\right] \quad (2.21)$$

Overall friction factor in above equation can be calculated by using equation below:

$$f = \int_f \left(\frac{A_f}{A_{total}}\right) + \int_t \left(1-\frac{A_f}{A_{total}}\right)\left(1-\frac{t_f}{S_F}\right) \quad (2.22)$$

The contribution of the fin and the tubes to the frictional factor of a finned tube compact heat exchanger modeled is calculated using equation (2.23) and (2.24) [26].

$$\int_f = 1.435 Re_D^{-0.562}\left(\frac{S_V}{S_H}\right)^{-0.365}+\left(\frac{S_F}{D_o}\right)^{-0.131}\left(\frac{S_V}{D_o}\right)^{1.22} \quad (2.23)$$

$$\int_t = \frac{4}{\pi}\left(0.25+\frac{0.118}{(S_V/D_o-1)^{1.08}}Re_D^{-0.16}\right)\left(\frac{S_T}{D_o}-1\right) \quad (2.24)$$

Consumed power of the condenser fan of refrigeration cycle:

Consumed power of the condenser fan ($\dot{W}$) is computed by using following equation:

$$\dot{W} = \Delta P_{air} \times \dot{V} \quad (2.25)$$

Operating parameters for different refrigerants and air side for the modelling of condenser are given in Table 2.4. When evaporator capacity is kept constant at 1183 W, condenser capacity is calculated for various refrigerants. These calculation results can be seen in Chapter 4, in Table 3.2. When the refrigerant inlet temperature of condenser is kept constant at 60^{o}C, the refrigerant inlet pressures of condenser are chosen 1000 kPa for R134a, 1800 kPa for R404A, 2400kPa for R410A, 1350 kPa for R290 because of the physical properties of refrigerants. Condensation temperature is kept constant at 40^{o}C for various refrigerants. Air side inlet temperature, pressure and volume flow rate are determined 20^{o}C, 100kPa and 0.095m^3/s, respectively. In addition, the refrigerant's mass flow rates are constant for the condenser component of the refrigeration cycle.

Table 2.4. Operating parameters used as input in condenser design

	Refrigerant-side				Air-side
	R134a	**R404a**	**R410a**	**R290**	
Inlet Temperature (^{o}C)	60				20
Inlet Pressure (kPa)	1000	1800	2400	1350	100
Condensing Temperature (^{o}C)	~ 40				
Mass Flow Rate (kg/s) $\dot{m}_{\mathbf{R}}$	0.0073	0.00710	0.00525	0.00345	-
Volume Flow rate (m^3/s) $\bar{V}_{air}$	-				0.095
Air Velocity (m/s)					0.5

2.2.4. Expansion valve model

The expansion valve is an ingredient in the refrigeration system that controls the amount of fluid released into the evaporator. It can be modelled as a fixed orifice, thermostatic expansion valve and capillary tube [34]. When it is modeled as a fixed orifice, following assumptions can be considered:

- Flow is one dimensional
- Gravity force and refrigerant side can be neglected,
- Flow coefficient can be considered as constant,
- Constant enthalpy is considered for expansion process. ($h_3 = h_4$)

Thus, mass flow rate in the orifice is defined as:

$$\dot{m}_e = C_e d_i^2 \sqrt{\rho_R (P_{cond} - P_{evap})} \tag{2.26}$$

where C_e is the mass flow factor depending on orifice geometry and (d_i) is the inner tube diameter.

2.2.5. Overall cycle model

The overall model is comprised of sub models for each ingredient of the system. The main ingredient models contain:

- Evaporator and condenser: detailed compact heat exchanger of which pipe type is circular finned.
- Expansion valve
- Compressor

An overview of relations in the vapor compression refrigeration cycle is indicated in Figure 2.8.

The coefficient of performance (COP) is computed by using;

$$COP = \frac{\dot{Q}_{tot,evap}}{\dot{W}_{comp}} = \frac{\dot{Q}_{tot,evap}}{\dot{Q}_{tot,cond} - \dot{Q}_{tot,evap}} \quad (2.27)$$

2.3. Engineering Equation Solver (EES) Software

Engineering Equation Solver (EES) is a commercial software program. This used for systems solution of non-linear equations. It ensures several practical privatized functions and equations in order to use solution of heat transfer and thermodynamics problems, thus these properties present a useful and widely used program for mechanical engineers working in these areas. In this software package, there are many thermodynamic properties. This feature of EES makes a lot easier. For example you can use different codes that call properties at the specified thermodynamic properties and so this eliminates iterative problem solving by hand through. EES also involves parametric tables that allow the user to analogies some variables at a time. Parametric tables can also be used to draw graphs.

Some basic properties of EES software are listed in below:

- High accuracy thermodynamic and transport functions for fluids.
- Unit conversion and automatic unit consistency checking
- Parametric studies with parametric tables
- Plotting (2-D) with automatic updating
- Graphical user input/output capabilities with Diagram window
- Heat transfer library functions for conduction, convection, and radiation [40].

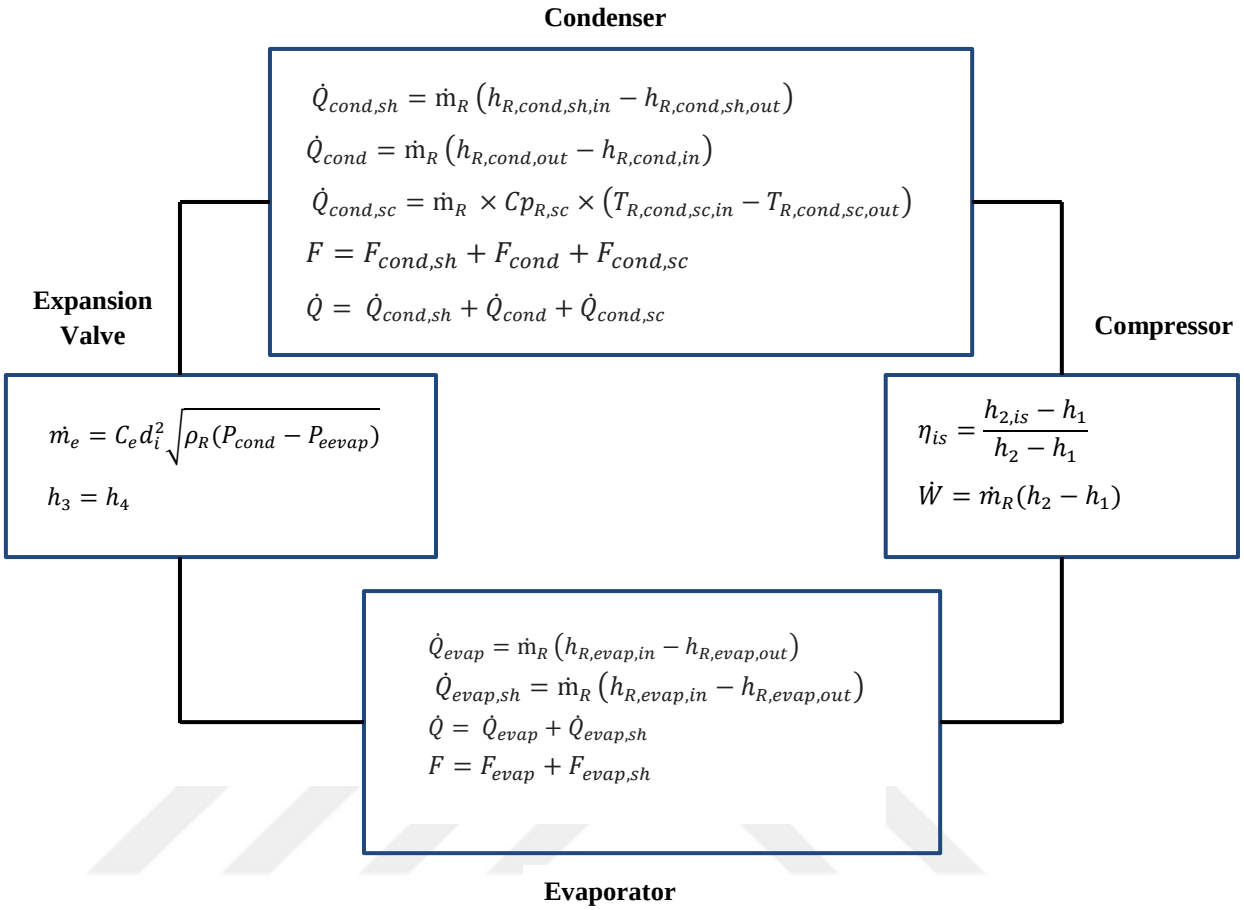

Figure 2.8. Overview of relations in vapor compression refrigeration cycle

2.4. Thermo Physical Properties of Refrigerants Used in the Model

In order to consider the trace of refrigerants on the environment, two main parameters (GWP and ODP) are used. One kg of R404A has a GWP of 3800, one kg of R134A has a GWP of 1370, one kg of R410a has a GWP of 1980 and one kg of R290 has a GWP of 20. Also, ODP value of R404A, R134a, R410a and R290 is zero [40].These values indicated that right choice of environmentally friendly refrigerant is very important to decrease the detrimental influences of them on the environment. Table 2.5 shows the properties of refrigerants examined in the present study.

In this study, one natural and three synthetic refrigerants have been examined. Among the refrigerants used, propane (R290) is natural refrigerant which has great thermodynamic properties. It is also to find easy and cost effective. The main advantage

of choosing propane as the refrigerant is that propane is non-toxic. However, safety design conditions must be provided due to the high flammability property of propone. In addition, R290 can be used for low temperature applications at -35^{o}C.

These three refrigerants, R404A, R134a and R410a, are selected as synthetic refrigerants because they are widely used in industrial refrigeration applications. Especially, R134a is more favorable for industrial refrigeration areas because it has outstanding thermo-physical characteristics and thermal stability. It is both non-flammable and nontoxic so it can be seen as a long-term replacement for the refrigerant CFC. But, because of high GWP values of these synthetic refrigerants, they would be completely phased out by 2020 in growing countries (Montreal Protocol) and its amendments from the United Nations Environment Program (UNEP, 1987).

Table 2.5. Thermo-physical and environmental properties of refrigerants used in model [41].

	R410a	**R134a**	**R404A**	**R290**
Classification of refrigerants	HFC	HFC	HFC	HC
Critical Temperature (^{o}C)	70.2	101.1	72	96.7
Critical Pressure (MPa)	4.77	4.05	3.731	4.25
ODP	0	0	0	0
GWP	1980	1370	3700	~20

3. RESULTS AND DISCUSSION

This study presented a mathematical model for refrigeration system components such as condenser, evaporator based on various empirical correlations of heat transfer coefficients in order to simulate the performance of system using four different

refrigerants. The improved model is able to predict inlet and outlet temperatures of air of evaporator for two regions ($T_{air,evap,in}$, $T_{air,evap,out}$), inlet and outlet temperatures of air of condenser for three regions ($T_{air,cond.,in}$, $T_{air,cond.,out}$). The developed model of condenser with two different surface types (8.03/8T and CF-7.0-5/8J) enables to calculate the pressure drop of the air (ΔP_{air}). Calculation of the pressure drop is used to determine the consumed power of condenser fan ($\dot{W}$). The modeling of overall refrigeration system results in calculation of coefficient of performance (COP) of system for different refrigerants and two various surface types.

3.1. Evaporator Simulation Results

Heat transfer rate for evaporator is kept constant of around 1183 W for different refrigerants (R134a, R404a, R410A and R290) and different surface types (8.03/8T and CF7.05). In addition the vapor quality of the refrigerant is assumed to be x=0.5. In this case, the convection coefficients and the overall heat transfer coefficients of various regions such as superheated, evaporation are calculated by using the modelling equations in Table 2.2. Mass flux values are calculated for different refrigerants and surface types. The calculated from the simulated model results can be seen in Table 3.1 in detail.

As can be seen in Table 3.1, the total surface area of type 8.03/8T and the total surface area of type CF-7.0-5/8J are calculated 2.717 m^2 and 2.40 m^2, respectively. For both surface types, the convection coefficient of superheated zone was found to be smaller than the convection coefficient of evaporation zone for all refrigerants. It has been seen that these results are consistent with the experimental values in the literature [36]. It is found that while the overall heat transfer surface area increases, the overall heat transfer coefficient values decreases for all refrigerants.

Table 3.1. Evaporator model results for different surface types and refrigerants

	Surface Type	Overall Surface Area (m^2)		Convection Coefficient (W/m^2K)		Overall Heat Transfer Coefficient (W/m^2K)		Mass Flux (kg/m^2s) (x=0.5)	Heat Transfer rate (W)	
		$A_{evap,sh}$	A_{evap}	$h_{evap,sh}$	h_{evap}	$U_{evap,sh}$	U_{evap}	G_{evap}	$Q_{evap,sh}$	Q_{evap}
R134a	**8.03/8T**	0.5434	2.173	41.6	369.4	1.976	14.95	**103.7**	50.93	1129
		2.717		**411**		**16.93**			**1180**	
	CF7.05	0.4806	1.922	24	218	2.234	16.9	**61.6**	50.93	1129
		2.40		**242**		**19.13**			**1180**	
R290	**8.03/8T**	0.5434	2.173	43.76	369.3	2.076	14.95	**50.42**	53.6	1129
		2.717		**413.1**		**17.03**			**1182**	
	CF7.05	0.4806	1.922	25.25	217.9	2.347	16.9	**29.94**	53.6	1129
		2.40		**243.2**		**19.25**			**1182**	
R404a	**8.03/8T**	0.5434	2.173	52.73	368	2.49	14.9	**102.1**	62.93	1120
		2.717		**420.6**		**17.4**			**1183**	
	CF7.05	0.4806	1.922	30.44	217.1	2.815	16.85	**60.62**	62.93	1120
		2.40		**247.5**		**19.67**			**1183**	
R410a	**8.03/8T**	0.5434	2.173	43.07	369.9	2.044	14.96	**105.5**	51.09	1132
		2.717		**413**		**17.01**			**1183**	
	CF7.05	0.4806	1.922	24.85	218.2	2.311	16.92	**62.65**	51.09	1132
		2.40		**243.1**		**19.23**			**1183**	

The calculated mass flux value varies depending on both the surface type and the refrigerant type. In addition, the calculated mass flux for type 8.03/8T is greater than the calculated mass flux for type CF-7.0-5/8J for the each refrigerant type. The results also show that the greatest mass flux is obtained for the R410a and the lowest mass flux for the R290 for both surface types.

Both the convection coefficient and the overall heat transfer coefficient of natural refrigerant (R290) were found to be approximately same as those of other refrigerants. However, the calculated mass flow rate (0.003875 kg/s) of R290 is considerably small compared with other refrigerants. Therefore, the natural refrigerant R290 may be suggested to the synthetic refrigerants (R134a, R410a and R404a) in refrigeration applications.

As can be seen in Table 3.1, convection coefficients for all refrigerants are found to be 369 W/m^{2}K for type 8.0-3/8T and 218 W/m^{2}K for type CF-7.0-5/8J for vapor quality of 0.5. The inlet and outlet temperatures of air in two different regions such as evaporation and superheated of evaporator are computed by using the modeling equations in Section 2.2. Calculated results can be seen in Figure 3.1.

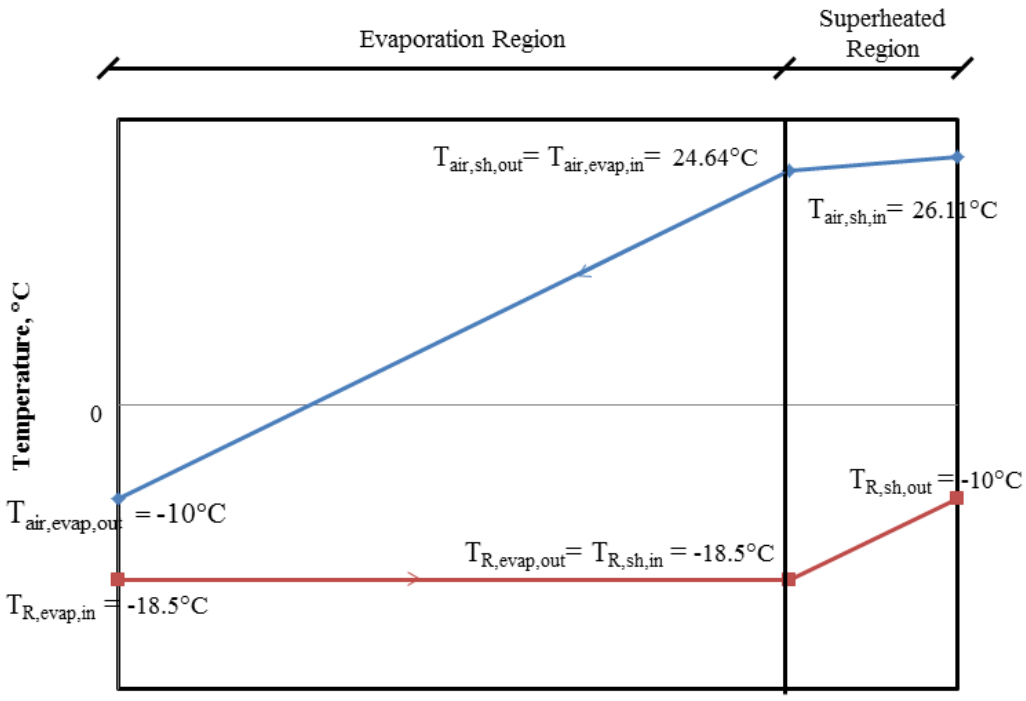

Figure 3.1. Simulation results of evaporator for the inlet and outlet conditions of air and refrigerants

3.1.1. Mathematical modeling results related with mass flux-heat transfer coefficient for different refrigerants

In Figures 3.2 and 3.3, the effect of different mass flux on the heat transfer coefficient of evaporation region is compared for various refrigerants R134a, R290, R404a and R410a. In this case, the heat transfer rate as1183 W and the vapor quality as 0.5 are assumed to be constant. Mass flux values range given as inputs to the model equations change from 50 to 500 kg/m^{2}s.

The results obtained for the surface type 8.0-3/8T are shown in Figure 3.2. It has been observed that the highest convection coefficients are calculated for the natural refrigerant (R290) at all mass flux values. The convection coefficient values of R290 are computed between 350-2350 W/m^2.K.

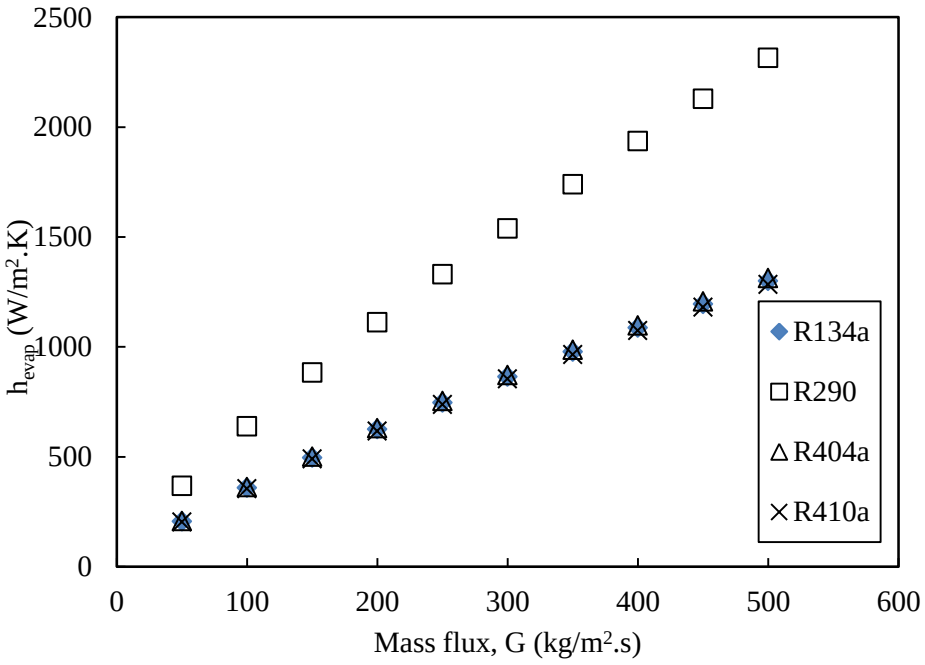

Figure 3.2. Influence of mass flux on the convection coefficient for different refrigerants (Type: 8.0-3/8T)

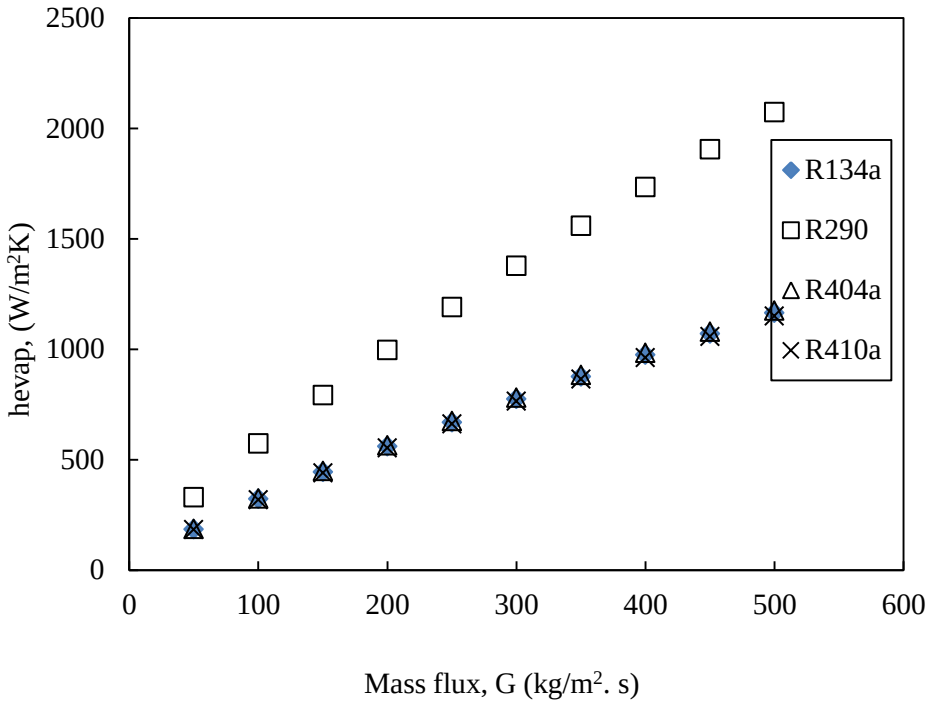

Figure 3.3. Influence of mass flux on the convection coefficient for different refrigerants (Type: CF-7.0-5/8J)

The convection coefficient values of the synthetic refrigerants (R134a, R404a, R410a) used in the system are calculated close the each other for the mass fluxes varying in the same range. Convection coefficient values for these refrigerants are found from 200 to 1250 W/m^2.K.

Figure 3.3 shows the calculation results for the type CF-7.0-5/8J. As can be clearly seen in Figure 3.3, the convection coefficients values against to mass flux variation of type CF-7.0-5/8J showed similar behavior as those of type 8.0-3/8T for different refrigerants. The convection coefficient values of R290 change between 270-2050 W/m^2.K while these values of R134a, R404a, R410a change between 125-1100 W/ m^2.K.

3.1.2. Mathematical modeling results related with mass flux-heat transfer coefficient for various surface types

In order to see the influence of the mass flux on the convection coefficient in the evaporation region for different surface types, the calculated values according to the improved model are plotted for each refrigerant in Figures 3-4 -3.7.

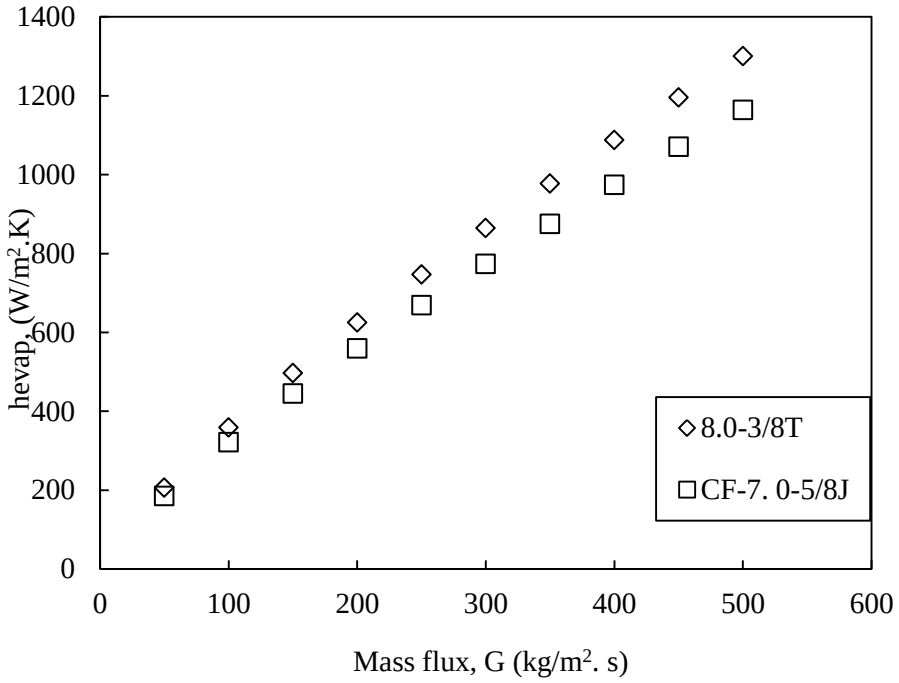

Figure 3.4. Effect of mass flux on the convection coefficient for R134a at different surface types

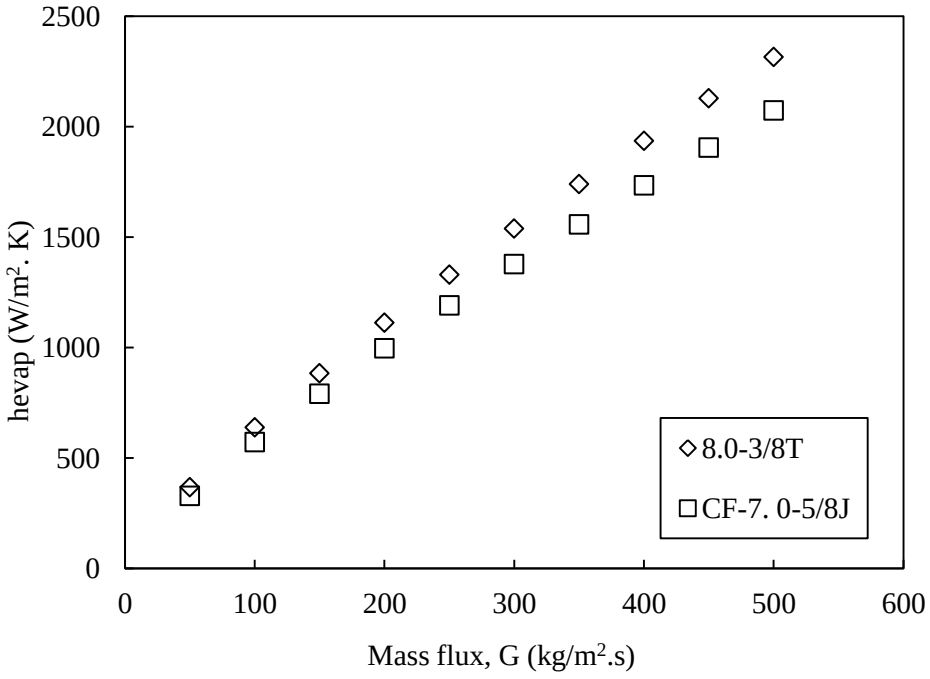

Figure 3.5. Effect of mass flux on the convection coefficient for R290 at different surface types

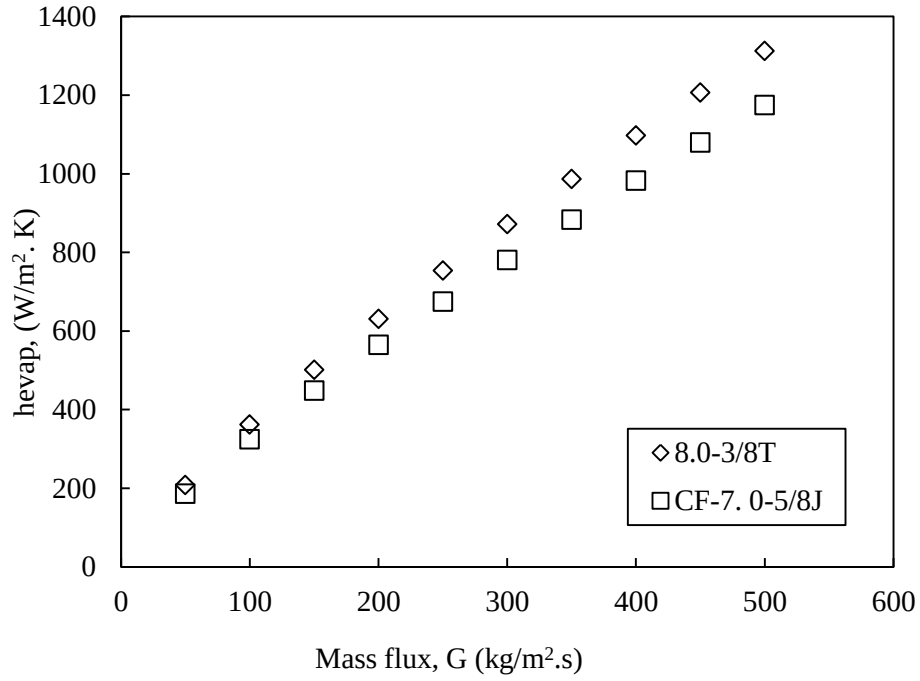

Figure 3.6. Effect of mass flux on the convection coefficient for R404a at different surface types

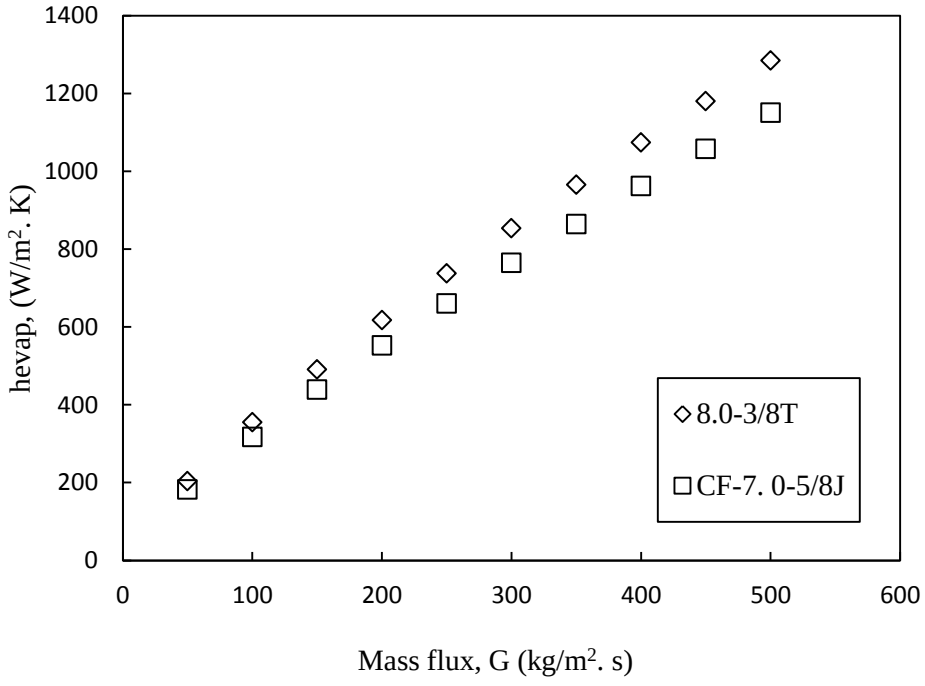

Figure 3.7. Effect of mass flux on the convection coefficient for R410a at different surface types

In literature [36], the design parameter $\propto$ of compact heat exchanger used as a condenser is described as the heat transfer surface area per total heat exchanger volume in this study. As can be seen in Table 2.1, $\propto$ values are given 587 m^2/m^3 and 269 m^2/m^3 for type 8.0-3 / 8T and type CF-7.0-5/8J, respectively. In addition, fin pitch of type 8.0-3/8T and fin pitch of type CF-7.0-5/8J are 315/meter and 275/meter, respectively.

In Figures 3.4 to 3.7, the calculated convection coefficient values of type 8.0-3/8T are higher than the calculated convection coefficient values of type CF-7.0-5/8J at the mass fluxes values between 50 and 500 kg/m^2s. As it is known, the large value of the convection coefficient requires that the large value of $\propto$ and fin pitch. Therefore, the calculated convection coefficient values of type 8.0-3/8T are higher than calculated the convection coefficient values of type CF-7.0-5/8J.

3.1.3. Mathematical modeling results related with vapor quality-mass flux for different refrigerants and surface types

In Figures 3.8 and 3.9, the effect of vapor quality on the mass flux in evaporation region for different refrigerants can be observed. In this case, the total heat transfer rate (1183 W) is kept constant. The vapor quality of liquid phase and vapor phase are 0 and 1, respectively. The mass flux calculations were done for vapor quality changing between 0.1 and 0.9.

As presented in Figure 3.8 and Figure 3.9, the change in mass flux versus vapor quality shows similar behavior for all refrigerants. While mass flux significantly decreases up to vapor quality of 0.3, slightly decreasing is observed between vapor quality of 0.3 and 0.9. This is an expected result. This is because the mass flux required to draw the same heat away from the liquid phase to the refrigerant fluid that is converted to the gas phase will decrease.

Natural refrigerant R290 has lower mass flux values than other synthetic refrigerants for the same vapor quality. In order to clearly see the effect of vapor quality on the mass flux in different surface types, the results obtained are shown in Figures 3.10 and 3.11 for only two refrigerants (R290 and R134a).

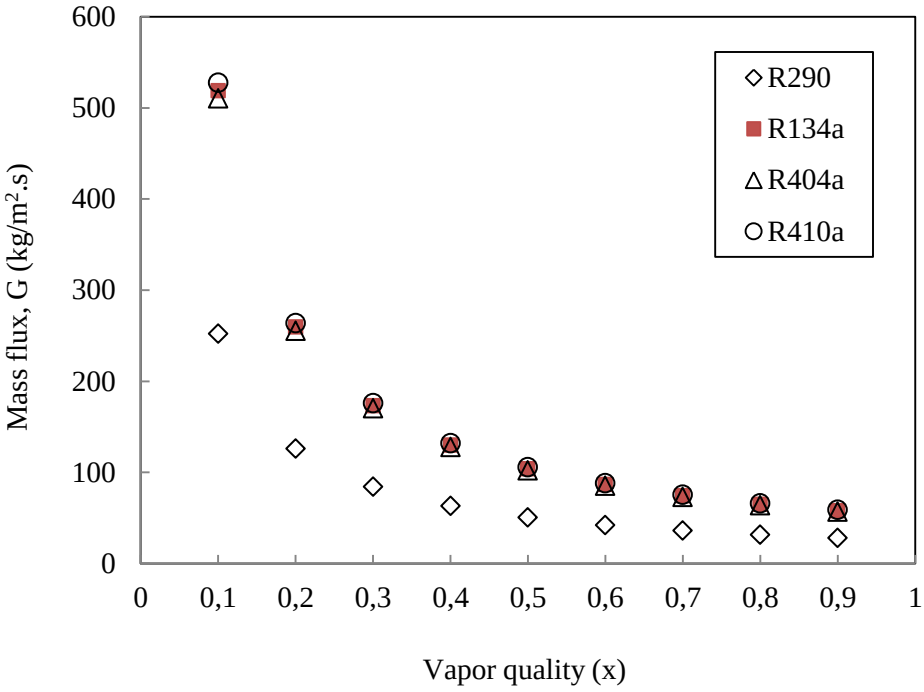

Figure 3.8. Influence of vapor quality on the mass flux for different refrigerants (Type: 8.0-3/8T)

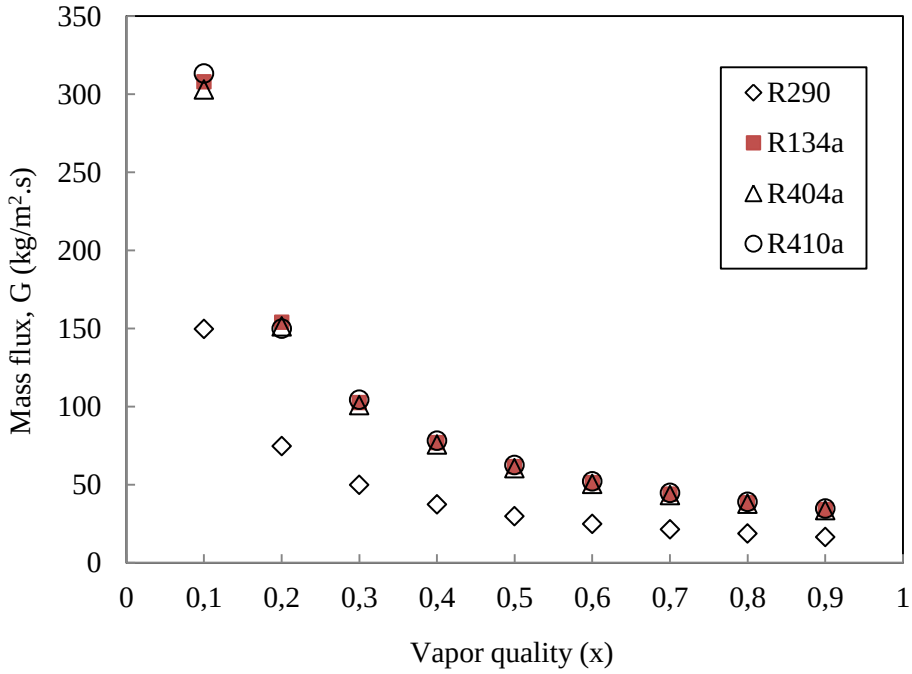

Figure 3.9. Influence of vapor quality on the mass flux for different refrigerants (Type: CF-7.0-5/8J)

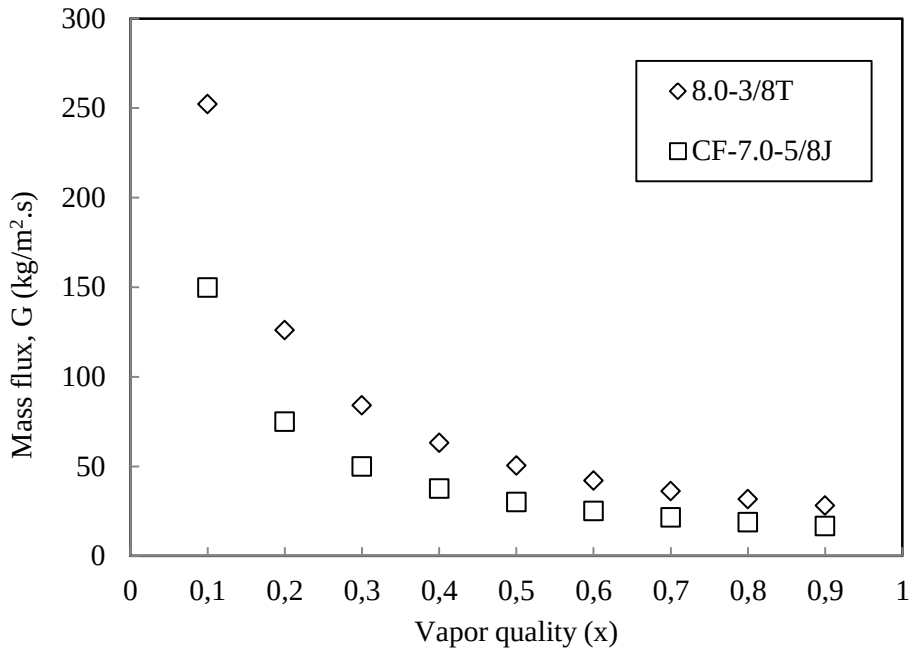

Figure 3.10. Influence of vapor quality on the mass flux for R290 at different surface types

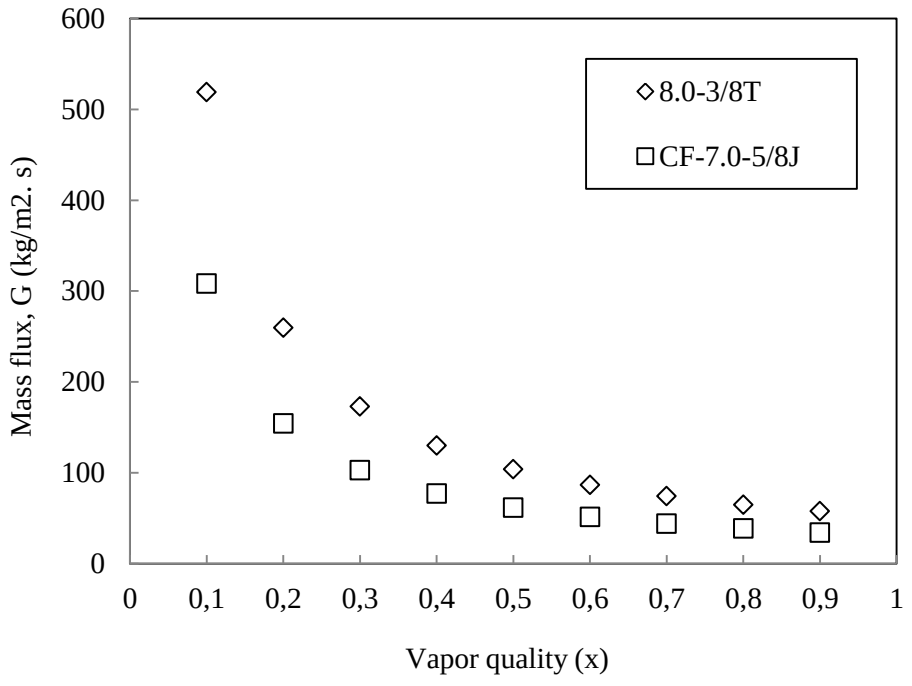

Figure 3.11. Influence of vapor quality on the mass flux for R134a at different surface types

As can be seen in Figure 3.10 and 3.11, calculated mass flux values corresponding to varying vapor quality for both refrigerants are found to be greater for type 8.0-3/8T than those of type CF-7. 0-5/8J. This result implies that for all vapor qualities values for a constant heat transfer rate (1183W), type 8.0-3/8T must have higher mass flux values. This result is inevitable because $\propto$ value of type 8.0-3/8T is higher than type CF-7.0-5/8J.

3.2. Condenser Simulation Results

Simulation results of the condenser model for different surface types and refrigerants were given in Table 3.2. As can be shown from Table 3.2, for both investigated surface types, heat transfer rates are calculated 1514 W, 1527 W, 1439 W and 1372 W for R134a, R290, R404a and R410A, respectively. In this case, the convection and the overall heat transfer coefficients of various regions such as superheated, condensation and subcooling are calculated by using the modelling equations in Table 2.2.

As seen in Table 3.2, the total surface area of type 8.03/8T is 2.717 m^2, the total surface area of type CF-7. 0-5/8J is 2.40 m^2. Considering all refrigerants, the lowest convective heat transfer coefficient is calculated at superheated regions for both surface types. In literature, it has been reported that the highest convective heat transfer coefficient should be in the subcooling region because the refrigerant is in liquid phase. According to the condenser simulation results, the highest convective heat transfer coefficients are calculated in the subcooling region for R404a and R410a. These results are consistent with the literature. However, for R290 and R134a, the convective heat transfer coefficients of subcooling region are calculated lower than the convective heat transfer coefficients of superheating region. In R134a and natural refrigerant R290 refrigerants, the convective heat transfer coefficients calculated for evaporation and subcooling regions are found to be very close to each other.

Table 3.2 also shows that the surface type having different surface areas is effective on the overall heat transfer coefficient. According to the calculated results, the overall heat transfer coefficient decreases with increasing the surface area for each refrigerant.

Table 3.2. Results of the condenser model for different surface types and refrigerant

	Surface Type	Overall Surface Area (m^2)			Convection Coefficient (W/m^2K)			Overall Heat Transfer Coefficient (W/m^2K)			Mass Flux (kg/m^2s)	Heat Transfer Rate (W)		
		$A_{cond,sh}$	A_{cond}	$A_{cond,sc}$	$h_{cond,sh}$	h_{cond}	$h_{cond,sc}$	$U_{cond,sh}$	U_{cond}	$U_{cond,sc}$	G	$Q_{cond,sh}$	Q_{cond}	$Q_{cond,sc}$
R134a	**8.03/8T**	0,5434	1,902	0,2717	564,1	3838	3652	20,98	60,5	59,52	**1364**	163,5	1195	155,3
		2,717			**8054**			**141**				**1514**		
	CF7.05	0,4806	1,682	0,2403	337,4	2978	2787	23,72	68,41	67,29	**1141**	163,5	1195	155,3
		2,403			**6103**			**159,4**				**1514**		
R290	**8.03/8T**	0,5434	1,902	0,2717	625.8	3924	3837	22.69	60.94	60.5	**720.4**	176.4	1193	157.9
		2,717			**8387**			**144.1**				**1527**		
	CF7.05	0,4806	1,682	0,2403	375.9	3070	2977	25.66	68.9	68.4	**608.4**	176.4	1193	157.9
		2,403			**6323**			**163**				**1527**		
R404a	**8.03/8T**	0,5434	1,902	0,2717	731.3	2237	7294	25.43	49.1	71.5	**674.6**	217.1	1032	189.8
		2,717			**10262**			**146**				**1439**		
	CF7.05	0,4806	1,682	0,2403	442.6	1515	8254	28.76	55.51	80.84	**476.1**	217.1	1032	189.8
		2,403			**10212**			**165.1**				**1439**		
R410a	**8.03/8T**	0,5434	1,902	0,2717	594	1879	3345	21.82	45.2	57.74	**543.9**	194.6	1019	159
		2,717			**5817**			**124.8**				**1372**		
	CF7.05	0,4806	1,682	0,2403	356	1237	2484	24.67	51.1	65.28	**370.6**	194.6	1019	159
		2,403			**4078**			**141.1**				**1372**		

Calculated inlet and outlet temperatures of air and refrigerants in three different regions are given in Figure 3.12.

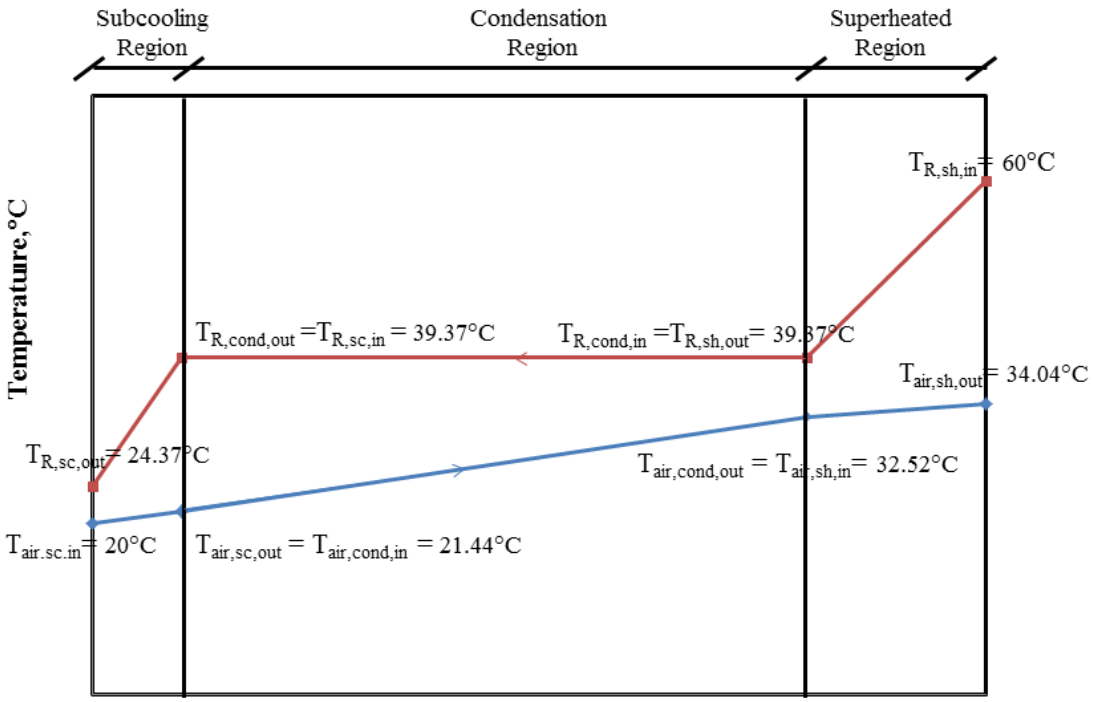

Figure 3.12. Simulation results of condenser for the inlet and outlet conditions of air and refrigerants

Inlet and outlet temperatures and pressures of refrigerants to the condenser superheated, saturation and subcooling regions are known. The inlet temperature to the subcooling region of the air blown to the condenser surface by a fan was assumed to be 20°C. The outlet air temperatures of the subcooling, condensing and superheated regions were calculated using the mean logarithmic temperature difference method (LMTD). According to the improved model, the air outlet temperatures of the subcooling region, the condensation region and the superheated region are found to be 21.44°C, 32.52 °C and 34.04 °C, respectively.

3.2.1. Mathematical modeling results related with vapor quality- mass flux for different refrigerants and surface types

As can be seen in Table 3.2, the heat transfer rates rejected to environment of R134a, R290, R404a and R410a are calculated to be 1514 W, 1527 W, 1439 W and 1372 W

respectively. In addition, the heat transfer rate of each refrigerant is found to be same for both surface types.

As shown in Figure 3.13 and Figure 3.14, the change in mass flux versus vapor quality shows similar behavior for all refrigerants. While there is a significant decrease in the mass flux value up to the vapor quality of 0.5, with increasing vapor quality after than 0.5, the mass flux slightly decreases. As it is known vapor quality is defined as the mass fraction of the vapor in a two-phase (liquid-vapor) region. Thus, the mass flux required to remove the same heat is expected to be less in the gas phase in where vapor quality is high. As seen in Figures 3.13 and 3.14, for both surface types, the natural refrigerant R290 behaves similarly to the synthetic refrigerants R404a and R410a in the condensation region. However, other synthetic refrigerant R134a has the highest mass flux during the condensation process compared to other refrigerants.

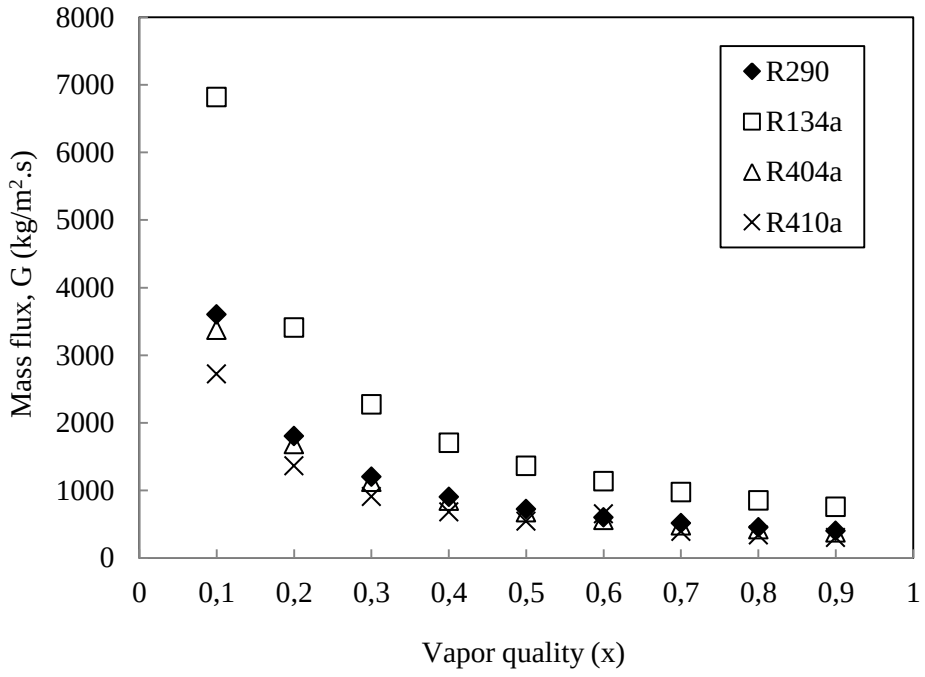

Figure 3.13. Effect of vapor quality on the mass flux for different refrigerants

(Type: 8.0-3/8T)

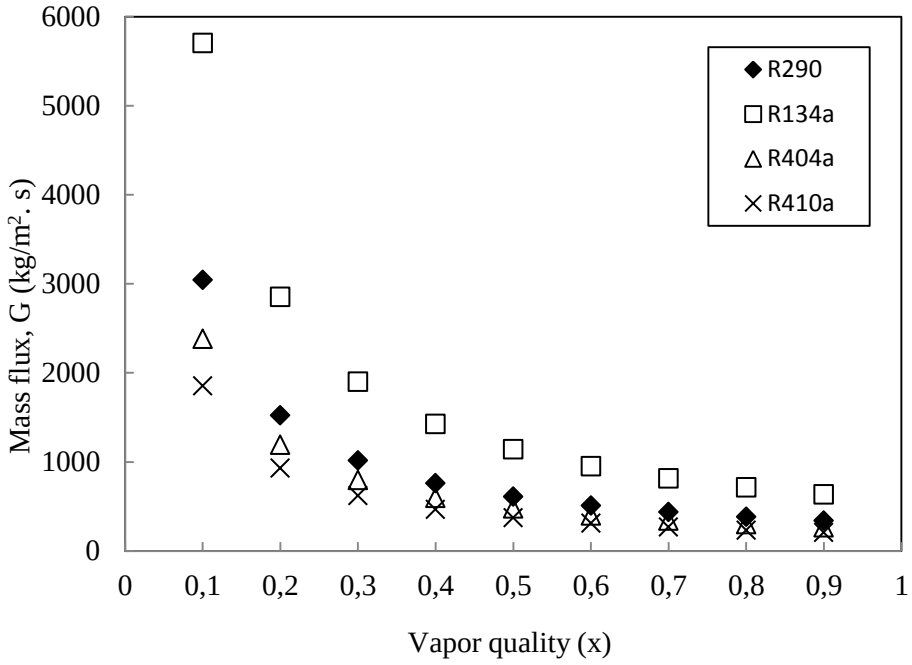

Figure 3.14. Effect of vapor quality on the mass flux for different refrigerants

(Type: CF-7.0-5/8J)

In order to see the effect of surface type on the relationship between vapor quality and mass flux, calculated results are replotted for R290 and R134a in Figures 3.15 and 3.16.

Figures 3.15 and 3.16 show that for type 8.0-3/8T the calculated mass flux values versus vapor quality are found higher than those of type CF-7.0-5/8J up to vapor quality of 0.3. However, at high vapor quality, it is observed that the variation of the mass flux versus vapor quality is independent from the surface type. It has been determined that the effect of the surface type increases in liquid phase in where the vapor quality changes from 0.1 to 0.3. As mentioned before this result is inevitable because $\propto$ value of type 8.0-3/8T is higher than type CF-7. 0-5/8J.

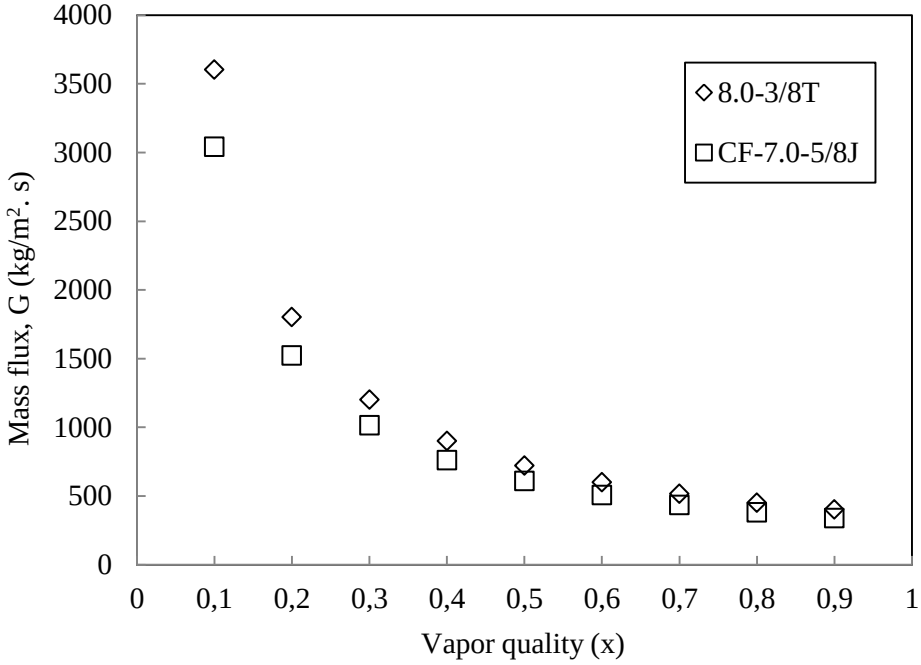

Figure 3.15. Influence of vapor quality on the mass flux for R290 at different surface types

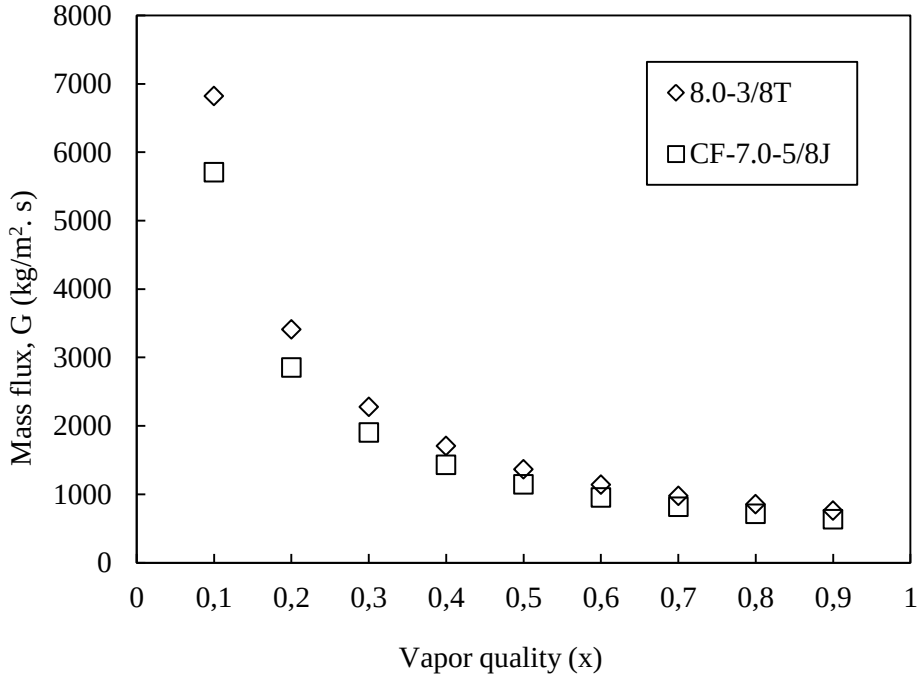

Figure 3.16 Influence of vapor quality on the mass flux for R134a at different surface types

3.2.2. Mathematical modeling results related with air velocity-fan power for various surface types

Figure 3.17 shows the effect of the air velocity change on fan power for both surface types examined. As can be clearly seen from Figure 3.17, the fan power slightly decreases with the increasing of air velocity in the range of 0.25 and 2.5 m/s in two surface types. As the air velocity increases, the Reynolds number increases thus the air flow becomes more turbulent. Decreasing of the friction coefficient between air and condenser outside surface as a result of transition of air flow from the laminar to the turbulence causes decrease of consumed fan power. As known, because the resistance force depends on the surface area, the velocity and the viscosity of the fluid, the consumed fan power of condensers having large surface area will be high. Therefore, the condenser with a surface type of 8.0-3/8T has higher consumed fan power than that of the condenser with a surface type of CF-7.0-5/8J.

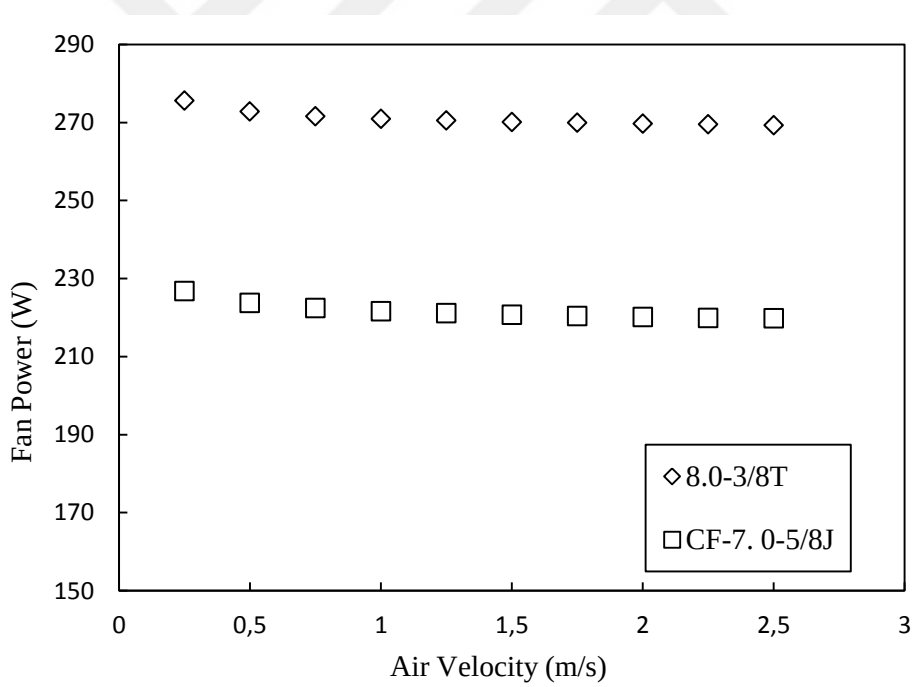

Figure 3.17. Effect of air velocity on fan power for different surface types

3.2.3. Mathematical modeling results related with air velocity-COP for different refrigerants and surface types

In order to see the influence of air velocity on the overall COP of system, the overall COPs are calculated from the improved model in the range of 0.25-2.5 m/s air velocity for all refrigerants. The results are presented in Figures 3.18 and 3.19 for type 8.0-3/8T and type CF-7.0-5/8J respectively.

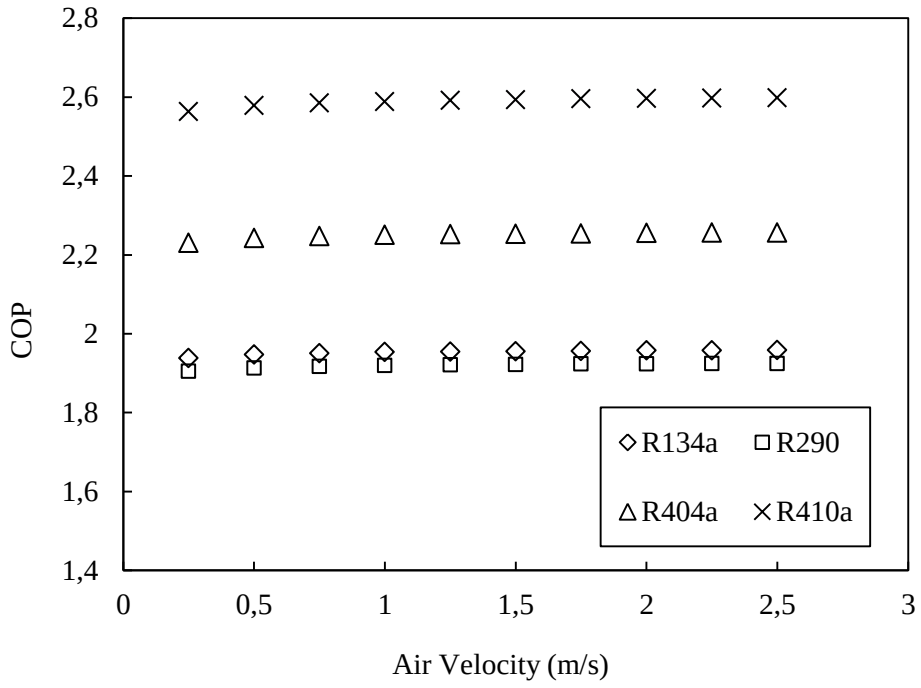

Figure 3.18. The effect of condenser air velocity on COP for different refrigerants (Type: 8.0-3/8T)

As seen in Figures 3.18 and 3.19, the increase in air velocity for all refrigerants has not been a significant effect on overall COP of system. Similar tendencies are observed for both types of surface. On the other hand, overall COP of system varied with the type of refrigerants on both surface types. According to obtained results, the overall COP of system for synthetic refrigerants R410a and R404a are found to be 2.9 and 2.5, respectively. The overall COP values for natural refrigerant R290 and synthetic refrigerant R134a are observed close to each other and calculated to be around 2.05.

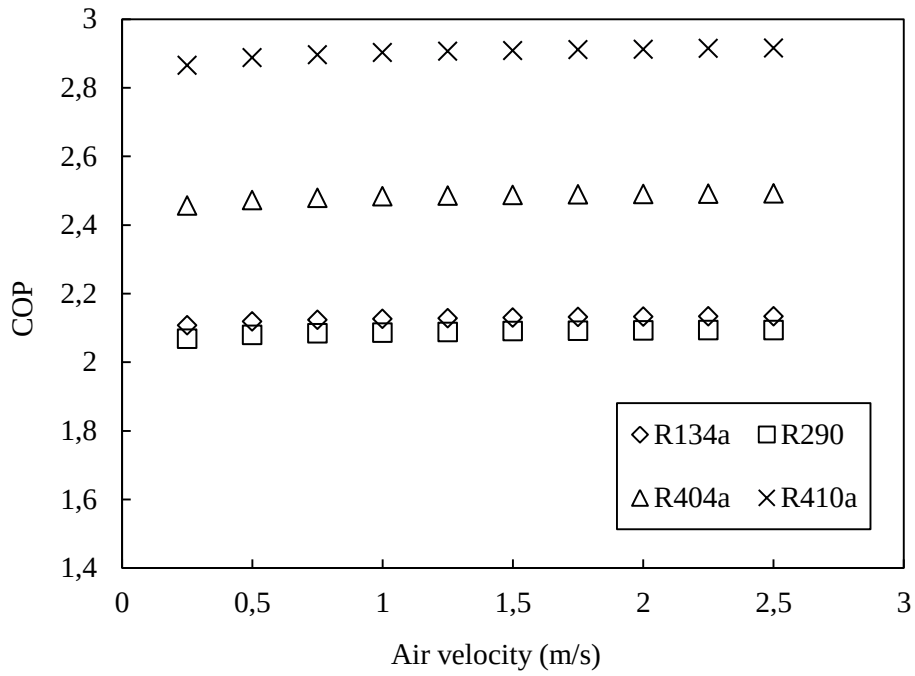

Figure 3.19. Effect of condenser air velocity on COP for different refrigerants (Type: CF-7.0-5/8J)

In order to see the effect of surface type on the overall COP of system, the overall COPs versus air velocity are shown in Figure 3.20 a-d. for all refrigerants. The overall COP of system using type CF-7.0-5/8J is calculated higher than that of type 8.0-3/8T. This is caused from being the consumed fan power for type 8.0-3/8T is higher than the consumed fan power for type CF-7.0-5/8J. In fact, the high consumed fan power means the high surface area of condenser. In this model selected condenser with a surface type of 8.0-3/8T has 587 m^2/m^3 of $\propto$, while for a condenser with surface type of CF-7.0-5/8J has 269 m^2/m^3 of $\propto$.

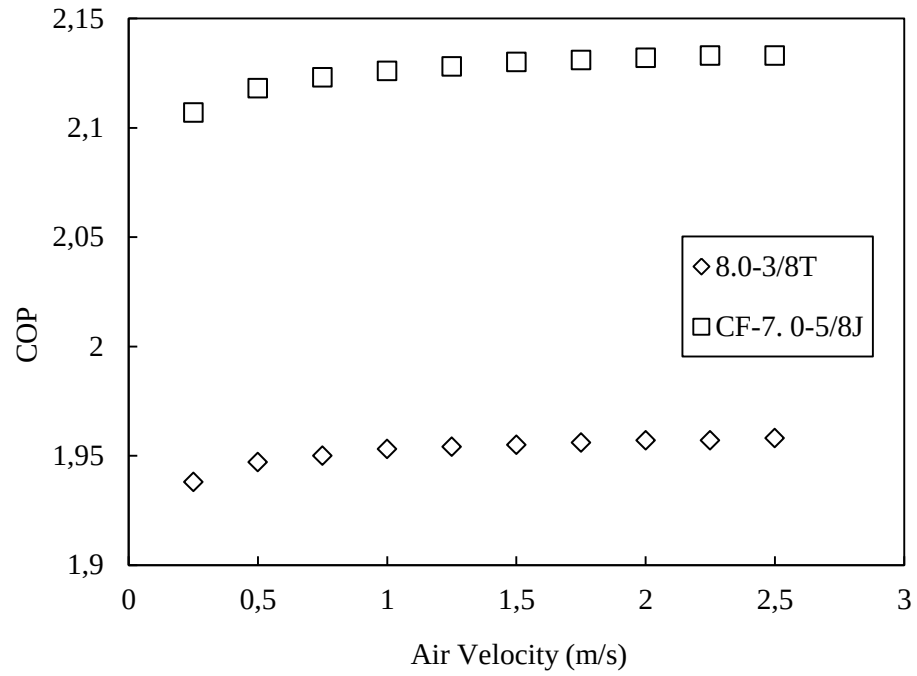
2,15
2,1
2,05
2
1,95
1,9
COP
0
0,5
1
1,5
2
2,5
3
Air Velocity (m/s)
8.0-3/8T
CF-7. 0-5/8J

(a)

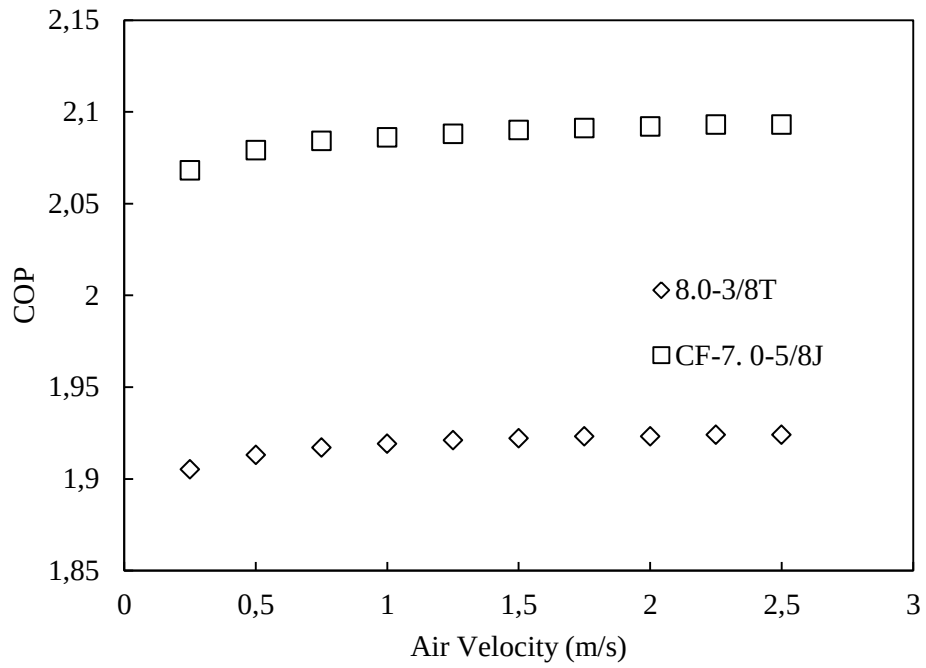
2,15
2,1
2,05
2
1,95
1,9
1,85
COP
0
0,5
1
1,5
2
2,5
3
Air Velocity (m/s)
8.0-3/8T
CF-7. 0-5/8J

(b)

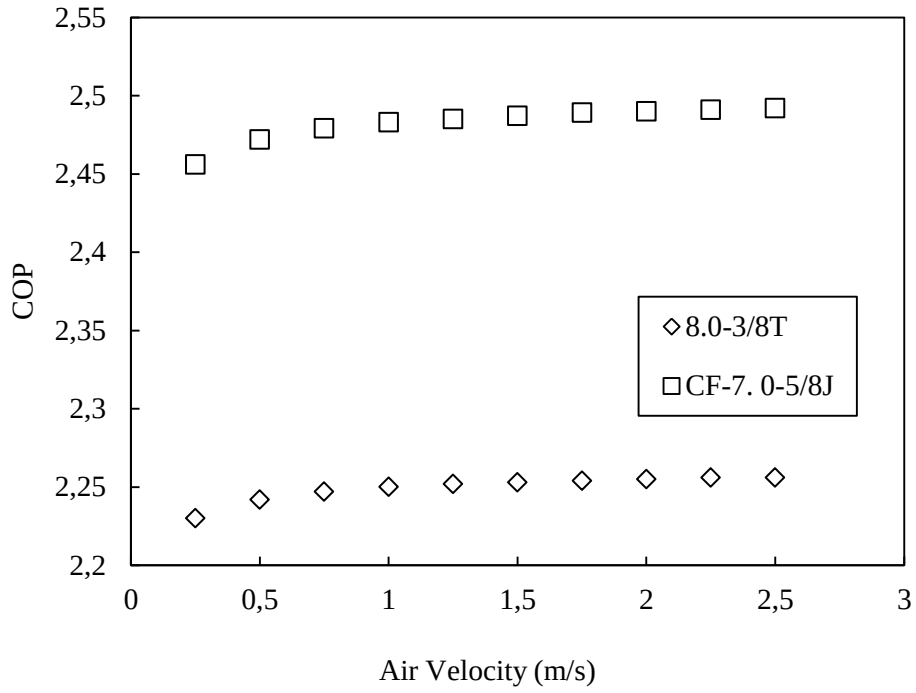

(c)

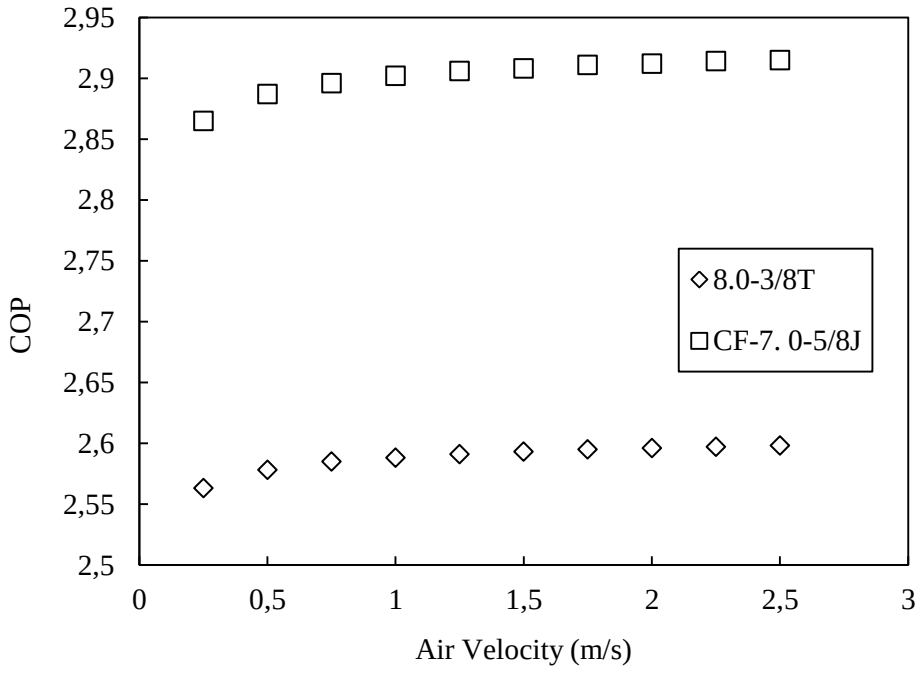

(d)

Figure 3.20. Effect of condenser air velocity on COP for different surface types

a) R134a b) R290 b) R404a d) R410a

3.3. Refrigeration System Simulation Results

Results of the simulated refrigeration system components (compressor power, fan power, evaporator capacity), system COP and overall COP for different refrigerants are given in Table 3.3. As can be seen from Table 3.3, the highest overall COP (2.58) is calculated for the synthetic refrigerant R410a whereas the lowest COP (1.91) is computed for the natural refrigerant (R290) for type 8.03/8T. Similar tendency is observed for type CF-7.0-5/8J**.** Nevertheless, when type 8.03/8T is compared to type CF-7.0-5/8J, type CF-7.0-5/8J appears to have higher overall COP values for all refrigerants. In addition, the compressor COP values are also calculated for different refrigerants. Considering the compressor COPs, the similar tendency is observed as in the overall COPs obtained for investigated refrigerants. The performance of refrigeration systems is expressed in terms of the coefficient of performance (COP), which was defined as the ratio of desired output and required input. In order to obtain the same desired output (Q_{evap}=1182W), the consumed required input (W_{comp}) are found different for selected refrigerants. Therefore, while the highest consumed compressor power is 344.8 W of R290, the lowest consumed compressor power is 189.3 W of R410a for type 8.03/8T**.** As can be seen from Table 3.3, there is no effect of surface type on consumed power. In calculations, air velocity is kept constant at 0.5 m/s.

Table 3.3. Results of the simulated refrigeration system for different refrigerants and surface types

Calculated Parameters	**8.03/8T**				**CF-7.0-5/8J**			
	R134a	**R290**	**R404a**	**R410a**	**R134a**	**R290**	**R404a**	**R410a**
Compressor power (W)	333.4	344.8	256.4	189.3	333.4	344.8	256.4	189.3
Fan power (W)	272.8	273.1	271.2	269.7	223.7	224	222.1	220.6
Evaporator capacity (W)	≈1182	≈1182	≈1182	≈1182	≈1182	≈1182	≈1182	≈1182
COP	3.54	3.43	4.61	6.25	3.54	3.43	4.61	6.25
$COP_{Overall}$	1.95	1.91	2.24	2.58	2.12	2.08	2.47	2.89

4. CONCLUSION

This study presented a mathematical model for refrigeration system components such as condenser, evaporator based on various empirical correlations of heat transfer coefficients in order to simulate the performance of system using four different refrigerants (R134a, R404a, R410A and R290) and different surface types (8.03/8T and CF7.05).In addition, the selected refrigerants are apprised in a refrigeration system relating to energy efficiency and environmental considerations.

The refrigeration system model has evaporation temperatures of -18°C and is referred to as medium low temperature applications. In addition, the model has condensation temperature is based on 40 °C. Cooling capacity of the evaporator (absorbed heat from refrigerated space) is selected to be 1.18 kW. For condenser, the heat transfer rates rejected to environment of R134a, R290, R404a and R410a are calculated to be 1514 W, 1527 W, 1439 W and 1372 W respectively. These operating parameters such as evaporation, condensation temperatures and evaporation capacity are kept constant. These type refrigeration systems are used for a small scale refrigerator. In selection of an appropriate refrigerant, several parameters are considered. First, selected refrigerants have to possess both thermosphysical and transport properties which are competitive with the refrigerant used nowadays. Secondly, it has been noted that selected refrigerants are not toxic and Global Warming Potential (GWP) is low.

The influences of different refrigerants and surface types on the system performance are calculated. The results obtained from improved model, it can be claimed that:

- In the case of refrigerated space temperature ($T_{air,evap,out}$) is desired to be constant at -10 °C, inlet air temperatures for evaporation region ($T_{air,evap,in}$) and for superheated region ($T_{air,sh,in}$) of evaporator are predicted as 24.64 °C and 26.11 °C, respectively.
- When it is assumed that the inlet temperature to the subcooling region of the air blown to the condenser surface by a fan as to be 20°C, the air outlet temperatures of the subcooling region ($T_{air,sc,out}$), the condensation region ($T_{air,cond,out}$) and the superheated region ($T_{air,sh,out}$) are found to be 21.44°C, 32.52 °C and 34.04 °C, respectively.

- The highest convection coefficients of evaporator evaporation region are calculated for the natural refrigerant (R290) at all mass flux values from 50 to 500 kg/m^{2}s for both surface type 8.03/8T and CF-7.0-5/8J**.** In the same range of mass flux, the convection coefficient values of the synthetic refrigerants (R134a, R404a, and R410a) used in the system is calculated close the each other. The convection coefficient values of type 8.0-3/8T are found higher than the calculated convection coefficient values of type CF-7.0-5/8J.
- For evaporator, calculated mass flux values corresponding to varying vapor quality for all refrigerants are found to be greater for type 8.0-3/8T than those of type CF-7. 0-5/8J. Among the refrigerants, natural refrigerant R290 has lower mass flux values than other synthetic refrigerants for the same vapor quality.
- For both condenser surface types, the synthetic refrigerant R134a has the highest mass flux versus vapor quality during the condensation process compared to other refrigerants. It is observed that, there is no significant effect of surface types on the variation of mass flux versus vapor quality.
- Calculated pressure drop of the condenser air (ΔP_{air}) side for two different surface types (8.03/8T and CF7.05) is used to determine the consumed power of condenser fan ($\dot{W}$). It is found that the condenser with a surface type of 8.0-3/8T has higher consumed fan power than that of surface type of CF-7.0-5/8J.
- The highest overall COP is computed for the synthetic refrigerant (R410a) while the lowest COP is computed for the natural refrigerant (R290) for both surface type 8.03/8T and CF-7.0-5/8J**.**
- When type 8.03/8T is compared to type CF-7.0-5/8J, type CF-7.0-5/8J appears to have higher overall COP values for all refrigerants. It can be recommended that the condenser with a surface type of CF-7.0-5/8J for all refrigerants to get high system COP.
- When the utilization of the system evaporator is considered, surface type CF-7.0-5/8J (2.40 m^2) which gives high overall heat transfer coefficient is preferred.

REFERENCES

[1] US Environmental Protection Agency, National Action Plan for Energy Efficiency: Sector Collaborative on Energy Efficiency Accomplishments and Next Steps. Available:<http://www.epa.gov/cleanenergy/documents/suca/sector_collaborative.pdf>.

[2] Çengel Y. A., Boles M. A., Thermodynamics an Engineering Approach, 5th Edition, USA

[3] Balmer R. T., Modern Engineering Thermodynamics, USA

[4] Horton, W.T., 2002. Modeling of secondary loop refrigeration systems in supermarket applications. Doctor of Philosophy Dissertation, Purdue University.

[5] Review of secondary loop refrigeration systems, Kai Wang, Magnus Eisele, Yunho Hwang*, Reinhard Radermacher, 2010

[6]http://www.hamburg.de/contentblob/1212096/data/vortrag-jakobs-gase-20-02-09.pdf

[7] http//:www.wikipedia.com,2014

[8] IIF/IIR. The environmental impact of the molecules used as refrigerants. 8th Informatory Note on CFC's and Refrigeration, August 1992.

[9] Singh, O., (2009), Applied Thermodynamics, 3rd Edition, Kanpur/INDIA

[10] ATALAY H., Soğutucu Akışkanların Termodinamik ve Termofiziksel Modellenmesi, Yüksek Lisans Tezi,(2011).

[11] Oró, E., et al., Review on phase change materials (PCMs) for cold thermal energy storage applications. Applied Energy, 2012. 99: p. 513-533.

[12] Sari, A., 2005. Eutectic mixtures of some fatty acids for low temperature solar heating applications: thermal properties and thermal reliability. Appl. Therm. Eng. 25, 2100–2107.

[13] Regin, A.F., Solanki, S.C., Saini, J.S., 2008. Heat transfer characteristics of thermal energy storage systems using PCM capsules: a review. Renew. Sustain. Energy Rev. 12, 2438– 2458.

[14] He, B., Setterwall, F., 2002. Technical grade paraffin waxes as phase change materials for cool thermal storage and cool storage systems capital cost estimation. Energy Convers. Manage. 43, 1709–1723.

[15] Qureshi,W.A., Nair, N.-K.C., Farid, M.M., 2011. Impact of energy storage in buildings on electricity demand side management. Energy Convers. Manage. 52, 2110–2120.

[16] Regin, A.F., Solanki, S.C., Saini, J.S., 2008. Heat transfer characteristics of thermal energy storage systems using PCM capsules: a review. Renew. Sustain. Energy Rev. 12, 2438–2458.

[17] Go, Z., Liu, H., and Li, Y., 2004, Thermal energy recovery of air conditioning system –heat recovery system calculation and phase change materials development, Applied Thermal Eng. **24**:2511−2526

[18] Demirel, Y., Heat storage by phase changing materials and thermoeconomics, in Thermal energy storage for sustainable energy consumption. 2007, Springer. p. 133-151.

[19] Lina, K. Zhang, Y. Xua, X. Dia, H. Yang, R. Qina, P., 2005, Experimental study of underfloor electric heating system with shape-stabilized PCM plates, Energy and Buildings **37**:215−220.

[20] Mehling, H., Cabeza, L.F., 2008. Heat and Cold Storage with PCM. An Up to Date Introduction into Basics and Applications. Springers-Verlag, Berlin Heidelberg.

[21] Sharma, A., Tyagi, V.V., Chen, C.R., Buddhi, D., 2009. Review on thermal energy storage with phase change materials and applications. Renew.Sustain. Energy Rev. 13, 318–345.

[22] Farid, M., Khudhair, M., Razack, K., Al-Hallaj, S., 2004. A review on phase change energy storage: materials and applications. Energy Convers. Manage. 45, 1597–1615.

[23] Parameshwaran, R., Kalaiselvam, S., 2015. Nanomaterialembedded phase-change materials (PCMs) for reducing building cooling needs. Eco-Efficient Mater. Mitigat. Build. Cool. Needs 401–439.

[24] Jiang, Y., Ding, E.Y., Li, G.K., 2002. Study on transition characteristics of PEG/CDA solid– solid phase change materials. Polymer (Guildf.) 43, 117–120.

[25]. Li,W.D., Ding, E.Y., 2007. Preparation and characterization of cross-linking PEG/MDI/ PE copolymer as solid-solid phase change heat storage material. Sol. Energy Mat. Sol. Cells 91, 764–765

[26] Getu, H. and P. Bansal, Modeling and performance analyses of evaporators in frozen-food supermarket display cabinets at low temperatures. International Journal of Refrigeration, 2007. 30(7): p. 1227-1243.

[27] F.C.McQuiston, Correlation of heat, mass and momentum transfer coefficients for plate-fine-tube heat transfer surface with staggered tubes, ASHRAE Transactions 84 (1) (1978) 294-301.

[28] Kim, N., B. Youn, and R. Webb, Air-side heat transfer and friction correlations for plain fin-and-tube heat exchangers with staggered tube arrangements. Journal of heat transfer, 1999. **121**(3): p. 662-667.

[29] Tassou, S. and R. Green, A mathematical model of the heat transfer process in a shell and tube condenser for use in refrigeration applications. Applied Mathematical Modelling, 1981. **5**(1): p. 29-33.

[30] Bejarano, G., et al., On the difficulty of globally optimally controlling refrigeration systems. Applied Thermal Engineering, 2017. 111: p. 1143-1157.

[31] Zabet, I., V. Lemort, and G.M. TÂRLEA, MATHEMATICAL MODEL OF A HEAT EXCHANGER WORKING WITH DIFFERENT REFRIGERANTS. Mathematical Modelling in Civil Engineering, 2012: p. 55.

[32] Liu, M., et al. Performance Study of Finned Tube Evaporators in a Humid Environment. in ASME 1997 Turbo Asia Conference. 1997. American Society of Mechanical Engineers.

[33] Zhuang, Z., et al., Modeling and performance analysis of the condenser using untreated sewage heat energy. Procedia Engineering, 2016. 146: p. 335-342.

[34] Bakhshipour, S., M. Valipour, and Y. Pahamli, Parametric analysis of domestic refrigerators using PCM heat exchanger. International Journal of Refrigeration, 2017. 83: p. 1-13.

[35] M.W. Brown and P.K. Bansal. Challenges in modeling vapor compression liquid chillers. ASHRAE Transaction: Research, 104(Pt 1A):474-486, 1998.

[36] Bergman, T.L., et al., Fundamentals of heat and mass transfer. 2011: John Wiley & Sons.

[37] Nellis, G. and S. Klein, Mass transfer. Heat transfer, 2009.

[38] Kays, W.M. and A.L. London, Compact heat exchangers. 1984.

[39] Wang, F., Maidment, G., Missenden,J., Tozer, R.,2007. The novel use of phase change materials in refrigeration plant. Part 2: Dynamic simulation model for the combined system. Appl. Therm. Eng. 27, 2902-2910.

[40] EES: Engineering Equation Solver, 2014, fChart Software Inc.

[41] Lemmon, E., W., Huber, M., L., Mclinden, M., O., (2007) NIST standard reference database 23, Version 8.0, Physical and Chemical properties Division

APPENDIX A

ENGINEERING EQUATION SOLVER RESULTS

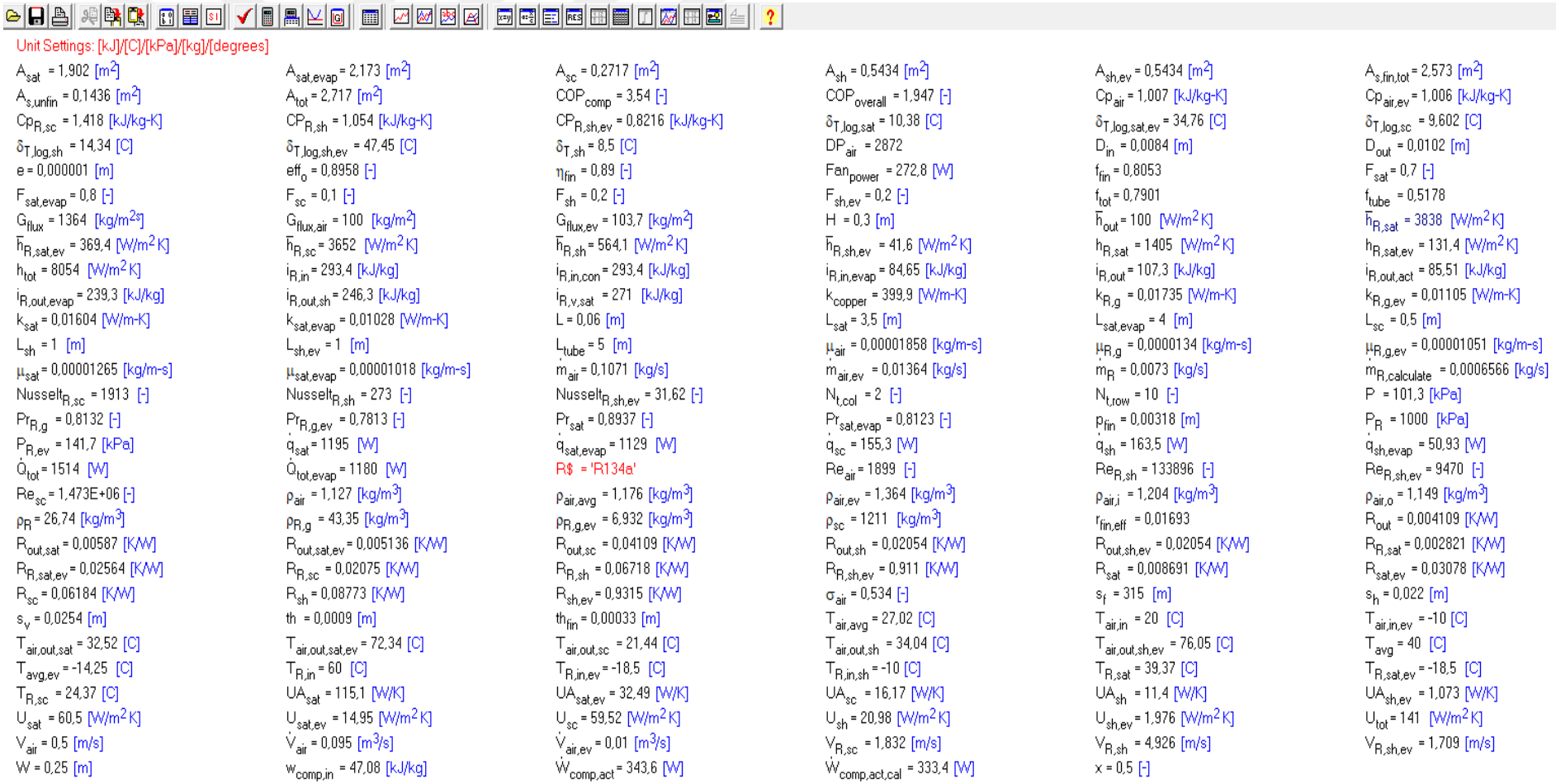

Unit Settings: [kJ]/[C]/[kPa]/[kg]/[degrees]

A_{sat} = 1,902 [m^2]
$A_{s,unfin}$ = 0,1436 [m^2]
$Cp_{R,sc}$ = 1,418 [kJ/kg-K]
$\delta_{T,log,sh}$ = 14,34 [C]
e = 0,000001 [m]
$F_{sat,evap}$ = 0,8 [-]
G_{flux} = 1364 [kg/m^2s]
$\bar{h}_{R,sat,ev}$ = 369,4 [W/m^2K]
h_{tot} = 8054 [W/m^2K]
$i_{R,out,evap}$ = 239,3 [kJ/kg]
k_{sat} = 0,01604 [W/m-K]
L_{sh} = 1 [m]
μ_{sat} = 0,00001265 [kg/m-s]
$Nusselt_{R,sc}$ = 1913 [-]
$Pr_{R,g}$ = 0,8132 [-]
$P_{R,ev}$ = 141,7 [kPa]
$\dot{Q}_{tot}$ = 1514 [W]
Re_{sc} = 1,473E+06 [-]
ρ_R = 26,74 [kg/m^3]
$R_{out,sat}$ = 0,00587 [K/W]
$R_{R,sat,ev}$ = 0,02564 [K/W]
R_{sc} = 0,06184 [K/W]
s_v = 0,0254 [m]
$T_{air,out,sat}$ = 32,52 [C]
$T_{avg,ev}$ = -14,25 [C]
$T_{R,sc}$ = 24,37 [C]
U_{sat} = 60,5 [W/m^2K]
V_{air} = 0,5 [m/s]
W = 0,25 [m]

$A_{sat,evap}$ = 2,173 [m^2]
A_{tot} = 2,717 [m^2]
$CP_{R,sh}$ = 1,054 [kJ/kg-K]
$\delta_{T,log,sh,ev}$ = 47,45 [C]
eff_0 = 0,8958 [-]
F_{sc} = 0,1 [-]
$G_{flux,air}$ = 100 [kg/m^2]
$\bar{h}_{R,sc}$ = 3652 [W/m^2K]
$i_{R,in}$ = 293,4 [kJ/kg]
$i_{R,out,sh}$ = 246,3 [kJ/kg]
$k_{sat,evap}$ = 0,01028 [W/m-K]
$L_{sh,ev}$ = 1 [m]
$\mu_{sat,evap}$ = 0,00001018 [kg/m-s]
$Nusselt_{R,sh}$ = 273 [-]
$Pr_{R,g,ev}$ = 0,7813 [-]
$\dot{q}_{sat}$ = 1195 [W]
$\dot{Q}_{tot,evap}$ = 1180 [W]
ρ_{air} = 1,127 [kg/m^3]
$\rho_{R,g}$ = 43,35 [kg/m^3]
$R_{out,sat,ev}$ = 0,005136 [K/W]
$R_{R,sc}$ = 0,02075 [K/W]
R_{sh} = 0,08773 [K/W]
th = 0,0009 [m]
$T_{air,out,sat,ev}$ = 72,34 [C]
$T_{R,in}$ = 60 [C]
UA_{sat} = 115,1 [W/K]
$U_{sat,ev}$ = 14,95 [W/m^2K]
$\dot{V}_{air}$ = 0,095 [m^3/s]
$w_{comp,in}$ = 47,08 [kJ/kg]

A_{sc} = 0,2717 [m^2]
COP_{comp} = 3,54 [-]
$CP_{R,sh,ev}$ = 0,8216 [kJ/kg-K]
$\delta_{T,sh}$ = 8,5 [C]
η_{fin} = 0,89 [-]
F_{sh} = 0,2 [-]
$G_{flux,ev}$ = 103,7 [kg/m^2]
$\bar{h}_{R,sh}$ = 564,1 [W/m^2K]
$i_{R,in,con}$ = 293,4 [kJ/kg]
$i_{R,v,sat}$ = 271 [kJ/kg]
L = 0,06 [m]
L_{tube} = 5 [m]
$\dot{m}_{air}$ = 0,1071 [kg/s]
$Nusselt_{R,sh,ev}$ = 31,62 [-]
Pr_{sat} = 0,8937 [-]
$\dot{q}_{sat,evap}$ = 1129 [W]
R$ = 'R134a'
$\rho_{air,avg}$ = 1,176 [kg/m^3]
$\rho_{R,g,ev}$ = 6,932 [kg/m^3]
$R_{out,sc}$ = 0,04109 [K/W]
$R_{R,sh}$ = 0,06718 [K/W]
$R_{sh,ev}$ = 0,9315 [K/W]
th_{fin} = 0,00033 [m]
$T_{air,out,sc}$ = 21,44 [C]
$T_{R,in,ev}$ = -18,5 [C]
$UA_{sat,ev}$ = 32,49 [W/K]
U_{sc} = 59,52 [W/m^2K]
$\dot{V}_{air,ev}$ = 0,01 [m^3/s]
$\dot{W}_{comp,act}$ = 343,6 [W]

A_{sh} = 0,5434 [m^2]
$COP_{overall}$ = 1,947 [-]
$\delta_{T,log,sat}$ = 10,38 [C]
DP_{air} = 2872
Fan_{power} = 272,8 [W]
$F_{sh,ev}$ = 0,2 [-]
H = 0,3 [m]
$\bar{h}_{R,sh,ev}$ = 41,6 [W/m^2K]
$i_{R,in,evap}$ = 84,65 [kJ/kg]
k_{copper} = 399,9 [W/m-K]
L_{sat} = 3,5 [m]
μ_{air} = 0,00001858 [kg/m-s]
$\dot{m}_{air,ev}$ = 0,01364 [kg/s]
$N_{t,col}$ = 2 [-]
$Pr_{sat,evap}$ = 0,8123 [-]
$\dot{q}_{sc}$ = 155,3 [W]
Re_{air} = 1899 [-]
$\rho_{air,ev}$ = 1,364 [kg/m^3]
ρ_{sc} = 1211 [kg/m^3]
$R_{out,sh}$ = 0,02054 [K/W]
$R_{R,sh,ev}$ = 0,911 [K/W]
σ_{air} = 0,534 [-]
$T_{air,avg}$ = 27,02 [C]
$T_{air,out,sh}$ = 34,04 [C]
$T_{R,in,sh}$ = -10 [C]
UA_{sc} = 16,17 [W/K]
U_{sh} = 20,98 [W/m^2K]
$V_{R,sc}$ = 1,832 [m/s]
$\dot{W}_{comp,act,cal}$ = 333,4 [W]

$A_{sh,ev}$ = 0,5434 [m^2]
Cp_{air} = 1,007 [kJ/kg-K]
$\delta_{T,log,sat,ev}$ = 34,76 [C]
D_{in} = 0,0084 [m]
f_{fin} = 0,8053
f_{tot} = 0,7901
$\bar{h}_{out}$ = 100 [W/m^2K]
$h_{R,sat}$ = 1405 [W/m^2K]
$i_{R,out}$ = 107,3 [kJ/kg]
$k_{R,g}$ = 0,01735 [W/m-K]
$L_{sat,evap}$ = 4 [m]
$\mu_{R,g}$ = 0,0000134 [kg/m-s]
$\dot{m}_R$ = 0,0073 [kg/s]
$N_{t,row}$ = 10 [-]
p_{fin} = 0,00318 [m]
$\dot{q}_{sh}$ = 163,5 [W]
$Re_{R,sh}$ = 133896 [-]
$\rho_{air,i}$ = 1,204 [kg/m^3]
$r_{fin,eff}$ = 0,01693
$R_{out,sh,ev}$ = 0,02054 [K/W]
R_{sat} = 0,008691 [K/W]
s_f = 315 [m]
$T_{air,in}$ = 20 [C]
$T_{air,out,sh,ev}$ = 76,05 [C]
$T_{R,sat}$ = 39,37 [C]
UA_{sh} = 11,4 [W/K]
$U_{sh,ev}$ = 1,976 [W/m^2K]
$V_{R,sh}$ = 4,926 [m/s]
x = 0,5 [-]

$A_{s,fin,tot}$ = 2,573 [m^2]
$Cp_{air,ev}$ = 1,006 [kJ/kg-K]
$\delta_{T,log,sc}$ = 9,602 [C]
D_{out} = 0,0102 [m]
F_{sat} = 0,7 [-]
f_{tube} = 0,5178
$\bar{h}_{R,sat}$ = 3838 [W/m^2K]
$h_{R,sat,ev}$ = 131,4 [W/m^2K]
$i_{R,out,act}$ = 85,51 [kJ/kg]
$k_{R,g,ev}$ = 0,01105 [W/m-K]
L_{sc} = 0,5 [m]
$\mu_{R,g,ev}$ = 0,00001051 [kg/m-s]
$\dot{m}_{R,calculate}$ = 0,0006566 [kg/s]
P = 101,3 [kPa]
P_R = 1000 [kPa]
$\dot{q}_{sh,evap}$ = 50,93 [W]
$Re_{R,sh,ev}$ = 9470 [-]
$\rho_{air,o}$ = 1,149 [kg/m^3]
R_{out} = 0,004109 [K/W]
$R_{R,sat}$ = 0,002821 [K/W]
$R_{sat,ev}$ = 0,03078 [K/W]
s_h = 0,022 [m]
$T_{air,in,ev}$ = -10 [C]
T_{avg} = 40 [C]
$T_{R,sat,ev}$ = -18,5 [C]
$UA_{sh,ev}$ = 1,073 [W/K]
U_{tot} = 141 [W/m^2K]
$V_{R,sh,ev}$ = 1,709 [m/s]

Appendix A.1. Simulation results of type 8.03/8T for R134a

Unit Settings: [kJ]/[C]/[kPa]/[kg]/[degrees]

A_{sat} = 1,902 [m^2]
$A_{s,unfin}$ = 0,1436 [m^2]
$Cp_{R,sc}$ = 2,717 [kJ/kg-K]
$\delta_{T,log,sh}$ = 14,3 [C]
e = 0,000001 [m]
$F_{sat,evap}$ = 0,8 [-]
G_{flux} = 720,4 [kg/m^2s]
$\bar{h}_{R,sat,ev}$ = 369,3 [W/m^2K]
h_{tot} = 8387 [W/m^2K]
$i_{R,out,evap}$ = 553,7 [kJ/kg]
k_{sat} = 0,02126 [W/m-K]
L_{sh} = 1 [m]
μ_{sat} = 0,000009385 [kg/m-s]
$Nusselt_{R,sc}$ = 1516 [-]
$Pr_{R,g}$ = 0,8981 [-]
$P_{R,ev}$ = 258 [kPa]
$\dot{Q}_{tot}$ = 1527 [W]
Re_{sc} = 1,052E+06 [-]
ρ_R = 15,55 [kg/m^3]
$R_{out,sat}$ = 0,00587 [K/W]
$R_{R,sat,ev}$ = 0,02565 [K/W]
R_{sc} = 0,06084 [K/W]
s_v = 0,0254 [m]
$T_{air,out,sat}$ = 32,53 [C]
$T_{avg,ev}$ = -14,25 [C]
$T_{R,sc}$ = 24,38 [C]
U_{sat} = 60,94 [W/m^2K]
V_{air} = 0,5 [m/s]
W = 0,25 [m]

$A_{sat,evap}$ = 2,173 [m^2]
A_{tot} = 2,717 [m^2]
$CP_{R,sh}$ = 2,155 [kJ/kg-K]
$\delta_{T,log,sh,ev}$ = 47,51 [C]
eff_o = 0,8958 [-]
F_{sc} = 0,1 [-]
$G_{flux,air}$ = 100 [kg/m^2]
$\bar{h}_{R,sc}$ = 3837 [W/m^2K]
$i_{R,in}$ = 659,3 [kJ/kg]
$i_{R,out,sh}$ = 567,5 [kJ/kg]
$k_{sat,evap}$ = 0,0138 [W/m-K]
$L_{sh,ev}$ = 1 [m]
$\mu_{sat,evap}$ = 0,000007184 [kg/m-s]
$Nusselt_{R,sh}$ = 222,6 [-]
$Pr_{R,g,ev}$ = 0,8244 [-]
$\dot{q}_{sat}$ = 1193 [W]
$\dot{Q}_{tot,evap}$ = 1182 [W]
ρ_{air} = 1,127 [kg/m^3]
$\rho_{R,g}$ = 26,03 [kg/m^3]
$R_{out,sat,ev}$ = 0,005136 [K/W]
$R_{R,sc}$ = 0,01975 [K/W]
R_{sh} = 0,0811 [K/W]
th = 0,0009 [m]
$T_{air,out,sat,ev}$ = 72,3 [C]
$T_{R,in}$ = 60 [C]
UA_{sat} = 115,9 [W/K]
$U_{sat,ev}$ = 14,95 [W/m^2K]
$\dot{V}_{air}$ = 0,095 [m^3/s]
$w_{comp,in}$ = 91,82 [kJ/kg]

A_{sc} = 0,2717 [m^2]
COP_{comp} = 3,429 [-]
$CP_{R,sh,ev}$ = 1,631 [kJ/kg-K]
$\delta_{T,sh}$ = 8,5 [C]
η_{fin} = 0,89 [-]
F_{sh} = 0,2 [-]
$G_{flux,ev}$ = 50,42 [kg/m^2]
$\bar{h}_{R,sh}$ = 625,8 [W/m^2K]
$i_{R,in,con}$ = 659,3 [kJ/kg]
$i_{R,v,sat}$ = 613,8 [kJ/kg]
L = 0,06 [m]
L_{tube} = 5 [m]
$\dot{m}_{air}$ = 0,1071 [kg/s]
$Nusselt_{R,sh,ev}$ = 25,09 [-]
Pr_{sat} = 1,011 [-]
$\dot{q}_{sat,evap}$ = 1129 [W]
R$ = 'R290'
$\rho_{air,avg}$ = 1,176 [kg/m^3]
$\rho_{R,g,ev}$ = 5,558 [kg/m^3]
$R_{out,sc}$ = 0,04109 [K/W]
$R_{R,sh}$ = 0,06055 [K/W]
$R_{sh,ev}$ = 0,8864 [K/W]
th_{fin} = 0,00033 [m]
$T_{air,out,sc}$ = 21,47 [C]
$T_{R,in,ev}$ = -18,5 [C]
$UA_{sat,ev}$ = 32,48 [W/K]
U_{sc} = 60,5 [W/m^2K]
$\dot{V}_{air,ev}$ = 0,01 [m^3/s]
$\dot{W}_{comp,act}$ = 355,8 [W]

A_{sh} = 0,5434 [m^2]
$COP_{overall}$ = 1,913 [-]
$\delta_{T,log,sat}$ = 10,29 [C]
DP_{air} = 2875
Fan_{power} = 273,1 [W]
$F_{sh,ev}$ = 0,2 [-]
H = 0,3 [m]
$\bar{h}_{R,sh,ev}$ = 43,76 [W/m^2K]
$i_{R,in,evap}$ = 262,4 [kJ/kg]
k_{copper} = 399,9 [W/m-K]
L_{sat} = 3,5 [m]
μ_{air} = 0,00001858 [kg/m-s]
$\dot{m}_{air,ev}$ = 0,01364 [kg/s]
$N_{t,col}$ = 2 [-]
$Pr_{sat,evap}$ = 0,8455 [-]
$\dot{q}_{sc}$ = 157,9 [W]
Re_{air} = 1898 [-]
$\rho_{air,ev}$ = 1,364 [kg/m^3]
ρ_{sc} = 494,3 [kg/m^3]
$R_{out,sh}$ = 0,02054 [K/W]
$R_{R,sh,ev}$ = 0,8659 [K/W]
σ_{air} = 0,534 [-]
$T_{air,avg}$ = 27,08 [C]
$T_{air,out,sh}$ = 34,16 [C]
$T_{R,in,sh}$ = -10 [C]
UA_{sc} = 16,44 [W/K]
U_{sh} = 22,69 [W/m^2K]
$V_{R,sc}$ = 2,377 [m/s]
$\dot{W}_{comp,act,cal}$ = 344,8 [W]

$A_{sh,ev}$ = 0,5434 [m^2]
Cp_{air} = 1,007 [kJ/kg-K]
$\delta_{T,log,sat,ev}$ = 34,75 [C]
D_{in} = 0,0084 [m]
f_{fin} = 0,8053
f_{tot} = 0,7901
$\bar{h}_{out}$ = 100 [W/m^2K]
$h_{R,sat}$ = 1491 [W/m^2K]
$i_{R,out}$ = 306 [kJ/kg]
$k_{R,g}$ = 0,02362 [W/m-K]
$L_{sat,evap}$ = 4 [m]
$\mu_{R,g}$ = 0,000009842 [kg/m-s]
$\dot{m}_R$ = 0,003875 [kg/s]
$N_{t,row}$ = 10 [-]
p_{fin} = 0,00318 [m]
$\dot{q}_{sh}$ = 176,4 [W]
$Re_{R,sh}$ = 99937 [-]
$\rho_{air,i}$ = 1,204 [kg/m^3]
$r_{fin,eff}$ = 0,01693
$R_{out,sh,ev}$ = 0,02054 [K/W]
R_{sat} = 0,008629 [K/W]
s_f = 315 [m]
$T_{air,in}$ = 20 [C]
$T_{air,out,sh,ev}$ = 76,21 [C]
$T_{R,sat}$ = 39,38 [C]
UA_{sh} = 12,33 [W/K]
$U_{sh,ev}$ = 2,076 [W/m^2K]
$V_{R,sh}$ = 4,498 [m/s]
x = 0,5 [-]

$A_{s,fin,tot}$ = 2,573 [m^2]
$Cp_{air,ev}$ = 1,006 [kJ/kg-K]
$\delta_{T,log,sc}$ = 9,609 [C]
D_{out} = 0,0102 [m]
F_{sat} = 0,7 [-]
f_{tube} = 0,5178
$\bar{h}_{R,sat}$ = 3924 [W/m^2K]
$h_{R,sat,ev}$ = 133 [W/m^2K]
$i_{R,out,act}$ = 263,9 [kJ/kg]
$k_{R,g,ev}$ = 0,01465 [W/m-K]
L_{sc} = 0,5 [m]
$\mu_{R,g,ev}$ = 0,000007407 [kg/m-s]
$\dot{m}_{R,calculate}$ = 0,0003374 [kg/s]
P = 101,3 [kPa]
P_R = 1350 [kPa]
$\dot{q}_{sh,evap}$ = 53,6 [W]
$Re_{R,sh,ev}$ = 6904 [-]
$\rho_{air,o}$ = 1,149 [kg/m^3]
R_{out} = 0,004109 [K/W]
$R_{R,sat}$ = 0,002759 [K/W]
$R_{sat,ev}$ = 0,03079 [K/W]
s_h = 0,022 [m]
$T_{air,in,ev}$ = -10 [C]
T_{avg} = 40 [C]
$T_{R,sat,ev}$ = -18,5 [C]
$UA_{sh,ev}$ = 1,128 [W/K]
U_{tot} = 144,1 [W/m^2K]
$V_{R,sh,ev}$ = 1,095 [m/s]

Appendix A.2. Simulation results of type 8.03/8T for R290

Unit Settings: [kJ]/[C]/[kPa]/[kg]/[degrees]

A_{sat} = 1,902 [m^2]
$A_{s,unfin}$ = 0,1436 [m^2]
$Cp_{R,sc}$ = 1,496 [kJ/kg-K]
$\delta_{T,log,sh}$ = 15,71 [C]
e = 0,000001 [m]
$F_{sat,evap}$ = 0,8 [-]
G_{flux} = 674,6 [kg/m^2s]
$\bar{h}_{R,sat,ev}$ = 368 [W/m^2K]
h_{tot} = 10262 [W/m^2K]
$i_{R,out,evap}$ = 208,3 [kJ/kg]
k_{sat} = 0,01783 [W/m-K]
L_{sh} = 1 [m]
μ_{sat} = 0,00001442 [kg/m-s]
$Nusselt_{R,sc}$ = 3436 [-]
$Pr_{R,g}$ = 0,9336 [-]
$P_{R,ev}$ = 320,5 [kPa]
$\dot{Q}_{tot}$ = 1439 [W]
Re_{sc} = 2,823E+06 [-]
ρ_R = 44,98 [kg/m^3]
$R_{out,sat}$ = 0,00587 [K/W]
$R_{R,sat,ev}$ = 0,02574 [K/W]
R_{sc} = 0,05148 [K/W]
s_v = 0,0254 [m]
$T_{air,out,sat}$ = 31,34 [C]
$T_{avg,ev}$ = -14,25 [C]
$T_{R,sc}$ = 24,6 [C]
U_{sat} = 49,1 [W/m^2K]
V_{air} = 0,5 [m/s]
W = 0,25 [m]

$A_{sat,evap}$ = 2,173 [m^2]
A_{tot} = 2,717 [m^2]
$CP_{R,sh}$ = 1,185 [kJ/kg-K]
$\delta_{T,log,sh,ev}$ = 46,52 [C]
eff_0 = 0,8958 [-]
F_{sc} = 0,1 [-]
$G_{flux,air}$ = 100 [kg/m^2]
$\bar{h}_{R,sc}$ = 7294 [W/m^2K]
$i_{R,in}$ = 259,4 [kJ/kg]
$i_{R,out,sh}$ = 215,7 [kJ/kg]
$k_{sat,evap}$ = 0,01065 [W/m-K]
$L_{sh,ev}$ = 1 [m]
$\mu_{sat,evap}$ = 0,00001061 [kg/m-s]
$Nusselt_{R,sh}$ = 328 [-]
$Pr_{R,g,ev}$ = 0,8513 [-]
$\dot{q}_{sat}$ = 1032 [W]
$\dot{Q}_{tot,evap}$ = 1183 [W]
ρ_{air} = 1,127 [kg/m^3]
$\rho_{R,g}$ = 82,8 [kg/m^3]
$R_{out,sat,ev}$ = 0,005136 [K/W]
$R_{R,sc}$ = 0,01039 [K/W]
R_{sh} = 0,07236 [K/W]
th = 0,0009 [m]
$T_{air,out,sat,ev}$ = 71,65 [C]
$T_{R,in}$ = 60 [C]
UA_{sat} = 93,37 [W/K]
$U_{sat,ev}$ = 14,9 [W/m^2K]
$\dot{V}_{air}$ = 0,095 [m^3/s]
$w_{comp,in}$ = 43,67 [kJ/kg]

A_{sc} = 0,2717 [m^2]
COP_{comp} = 4,612 [-]
$CP_{R,sh,ev}$ = 0,8764 [kJ/kg-K]
$\delta_{T,sh}$ = 8,5 [C]
η_{fin} = 0,89 [-]
F_{sh} = 0,2 [-]
$G_{flux,ev}$ = 102,1 [kg/m^2]
$\bar{h}_{R,sh}$ = 731,3 [W/m^2K]
$i_{R,in,con}$ = 259,4 [kJ/kg]
$i_{R,v,sat}$ = 233,7 [kJ/kg]
L = 0,06 [m]
L_{tube} = 5 [m]
$\dot{m}_{air}$ = 0,1071 [kg/s]
$Nusselt_{R,sh,ev}$ = 39,36 [-]
Pr_{sat} = 1,112 [-]
$\dot{q}_{sat,evap}$ = 1120 [W]
R$ = 'R404a'
$\rho_{air,avg}$ = 1,177 [kg/m^3]
$\rho_{R,g,ev}$ = 15,62 [kg/m^3]
$R_{out,sc}$ = 0,04109 [K/W]
$R_{R,sh}$ = 0,05182 [K/W]
$R_{sh,ev}$ = 0,7392 [K/W]
th_{fin} = 0,00033 [m]
$T_{air,out,sc}$ = 21,76 [C]
$T_{R,in,ev}$ = -18,5 [C]
$UA_{sat,ev}$ = 32,38 [W/K]
U_{sc} = 71,5 [W/m^2K]
$\dot{V}_{air,ev}$ = 0,01 [m^3/s]
$\dot{W}_{comp,act}$ = 369,4 [W]

A_{sh} = 0,5434 [m^2]
$COP_{overall}$ = 2,242 [-]
$\delta_{T,log,sat}$ = 11,05 [C]
DP_{air} = 2854
Fan_{power} = 271,2 [W]
$F_{sh,ev}$ = 0,2 [-]
H = 0,3 [m]
$\bar{h}_{R,sh,ev}$ = 52,73 [W/m^2K]
$i_{R,in,evap}$ = 75,92 [kJ/kg]
k_{copper} = 399,9 [W/m-K]
L_{sat} = 3,5 [m]
μ_{air} = 0,00001857 [kg/m-s]
$\dot{m}_{air,ev}$ = 0,01364 [kg/s]
$N_{t,col}$ = 2 [-]
$Pr_{sat,evap}$ = 0,8709 [-]
$\dot{q}_{sc}$ = 189,8 [W]
Re_{air} = 1903 [-]
$\rho_{air,ev}$ = 1,364 [kg/m^3]
ρ_{sc} = 1045 [kg/m^3]
$R_{out,sh}$ = 0,02054 [K/W]
$R_{R,sh,ev}$ = 0,7187 [K/W]
σ_{air} = 0,534 [-]
$T_{air,avg}$ = 26,67 [C]
$T_{air,out,sh}$ = 33,35 [C]
$T_{R,in,sh}$ = -10 [C]
UA_{sc} = 19,43 [W/K]
U_{sh} = 25,43 [W/m^2K]
$V_{R,sc}$ = 4,635 [m/s]
$\dot{W}_{comp,act,cal}$ = 256,4 [W]

$A_{sh,ev}$ = 0,5434 [m^2]
Cp_{air} = 1,007 [kJ/kg-K]
$\delta_{T,log,sat,ev}$ = 34,58 [C]
D_{in} = 0,0084 [m]
f_{fin} = 0,8052
f_{tot} = 0,79
$\bar{h}_{out}$ = 100 [W/m^2K]
$h_{R,sat}$ = 874,6 [W/m^2K]
$i_{R,out}$ = 111,7 [kJ/kg]
$k_{R,g}$ = 0,01873 [W/m-K]
$L_{sat,evap}$ = 4 [m]
$\mu_{R,g}$ = 0,00001476 [kg/m-s]
$\dot{m}_R$ = 0,00846 [kg/s]
$N_{t,row}$ = 10 [-]
p_{fin} = 0,00318 [m]
$\dot{q}_{sh}$ = 217,1 [W]
$Re_{R,sh}$ = 159937 [-]
$\rho_{air,i}$ = 1,204 [kg/m^3]
$r_{fin,eff}$ = 0,01693
$R_{out,sh,ev}$ = 0,02054 [K/W]
R_{sat} = 0,01071 [K/W]
s_f = 315 [m]
$T_{air,in}$ = 20 [C]
$T_{air,out,sh,ev}$ = 76,24 [C]
$T_{R,sat}$ = 39,6 [C]
UA_{sh} = 13,82 [W/K]
$U_{sh,ev}$ = 2,49 [W/m^2K]
$V_{R,sh}$ = 3,394 [m/s]
x = 0,5 [-]

$A_{s,fin,tot}$ = 2,573 [m^2]
$Cp_{air,ev}$ = 1,006 [kJ/kg-K]
$\delta_{T,log,sc}$ = 9,773 [C]
D_{out} = 0,0102 [m]
F_{sat} = 0,7 [-]
f_{tube} = 0,5178
$\bar{h}_{R,sat}$ = 2237 [W/m^2K]
$h_{R,sat,ev}$ = 133,7 [W/m^2K]
$i_{R,out,act}$ = 89,09 [kJ/kg]
$k_{R,g,ev}$ = 0,01125 [W/m-K]
L_{sc} = 0,5 [m]
$\mu_{R,g,ev}$ = 0,00001093 [kg/m-s]
$\dot{m}_{R,calculate}$ = 0,0008602 [kg/s]
P = 101,3 [kPa]
P_R = 1800 [kPa]
$\dot{q}_{sh,evap}$ = 62,93 [W]
$Re_{R,sh,ev}$ = 11929 [-]
$\rho_{air,o}$ = 1,152 [kg/m^3]
R_{out} = 0,004109 [K/W]
$R_{R,sat}$ = 0,00484 [K/W]
$R_{sat,ev}$ = 0,03088 [K/W]
s_h = 0,022 [m]
$T_{air,in,ev}$ = -10 [C]
T_{avg} = 40 [C]
$T_{R,sat,ev}$ = -18,5 [C]
$UA_{sh,ev}$ = 1,353 [W/K]
U_{tot} = 146 [W/m^2K]
$V_{R,sh,ev}$ = 0,9935 [m/s]

Appendix A.3. Simulation results of type 8.03/8T for R404a

Unit Settings: [kJ]/[C]/[kPa]/[kg]/[degrees]

A_{sat} = 1,902 [m^2]
$A_{s,unfin}$ = 0,1436 [m^2]
$Cp_{R,sc}$ = 1,672 [kJ/kg-K]
$\delta_{T,log,sh}$ = 16,41 [C]
e = 0,000001 [m]
$F_{sat,evap}$ = 0,8 [-]
G_{flux} = 543,9 [kg/m^2s]
$\bar{h}_{R,sat,ev}$ = 369,9 [W/m^2K]
h_{tot} = 5817 [W/m^2K]
$i_{R,out,evap}$ = 275,1 [kJ/kg]
k_{sat} = 0,01792 [W/m-K]
L_{sh} = 1 [m]
μ_{sat} = 0,00001517 [kg/m-s]
$Nusselt_{R,sc}$ = 1568 [-]
$Pr_{R,g}$ = 1,123 [-]
$P_{R,ev}$ = 422,6 [kPa]
$\dot{Q}_{tot}$ = 1372 [W]
Re_{sc} = 940335 [-]
ρ_R = 44,39 [kg/m^3]
$R_{out,sat}$ = 0,00587 [K/W]
$R_{R,sat,ev}$ = 0,02561 [K/W]
R_{sc} = 0,06375 [K/W]
s_v = 0,0254 [m]
$T_{air,out,sat}$ = 30,93 [C]
$T_{avg,ev}$ = -14,25 [C]
$T_{R,sc}$ = 24,83 [C]
U_{sat} = 45,2 [W/m^2K]
V_{air} = 0,5 [m/s]
W = 0,25 [m]

$A_{sat,evap}$ = 2,173 [m^2]
A_{tot} = 2,717 [m^2]
$CP_{R,sh}$ = 1,346 [kJ/kg-K]
$\delta_{T,log,sh,ev}$ = 46 [C]
eff_o = 0,8958 [-]
F_{sc} = 0,1 [-]
$G_{flux,air}$ = 100 [kg/m^2]
$\bar{h}_{R,sc}$ = 3345 [W/m^2K]
$i_{R,in}$ = 316,6 [kJ/kg]
$i_{R,out,sh}$ = 283,2 [kJ/kg]
$k_{sat,evap}$ = 0,01058 [W/m-K]
$L_{sh,ev}$ = 1 [m]
$\mu_{sat,evap}$ = 0,00001099 [kg/m-s]
$Nusselt_{R,sh}$ = 266,2 [-]
$Pr_{R,g,ev}$ = 0,9537 [-]
$\dot{q}_{sat}$ = 1019 [W]
$\dot{Q}_{tot,evap}$ = 1183 [W]
ρ_{air} = 1,127 [kg/m^3]
$\rho_{R,g}$ = 83,04 [kg/m^3]
$R_{out,sat,ev}$ = 0,005136 [K/W]
$R_{R,sc}$ = 0,02266 [K/W]
R_{sh} = 0,08433 [K/W]
th = 0,0009 [m]
$T_{air,out,sat,ev}$ = 72,55 [C]
$T_{R,in}$ = 60 [C]
UA_{sat} = 85,96 [W/K]
$U_{sat,ev}$ = 14,96 [W/m^2K]
$\dot{V}_{air}$ = 0,095 [m^3/s]
$w_{comp,in}$ = 33,38 [kJ/kg]

A_{sc} = 0,2717 [m^2]
COP_{comp} = 6,251 [-]
$CP_{R,sh,ev}$ = 0,9371 [kJ/kg-K]
$\delta_{T,sh}$ = 8,5 [C]
η_{fin} = 0,89 [-]
F_{sh} = 0,2 [-]
$G_{flux,ev}$ = 105,5 [kg/m^2]
$\bar{h}_{R,sh}$ = 594 [W/m^2K]
$i_{R,in,con}$ = 316,6 [kJ/kg]
$i_{R,v,sat}$ = 285,9 [kJ/kg]
L = 0,06 [m]
L_{tube} = 5 [m]
$\dot{m}_{air}$ = 0,1071 [kg/s]
$Nusselt_{R,sh,ev}$ = 32,36 [-]
Pr_{sat} = 1,524 [-]
$\dot{q}_{sat,evap}$ = 1132 [W]
R$ = 'R410a'
$\rho_{air,avg}$ = 1,179 [kg/m^3]
$\rho_{R,g,ev}$ = 15,55 [kg/m^3]
$R_{out,sc}$ = 0,04109 [K/W]
$R_{R,sh}$ = 0,06379 [K/W]
$R_{sh,ev}$ = 0,9003 [K/W]
th_{fin} = 0,00033 [m]
$T_{air,out,sc}$ = 21,47 [C]
$T_{R,in,ev}$ = -18,5 [C]
$UA_{sat,ev}$ = 32,52 [W/K]
U_{sc} = 57,74 [W/m^2K]
$\dot{V}_{air,ev}$ = 0,01 [m^3/s]
$\dot{W}_{comp,act}$ = 211,7 [W]

A_{sh} = 0,5434 [m^2]
$COP_{overall}$ = 2,578 [-]
$\delta_{T,log,sat}$ = 11,85 [C]
DP_{air} = 2839
Fan_{power} = 269,7 [W]
$F_{sh,ev}$ = 0,2 [-]
H = 0,3 [m]
$\bar{h}_{R,sh,ev}$ = 43,07 [W/m^2K]
$i_{R,in,evap}$ = 96,57 [kJ/kg]
k_{copper} = 399,9 [W/m-K]
L_{sat} = 3,5 [m]
μ_{air} = 0,00001855 [kg/m-s]
$\dot{m}_{air,ev}$ = 0,01364 [kg/s]
$N_{t,col}$ = 2 [-]
$Pr_{sat,evap}$ = 0,9974 [-]
$\dot{q}_{sc}$ = 159 [W]
Re_{air} = 1906 [-]
$\rho_{air,ev}$ = 1,364 [kg/m^3]
ρ_{sc} = 1063 [kg/m^3]
$R_{out,sh}$ = 0,02054 [K/W]
$R_{R,sh,ev}$ = 0,8798 [K/W]
σ_{air} = 0,534 [-]
$T_{air,avg}$ = 26,37 [C]
$T_{air,out,sh}$ = 32,73 [C]
$T_{R,in,sh}$ = -10 [C]
UA_{sc} = 15,69 [W/K]
U_{sh} = 21,82 [W/m^2K]
$V_{R,sc}$ = 1,597 [m/s]
$\dot{W}_{comp,act,cal}$ = 189,3 [W]

$A_{sh,ev}$ = 0,5434 [m^2]
Cp_{air} = 1,007 [kJ/kg-K]
$\delta_{T,log,sat,ev}$ = 34,81 [C]
D_{in} = 0,0084 [m]
f_{fin} = 0,8052
f_{tot} = 0,79
$\bar{h}_{out}$ = 100 [W/m^2K]
$h_{R,sat}$ = 806 [W/m^2K]
$i_{R,out}$ = 125,2 [kJ/kg]
$k_{R,g}$ = 0,01875 [W/m-K]
$L_{sat,evap}$ = 4 [m]
$\mu_{R,g}$ = 0,00001565 [kg/m-s]
$\dot{m}_R$ = 0,00634 [kg/s]
$N_{t,row}$ = 10 [-]
p_{fin} = 0,00318 [m]
$\dot{q}_{sh}$ = 194,6 [W]
$Re_{R,sh}$ = 114920 [-]
$\rho_{air,i}$ = 1,204 [kg/m^3]
$r_{fin,eff}$ = 0,01693
$R_{out,sh,ev}$ = 0,02054 [K/W]
R_{sat} = 0,01163 [K/W]
s_f = 315 [m]
$T_{air,in}$ = 20 [C]
$T_{air,out,sh,ev}$ = 76,28 [C]
$T_{R,sat}$ = 39,83 [C]
UA_{sh} = 11,86 [W/K]
$U_{sh,ev}$ = 2,044 [W/m^2K]
$V_{R,sh}$ = 2,578 [m/s]
x = 0,5 [-]

$A_{s,fin,tot}$ = 2,573 [m^2]
$Cp_{air,ev}$ = 1,006 [kJ/kg-K]
$\delta_{T,log,sc}$ = 10,14 [C]
D_{out} = 0,0102 [m]
F_{sat} = 0,7 [-]
f_{tube} = 0,5178
$\bar{h}_{R,sat}$ = 1879 [W/m^2K]
$h_{R,sat,ev}$ = 140 [W/m^2K]
$i_{R,out,act}$ = 99,27 [kJ/kg]
$k_{R,g,ev}$ = 0,01118 [W/m-K]
L_{sc} = 0,5 [m]
$\mu_{R,g,ev}$ = 0,00001138 [kg/m-s]
$\dot{m}_{R,calculate}$ = 0,0006624 [kg/s]
P = 101,3 [kPa]
P_R = 2400 [kPa]
$\dot{q}_{sh,evap}$ = 51,09 [W]
$Re_{R,sh,ev}$ = 8823 [-]
$\rho_{air,o}$ = 1,154 [kg/m^3]
R_{out} = 0,004109 [K/W]
$R_{R,sat}$ = 0,005763 [K/W]
$R_{sat,ev}$ = 0,03075 [K/W]
s_h = 0,022 [m]
$T_{air,in,ev}$ = -10 [C]
T_{avg} = 40 [C]
$T_{R,sat,ev}$ = -18,5 [C]
$UA_{sh,ev}$ = 1,111 [W/K]
U_{tot} = 124,8 [W/m^2K]
$V_{R,sh,ev}$ = 0,7685 [m/s]

Appendix A.4. Simulation results of type 8.03/8T for R410a

Unit Settings: [kJ]/[C]/[kPa]/[kg]/[degrees]

A_{sat} = 1,682 [m^2]
$A_{s,unfin}$ = 0,237 [m^2]
$Cp_{R,sc}$ = 1,418 [kJ/kg-K]
$\delta_{T,log,sh}$ = 14,34 [C]
e = 0,000001 [m]
$F_{sat,evap}$ = 0,8 [-]
G_{flux} = 1141 [kg/m^2s]
$\bar{h}_{R,sat,ev}$ = 218 [W/m^2K]
h_{tot} = 6103 [W/m^2K]
$i_{R,out,evap}$ = 239,3 [kJ/kg]
k_{sat} = 0,01604 [W/m-K]
L_{sh} = 1 [m]
μ_{sat} = 0,00001265 [kg/m-s]
$Nusselt_{R,sc}$ = 2537 [-]
$Pr_{R,g}$ = 0,8132 [-]
$P_{R,ev}$ = 141,7 [kPa]
$\dot{Q}_{tot}$ = 1514 [W]
Re_{sc} = 2,097E+06 [-]
ρ_R = 14,66 [kg/m^3]
$R_{out,sat}$ = 0,006599 [K/W]
$R_{R,sat,ev}$ = 0,02501 [K/W]
R_{sc} = 0,06184 [K/W]
s_v = 0,0313 [m]
$T_{air,out,sat}$ = 32,52 [C]
$T_{avg,ev}$ = -14,25 [C]
$T_{R,sc}$ = 24,37 [C]
U_{sat} = 68,41 [W/m^2K]
V_{air} = 0,5 [m/s]
W = 0,25 [m]

$A_{sat,evap}$ = 1,922 [m^2]
A_{tot} = 2,403 [m^2]
$CP_{R,sh}$ = 1,054 [kJ/kg-K]
$\delta_{T,log,sh,ev}$ = 47,45 [C]
eff_o = 0,9009 [-]
F_{sc} = 0,1 [-]
$G_{flux,air}$ = 100 [kg/m^2]
$\bar{h}_{R,sc}$ = 2787 [W/m^2K]
$i_{R,in}$ = 293,4 [kJ/kg]
$i_{R,out,sh}$ = 246,3 [kJ/kg]
$k_{sat,evap}$ = 0,01028 [W/m-K]
$L_{sh,ev}$ = 1 [m]
$\mu_{sat,evap}$ = 0,00001018 [kg/m-s]
$Nusselt_{R,sh}$ = 283,8 [-]
$Pr_{R,g,ev}$ = 0,7813 [-]
$\dot{q}_{sat}$ = 1195 [W]
$\dot{Q}_{tot,evap}$ = 1180 [W]
ρ_{air} = 1,127 [kg/m^3]
$\rho_{R,g}$ = 43,35 [kg/m^3]
$R_{out,sat,ev}$ = 0,005774 [K/W]
$R_{R,sc}$ = 0,01565 [K/W]
R_{sh} = 0,08773 [K/W]
th = 0,0009 [m]
$T_{air,out,sat,ev}$ = 72,34 [C]
$T_{R,in}$ = 60 [C]
UA_{sat} = 115,1 [W/K]
$U_{sat,ev}$ = 16,9 [W/m^2K]
$\dot{V}_{air}$ = 0,095 [m^3/s]
$w_{comp,in}$ = 47,08 [kJ/kg]

A_{sc} = 0,2403 [m^2]
COP_{comp} = 3,54 [-]
$CP_{R,sh,ev}$ = 0,8216 [kJ/kg-K]
$\delta_{T,sh}$ = 8,5 [C]
η_{fin} = 0,89 [-]
F_{sh} = 0,2 [-]
$G_{flux,ev}$ = 61,6 [kg/m^2]
$\bar{h}_{R,sh}$ = 337,4 [W/m^2K]
$i_{R,in,con}$ = 293,4 [kJ/kg]
$i_{R,v,sat}$ = 271 [kJ/kg]
L = 0,06 [m]
L_{tube} = 5 [m]
$\dot{m}_{air}$ = 0,1071 [kg/s]
$Nusselt_{R,sh,ev}$ = 31,71 [-]
Pr_{sat} = 0,8937 [-]
$\dot{q}_{sat,evap}$ = 1129 [W]
R$ = 'R134a'
$\rho_{air,avg}$ = 1,176 [kg/m^3]
$\rho_{R,g,ev}$ = 6,932 [kg/m^3]
$R_{out,sc}$ = 0,0462 [K/W]
$R_{R,sh}$ = 0,06463 [K/W]
$R_{sh,ev}$ = 0,9315 [K/W]
th_{fin} = 0,000254 [m]
$T_{air,out,sc}$ = 21,44 [C]
$T_{R,in,ev}$ = -18,5 [C]
$UA_{sat,ev}$ = 32,49 [W/K]
U_{sc} = 67,29 [W/m^2K]
$\dot{V}_{air,ev}$ = 0,01 [m^3/s]
$\dot{W}_{comp,act}$ = 343,6 [W]

A_{sh} = 0,4806 [m^2]
$COP_{overall}$ = 2,118 [-]
$\delta_{T,log,sat}$ = 10,38 [C]
DP_{air} = 2355
Fan_{power} = 223,7 [W]
$F_{sh,ev}$ = 0,2 [-]
H = 0,3 [m]
$\bar{h}_{R,sh,ev}$ = 24 [W/m^2K]
$i_{R,in,evap}$ = 84,65 [kJ/kg]
k_{copper} = 399,9 [W/m-K]
L_{sat} = 3,5 [m]
μ_{air} = 0,00001858 [kg/m-s]
$\dot{m}_{air,ev}$ = 0,01364 [kg/s]
$N_{t,col}$ = 2 [-]
$Pr_{sat,evap}$ = 0,8123 [-]
$\dot{q}_{sc}$ = 155,3 [W]
Re_{air} = 1899 [-]
$\rho_{air,ev}$ = 1,364 [kg/m^3]
ρ_{sc} = 1211 [kg/m^3]
$R_{out,sh}$ = 0,0231 [K/W]
$R_{R,sh,ev}$ = 0,9084 [K/W]
σ_{air} = 0,534 [-]
$T_{air,avg}$ = 27,02 [C]
$T_{air,out,sh}$ = 34,04 [C]
$T_{R,in,sh}$ = -10 [C]
UA_{sc} = 16,17 [W/K]
U_{sh} = 23,72 [W/m^2K]
$V_{R,sc}$ = 1,5 [m/s]
$\dot{W}_{comp,act,cal}$ = 333,4 [W]

$A_{sh,ev}$ = 0,4806 [m^2]
Cp_{air} = 1,007 [kJ/kg-K]
$\delta_{T,log,sat,ev}$ = 34,76 [C]
D_{in} = 0,0146 [m]
f_{fin} = 0,6257
f_{tot} = 0,597
$\bar{h}_{out}$ = 100 [W/m^2K]
$h_{R,sat}$ = 1091 [W/m^2K]
$i_{R,out}$ = 107,3 [kJ/kg]
$k_{R,g}$ = 0,01735 [W/m-K]
$L_{sat,evap}$ = 4 [m]
$\mu_{R,g}$ = 0,0000134 [kg/m-s]
$\dot{m}_R$ = 0,0073 [kg/s]
$N_{t,row}$ = 10 [-]
p_{fin} = 0,00318 [m]
$\dot{q}_{sh}$ = 163,5 [W]
$Re_{R,sh}$ = 140542 [-]
$\rho_{air,i}$ = 1,204 [kg/m^3]
$r_{fin,eff}$ = 0,01693
$R_{out,sh,ev}$ = 0,0231 [K/W]
R_{sat} = 0,008691 [K/W]
s_f = 315 [m]
$T_{air,in}$ = 20 [C]
$T_{air,out,sh,ev}$ = 76,05 [C]
$T_{R,sat}$ = 39,37 [C]
UA_{sh} = 11,4 [W/K]
$U_{sh,ev}$ = 2,234 [W/m^2K]
$V_{R,sh}$ = 2,975 [m/s]
x = 0,5 [-]

$A_{s,fin,tot}$ = 2,166 [m^2]
$Cp_{air,ev}$ = 1,006 [kJ/kg-K]
$\delta_{T,log,sc}$ = 9,602 [C]
D_{out} = 0,0164 [m]
F_{sat} = 0,7 [-]
f_{tube} = 0,3344
$\bar{h}_{R,sat}$ = 2978 [W/m^2K]
$h_{R,sat,ev}$ = 77,52 [W/m^2K]
$i_{R,out,act}$ = 85,51 [kJ/kg]
$k_{R,g,ev}$ = 0,01105 [W/m-K]
L_{sc} = 0,5 [m]
$\mu_{R,g,ev}$ = 0,00001051 [kg/m-s]
$\dot{m}_{R,calculate}$ = 0,001145 [kg/s]
P = 101,3 [kPa]
P_R = 1000 [kPa]
$\dot{q}_{sh,evap}$ = 50,93 [W]
$Re_{R,sh,ev}$ = 9504 [-]
$\rho_{air,o}$ = 1,149 [kg/m^3]
R_{out} = 0,00462 [K/W]
$R_{R,sat}$ = 0,002091 [K/W]
$R_{sat,ev}$ = 0,03078 [K/W]
s_h = 0,0343 [m]
$T_{air,in,ev}$ = -10 [C]
T_{avg} = 40 [C]
$T_{R,sat,ev}$ = -18,5 [C]
$UA_{sh,ev}$ = 1,073 [W/K]
U_{tot} = 159,4 [W/m^2K]
$V_{R,sh,ev}$ = 0,9869 [m/s]

Appendix A.5. Simulation results of type CF-7.0-5/8J for R134a

Unit Settings: [kJ]/[C]/[kPa]/[kg]/[degrees]

A_{sat} = 1,682 [m^2]
$A_{s,unfin}$ = 0,237 [m^2]
$Cp_{R,sc}$ = 2,717 [kJ/kg-K]
$\delta_{T,log,sh}$ = 14,3 [C]
e = 0,000001 [m]
$F_{sat,evap}$ = 0,8 [-]
G_{flux} = 608,4 [kg/m^2s]
$\bar{h}_{R,sat,ev}$ = 217,9 [W/m^2K]
h_{tot} = 6423 [W/m^2K]
$i_{R,out,evap}$ = 553,7 [kJ/kg]
k_{sat} = 0,02126 [W/m-K]
L_{sh} = 1 [m]
μ_{sat} = 0,000009385 [kg/m-s]
$Nusselt_{R,sc}$ = 2044 [-]
$Pr_{R,g}$ = 0,8981 [-]
$P_{R,ev}$ = 258 [kPa]
$\dot{Q}_{tot}$ = 1527 [W]
Re_{sc} = 1,529E+06 [-]
ρ_R = 8,475 [kg/m^3]
$R_{out,sat}$ = 0,006599 [K/W]
$R_{R,sat,ev}$ = 0,02501 [K/W]
R_{sc} = 0,06084 [K/W]
s_v = 0,0313 [m]
$T_{air,out,sat}$ = 32,53 [C]
$T_{avg,ev}$ = -14,25 [C]
$T_{R,sc}$ = 24,38 [C]
U_{sat} = 68,9 [W/m^2K]
V_{air} = 0,5 [m/s]
W = 0,25 [m]

$A_{sat,evap}$ = 1,922 [m^2]
A_{tot} = 2,403 [m^2]
$CP_{R,sh}$ = 2,155 [kJ/kg-K]
$\delta_{T,log,sh,ev}$ = 47,51 [C]
eff_0 = 0,9009 [-]
F_{sc} = 0,1 [-]
$G_{flux,air}$ = 100 [kg/m^2]
$\bar{h}_{R,sc}$ = 2977 [W/m^2K]
$i_{R,in}$ = 659,3 [kJ/kg]
$i_{R,out,sh}$ = 567,5 [kJ/kg]
$k_{sat,evap}$ = 0,0138 [W/m-K]
$L_{sh,ev}$ = 1 [m]
$\mu_{sat,evap}$ = 0,000007184 [kg/m-s]
$Nusselt_{R,sh}$ = 232,4 [-]
$Pr_{R,g,ev}$ = 0,8244 [-]
$\dot{q}_{sat}$ = 1193 [W]
$\dot{Q}_{tot,evap}$ = 1182 [W]
ρ_{air} = 1,127 [kg/m^3]
$\rho_{R,g}$ = 26,03 [kg/m^3]
$R_{out,sat,ev}$ = 0,005774 [K/W]
$R_{R,sc}$ = 0,01465 [K/W]
R_{sh} = 0,0811 [K/W]
th = 0,0009 [m]
$T_{air,out,sat,ev}$ = 72,3 [C]
$T_{R,in}$ = 60 [C]
UA_{sat} = 115,9 [W/K]
$U_{sat,ev}$ = 16,9 [W/m^2K]
$\dot{V}_{air}$ = 0,095 [m^3/s]
$w_{comp,in}$ = 91,82 [kJ/kg]

A_{sc} = 0,2403 [m^2]
COP_{comp} = 3,429 [-]
$CP_{R,sh,ev}$ = 1,631 [kJ/kg-K]
$\delta_{T,sh}$ = 8,5 [C]
η_{fin} = 0,89 [-]
F_{sh} = 0,2 [-]
$G_{flux,ev}$ = 29,94 [kg/m^2]
$\bar{h}_{R,sh}$ = 375,9 [W/m^2K]
$i_{R,in,con}$ = 659,3 [kJ/kg]
$i_{R,v,sat}$ = 613,8 [kJ/kg]
L = 0,06 [m]
L_{tube} = 5 [m]
$\dot{m}_{air}$ = 0,1071 [kg/s]
$Nusselt_{R,sh,ev}$ = 25,16 [-]
Pr_{sat} = 1,011 [-]
$\dot{q}_{sat,evap}$ = 1129 [W]
R$ = 'R290'
$\rho_{air,avg}$ = 1,176 [kg/m^3]
$\rho_{R,g,ev}$ = 5,558 [kg/m^3]
$R_{out,sc}$ = 0,0462 [K/W]
$R_{R,sh}$ = 0,058 [K/W]
$R_{sh,ev}$ = 0,8864 [K/W]
th_{fin} = 0,000254 [m]
$T_{air,out,sc}$ = 21,47 [C]
$T_{R,in,ev}$ = -18,5 [C]
$UA_{sat,ev}$ = 32,48 [W/K]
U_{sc} = 68,4 [W/m^2K]
$\dot{V}_{air,ev}$ = 0,01 [m^3/s]
$\dot{W}_{comp,act}$ = 355,8 [W]

A_{sh} = 0,4806 [m^2]
$COP_{overall}$ = 2,079 [-]
$\delta_{T,log,sat}$ = 10,29 [C]
DP_{air} = 2358
Fan_{power} = 224 [W]
$F_{sh,ev}$ = 0,2 [-]
H = 0,3 [m]
$\bar{h}_{R,sh,ev}$ = 25,25 [W/m^2K]
$i_{R,in,evap}$ = 262,4 [kJ/kg]
k_{copper} = 399,9 [W/m-K]
L_{sat} = 3,5 [m]
μ_{air} = 0,00001858 [kg/m-s]
$\dot{m}_{air,ev}$ = 0,01364 [kg/s]
$N_{t,col}$ = 2 [-]
$Pr_{sat,evap}$ = 0,8455 [-]
$\dot{q}_{sc}$ = 157,9 [W]
Re_{air} = 1898 [-]
$\rho_{air,ev}$ = 1,364 [kg/m^3]
ρ_{sc} = 494,3 [kg/m^3]
$R_{out,sh}$ = 0,0231 [K/W]
$R_{R,sh,ev}$ = 0,8633 [K/W]
σ_{air} = 0,534 [-]
$T_{air,avg}$ = 27,08 [C]
$T_{air,out,sh}$ = 34,16 [C]
$T_{R,in,sh}$ = -10 [C]
UA_{sc} = 16,44 [W/K]
U_{sh} = 25,66 [W/m^2K]
$V_{R,sc}$ = 1,988 [m/s]
$\dot{W}_{comp,act,cal}$ = 344,8 [W]

$A_{sh,ev}$ = 0,4806 [m^2]
Cp_{air} = 1,007 [kJ/kg-K]
$\delta_{T,log,sat,ev}$ = 34,75 [C]
D_{in} = 0,0146 [m]
f_{fin} = 0,6257
f_{tot} = 0,597
$\bar{h}_{out}$ = 100 [W/m^2K]
$h_{R,sat}$ = 1167 [W/m^2K]
$i_{R,out}$ = 306 [kJ/kg]
$k_{R,g}$ = 0,02362 [W/m-K]
$L_{sat,evap}$ = 4 [m]
$\mu_{R,g}$ = 0,000009842 [kg/m-s]
$\dot{m}_R$ = 0,003875 [kg/s]
$N_{t,row}$ = 10 [-]
p_{fin} = 0,00318 [m]
$\dot{q}_{sh}$ = 176,4 [W]
$Re_{R,sh}$ = 105467 [-]
$\rho_{air,i}$ = 1,204 [kg/m^3]
$r_{fin,eff}$ = 0,01693
$R_{out,sh,ev}$ = 0,0231 [K/W]
R_{sat} = 0,008629 [K/W]
s_f = 315 [m]
$T_{air,in}$ = 20 [C]
$T_{air,out,sh,ev}$ = 76,21 [C]
$T_{R,sat}$ = 39,38 [C]
UA_{sh} = 12,33 [W/K]
$U_{sh,ev}$ = 2,347 [W/m^2K]
$V_{R,sh}$ = 2,731 [m/s]
x = 0,5 [-]

$A_{s,fin,tot}$ = 2,166 [m^2]
$Cp_{air,ev}$ = 1,006 [kJ/kg-K]
$\delta_{T,log,sc}$ = 9,609 [C]
D_{out} = 0,0164 [m]
F_{sat} = 0,7 [-]
f_{tube} = 0,3344
$\bar{h}_{R,sat}$ = 3070 [W/m^2K]
$h_{R,sat,ev}$ = 78,46 [W/m^2K]
$i_{R,out,act}$ = 263,9 [kJ/kg]
$k_{R,g,ev}$ = 0,01465 [W/m-K]
L_{sc} = 0,5 [m]
$\mu_{R,g,ev}$ = 0,000007407 [kg/m-s]
$\dot{m}_{R,calculate}$ = 0,0005885 [kg/s]
P = 101,3 [kPa]
P_R = 1350 [kPa]
$\dot{q}_{sh,evap}$ = 53,6 [W]
$Re_{R,sh,ev}$ = 6930 [-]
$\rho_{air,o}$ = 1,149 [kg/m^3]
R_{out} = 0,00462 [K/W]
$R_{R,sat}$ = 0,002029 [K/W]
$R_{sat,ev}$ = 0,03079 [K/W]
s_h = 0,0343 [m]
$T_{air,in,ev}$ = -10 [C]
T_{avg} = 40 [C]
$T_{R,sat,ev}$ = -18,5 [C]
$UA_{sh,ev}$ = 1,128 [W/K]
U_{tot} = 163 [W/m^2K]
$V_{R,sh,ev}$ = 0,6325 [m/s]

Appendix A.6. Simulation results of type CF-7.0-5/8J for R290

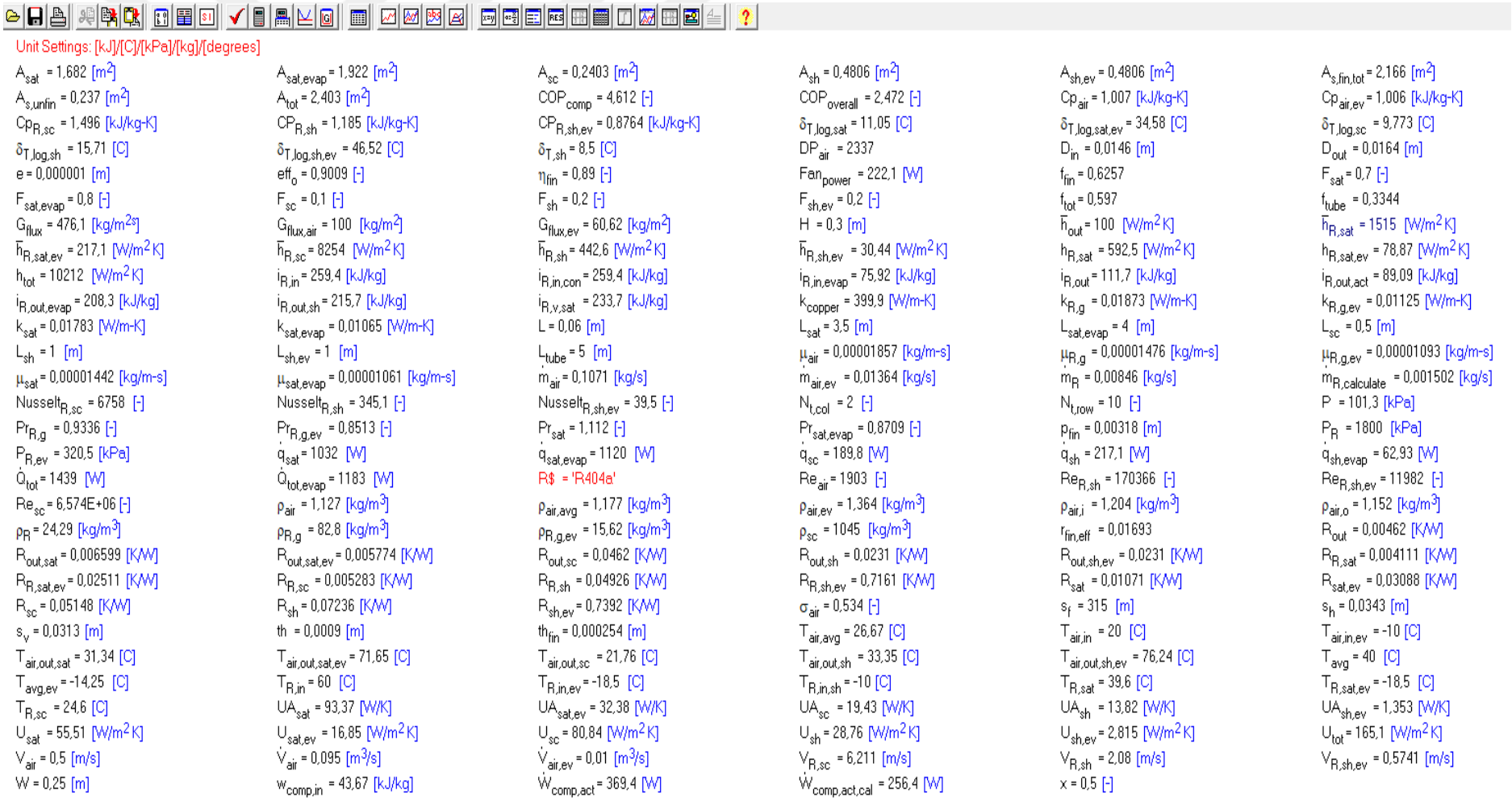

Unit Settings: [kJ]/[C]/[kPa]/[kg]/[degrees]

A_{sat} = 1,682 [m^2]
$A_{s,unfin}$ = 0,237 [m^2]
$Cp_{R,sc}$ = 1,496 [kJ/kg-K]
$\delta_{T,log,sh}$ = 15,71 [C]
e = 0,000001 [m]
$F_{sat,evap}$ = 0,8 [-]
G_{flux} = 476,1 [kg/m^2s]
$\bar{h}_{R,sat,ev}$ = 217,1 [W/m^2K]
h_{tot} = 10212 [W/m^2K]
$i_{R,out,evap}$ = 208,3 [kJ/kg]
k_{sat} = 0,01783 [W/m-K]
L_{sh} = 1 [m]
μ_{sat} = 0,00001442 [kg/m-s]
$Nusselt_{R,sc}$ = 6758 [-]
$Pr_{R,g}$ = 0,9336 [-]
$P_{R,ev}$ = 320,5 [kPa]
$\dot{Q}_{tot}$ = 1439 [W]
Re_{sc} = 6,574E+06 [-]
ρ_R = 24,29 [kg/m^3]
$R_{out,sat}$ = 0,006599 [K/W]
$R_{R,sat,ev}$ = 0,02511 [K/W]
R_{sc} = 0,05148 [K/W]
s_v = 0,0313 [m]
$T_{air,out,sat}$ = 31,34 [C]
$T_{avg,ev}$ = -14,25 [C]
$T_{R,sc}$ = 24,6 [C]
U_{sat} = 55,51 [W/m^2K]
V_{air} = 0,5 [m/s]
W = 0,25 [m]

$A_{sat,evap}$ = 1,922 [m^2]
A_{tot} = 2,403 [m^2]
$CP_{R,sh}$ = 1,185 [kJ/kg-K]
$\delta_{T,log,sh,ev}$ = 46,52 [C]
eff_o = 0,9009 [-]
F_{sc} = 0,1 [-]
$G_{flux,air}$ = 100 [kg/m^2]
$\bar{h}_{R,sc}$ = 8254 [W/m^2K]
$i_{R,in}$ = 259,4 [kJ/kg]
$i_{R,out,sh}$ = 215,7 [kJ/kg]
$k_{sat,evap}$ = 0,01065 [W/m-K]
$L_{sh,ev}$ = 1 [m]
$\mu_{sat,evap}$ = 0,00001061 [kg/m-s]
$Nusselt_{R,sh}$ = 345,1 [-]
$Pr_{R,g,ev}$ = 0,8513 [-]
$\dot{q}_{sat}$ = 1032 [W]
$\dot{Q}_{tot,evap}$ = 1183 [W]
ρ_{air} = 1,127 [kg/m^3]
$\rho_{R,g}$ = 82,8 [kg/m^3]
$R_{out,sat,ev}$ = 0,005774 [K/W]
$R_{R,sc}$ = 0,005283 [K/W]
R_{sh} = 0,07236 [K/W]
th = 0,0009 [m]
$T_{air,out,sat,ev}$ = 71,65 [C]
$T_{R,in}$ = 60 [C]
UA_{sat} = 93,37 [W/K]
$U_{sat,ev}$ = 16,85 [W/m^2K]
$\dot{V}_{air}$ = 0,095 [m^3/s]
$w_{comp,in}$ = 43,67 [kJ/kg]

A_{sc} = 0,2403 [m^2]
COP_{comp} = 4,612 [-]
$CP_{R,sh,ev}$ = 0,8764 [kJ/kg-K]
$\delta_{T,sh}$ = 8,5 [C]
η_{fin} = 0,89 [-]
F_{sh} = 0,2 [-]
$G_{flux,ev}$ = 60,62 [kg/m^2]
$\bar{h}_{R,sh}$ = 442,6 [W/m^2K]
$i_{R,in,con}$ = 259,4 [kJ/kg]
$i_{R,v,sat}$ = 233,7 [kJ/kg]
L = 0,06 [m]
L_{tube} = 5 [m]
$\dot{m}_{air}$ = 0,1071 [kg/s]
$Nusselt_{R,sh,ev}$ = 39,5 [-]
Pr_{sat} = 1,112 [-]
$\dot{q}_{sat,evap}$ = 1120 [W]
R$ = 'R404a'
$\rho_{air,avg}$ = 1,177 [kg/m^3]
$\rho_{R,g,ev}$ = 15,62 [kg/m^3]
$R_{out,sc}$ = 0,0462 [K/W]
$R_{R,sh}$ = 0,04926 [K/W]
$R_{sh,ev}$ = 0,7392 [K/W]
th_{fin} = 0,000254 [m]
$T_{air,out,sc}$ = 21,76 [C]
$T_{R,in,ev}$ = -18,5 [C]
$UA_{sat,ev}$ = 32,38 [W/K]
U_{sc} = 80,84 [W/m^2K]
$\dot{V}_{air,ev}$ = 0,01 [m^3/s]
$\dot{W}_{comp,act}$ = 369,4 [W]

A_{sh} = 0,4806 [m^2]
$COP_{overall}$ = 2,472 [-]
$\delta_{T,log,sat}$ = 11,05 [C]
DP_{air} = 2337
Fan_{power} = 222,1 [W]
$F_{sh,ev}$ = 0,2 [-]
H = 0,3 [m]
$\bar{h}_{R,sh,ev}$ = 30,44 [W/m^2K]
$i_{R,in,evap}$ = 75,92 [kJ/kg]
k_{copper} = 399,9 [W/m-K]
L_{sat} = 3,5 [m]
μ_{air} = 0,00001857 [kg/m-s]
$\dot{m}_{air,ev}$ = 0,01364 [kg/s]
$N_{t,col}$ = 2 [-]
$Pr_{sat,evap}$ = 0,8709 [-]
$\dot{q}_{sc}$ = 189,8 [W]
Re_{air} = 1903 [-]
$\rho_{air,ev}$ = 1,364 [kg/m^3]
ρ_{sc} = 1045 [kg/m^3]
$R_{out,sh}$ = 0,0231 [K/W]
$R_{R,sh,ev}$ = 0,7161 [K/W]
σ_{air} = 0,534 [-]
$T_{air,avg}$ = 26,67 [C]
$T_{air,out,sh}$ = 33,35 [C]
$T_{R,in,sh}$ = -10 [C]
UA_{sc} = 19,43 [W/K]
U_{sh} = 28,76 [W/m^2K]
$V_{R,sc}$ = 6,211 [m/s]
$\dot{W}_{comp,act,cal}$ = 256,4 [W]

$A_{sh,ev}$ = 0,4806 [m^2]
Cp_{air} = 1,007 [kJ/kg-K]
$\delta_{T,log,sat,ev}$ = 34,58 [C]
D_{in} = 0,0146 [m]
f_{fin} = 0,6257
f_{tot} = 0,597
$\bar{h}_{out}$ = 100 [W/m^2K]
$h_{R,sat}$ = 592,5 [W/m^2K]
$i_{R,out}$ = 111,7 [kJ/kg]
$k_{R,g}$ = 0,01873 [W/m-K]
$L_{sat,evap}$ = 4 [m]
$\mu_{R,g}$ = 0,00001476 [kg/m-s]
$\dot{m}_R$ = 0,00846 [kg/s]
$N_{t,row}$ = 10 [-]
p_{fin} = 0,00318 [m]
$\dot{q}_{sh}$ = 217,1 [W]
$Re_{R,sh}$ = 170366 [-]
$\rho_{air,i}$ = 1,204 [kg/m^3]
$r_{fin,eff}$ = 0,01693
$R_{out,sh,ev}$ = 0,0231 [K/W]
R_{sat} = 0,01071 [K/W]
s_f = 315 [m]
$T_{air,in}$ = 20 [C]
$T_{air,out,sh,ev}$ = 76,24 [C]
$T_{R,sat}$ = 39,6 [C]
UA_{sh} = 13,82 [W/K]
$U_{sh,ev}$ = 2,815 [W/m^2K]
$V_{R,sh}$ = 2,08 [m/s]
x = 0,5 [-]

$A_{s,fin,tot}$ = 2,166 [m^2]
$Cp_{air,ev}$ = 1,006 [kJ/kg-K]
$\delta_{T,log,sc}$ = 9,773 [C]
D_{out} = 0,0164 [m]
F_{sat} = 0,7 [-]
f_{tube} = 0,3344
$\bar{h}_{R,sat}$ = 1515 [W/m^2K]
$h_{R,sat,ev}$ = 78,87 [W/m^2K]
$i_{R,out,act}$ = 89,09 [kJ/kg]
$k_{R,g,ev}$ = 0,01125 [W/m-K]
L_{sc} = 0,5 [m]
$\mu_{R,g,ev}$ = 0,00001093 [kg/m-s]
$\dot{m}_{R,calculate}$ = 0,001502 [kg/s]
P = 101,3 [kPa]
P_R = 1800 [kPa]
$\dot{q}_{sh,evap}$ = 62,93 [W]
$Re_{R,sh,ev}$ = 11982 [-]
$\rho_{air,o}$ = 1,152 [kg/m^3]
R_{out} = 0,00462 [K/W]
$R_{R,sat}$ = 0,004111 [K/W]
$R_{sat,ev}$ = 0,03088 [K/W]
s_h = 0,0343 [m]
$T_{air,in,ev}$ = -10 [C]
T_{avg} = 40 [C]
$T_{R,sat,ev}$ = -18,5 [C]
$UA_{sh,ev}$ = 1,353 [W/K]
U_{tot} = 165,1 [W/m^2K]
$V_{R,sh,ev}$ = 0,5741 [m/s]

Appendix A.7. Simulation results of type CF-7.0-5/8J for R404a

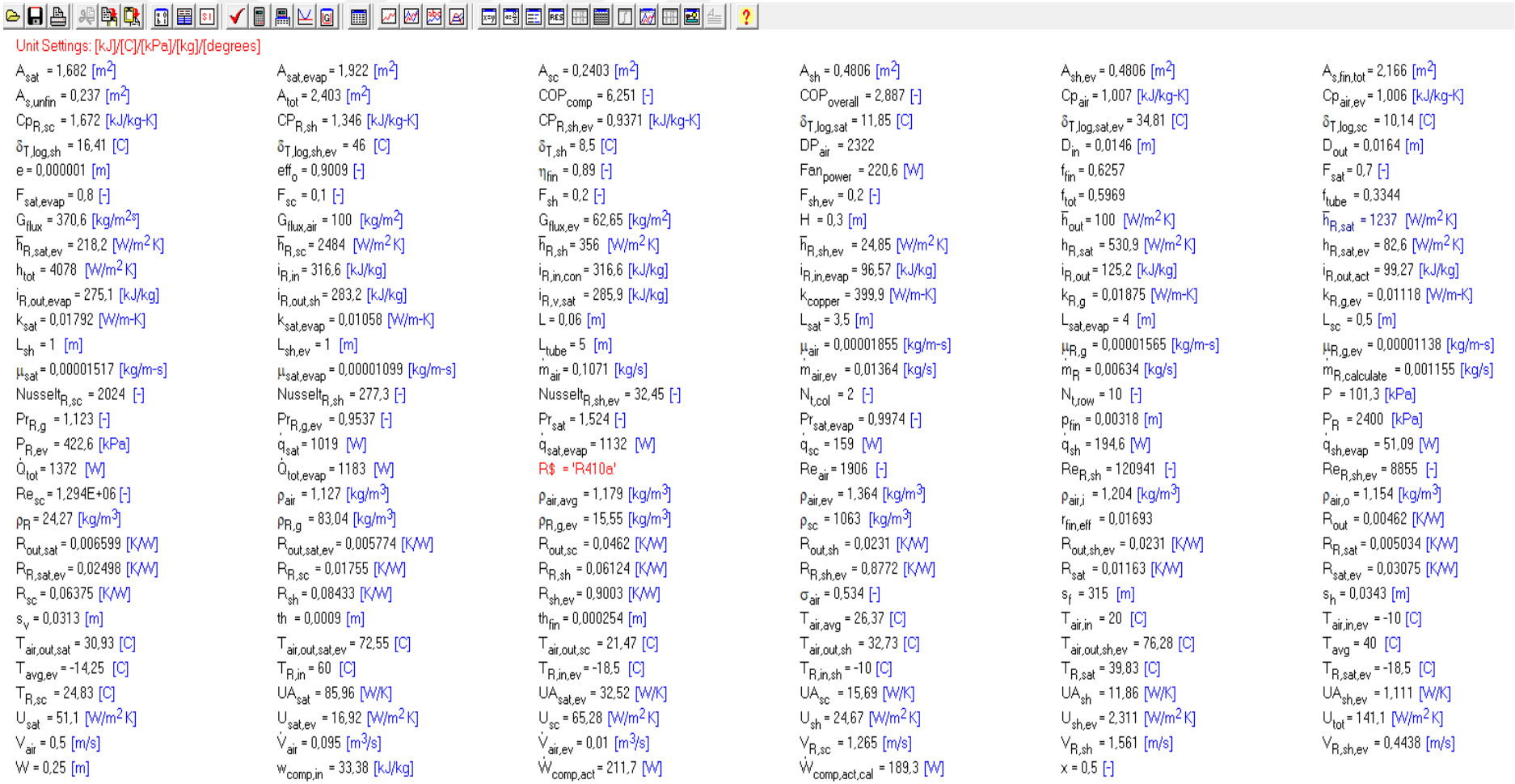

Unit Settings: [kJ]/[C]/[kPa]/[kg]/[degrees]

A_{sat} = 1,682 [m^2]
$A_{s,unfin}$ = 0,237 [m^2]
$Cp_{R,sc}$ = 1,672 [kJ/kg-K]
$\delta_{T,log,sh}$ = 16,41 [C]
e = 0,000001 [m]
$F_{sat,evap}$ = 0,8 [-]
G_{flux} = 370,6 [kg/m^2s]
$\bar{h}_{R,sat,ev}$ = 218,2 [W/m^2K]
h_{tot} = 4078 [W/m^2K]
$i_{R,out,evap}$ = 275,1 [kJ/kg]
k_{sat} = 0,01792 [W/m-K]
L_{sh} = 1 [m]
μ_{sat} = 0,00001517 [kg/m-s]
$Nusselt_{R,sc}$ = 2024 [-]
$Pr_{R,g}$ = 1,123 [-]
$P_{R,ev}$ = 422,6 [kPa]
$\dot{Q}_{tot}$ = 1372 [W]
Re_{sc} = 1,294E+06 [-]
ρ_R = 24,27 [kg/m^3]
$R_{out,sat}$ = 0,006599 [K/W]
$R_{R,sat,ev}$ = 0,02498 [K/W]
R_{sc} = 0,06375 [K/W]
s_v = 0,0313 [m]
$T_{air,out,sat}$ = 30,93 [C]
$T_{avg,ev}$ = -14,25 [C]
$T_{R,sc}$ = 24,83 [C]
U_{sat} = 51,1 [W/m^2K]
V_{air} = 0,5 [m/s]
W = 0,25 [m]

$A_{sat,evap}$ = 1,922 [m^2]
A_{tot} = 2,403 [m^2]
$CP_{R,sh}$ = 1,346 [kJ/kg-K]
$\delta_{T,log,sh,ev}$ = 46 [C]
eff_o = 0,9009 [-]
F_{sc} = 0,1 [-]
$G_{flux,air}$ = 100 [kg/m^2]
$\bar{h}_{R,sc}$ = 2484 [W/m^2K]
$i_{R,in}$ = 316,6 [kJ/kg]
$i_{R,out,sh}$ = 283,2 [kJ/kg]
$k_{sat,evap}$ = 0,01058 [W/m-K]
$L_{sh,ev}$ = 1 [m]
$\mu_{sat,evap}$ = 0,00001099 [kg/m-s]
$Nusselt_{R,sh}$ = 277,3 [-]
$Pr_{R,g,ev}$ = 0,9537 [-]
$\dot{q}_{sat}$ = 1019 [W]
$\dot{Q}_{tot,evap}$ = 1183 [W]
ρ_{air} = 1,127 [kg/m^3]
$\rho_{R,g}$ = 83,04 [kg/m^3]
$R_{out,sat,ev}$ = 0,005774 [K/W]
$R_{R,sc}$ = 0,01755 [K/W]
R_{sh} = 0,08433 [K/W]
th = 0,0009 [m]
$T_{air,out,sat,ev}$ = 72,55 [C]
$T_{R,in}$ = 60 [C]
UA_{sat} = 85,96 [W/K]
$U_{sat,ev}$ = 16,92 [W/m^2K]
$\dot{V}_{air}$ = 0,095 [m^3/s]
$w_{comp,in}$ = 33,38 [kJ/kg]

A_{sc} = 0,2403 [m^2]
COP_{comp} = 6,251 [-]
$CP_{R,sh,ev}$ = 0,9371 [kJ/kg-K]
$\delta_{T,sh}$ = 8,5 [C]
η_{fin} = 0,89 [-]
F_{sh} = 0,2 [-]
$G_{flux,ev}$ = 62,65 [kg/m^2]
$\bar{h}_{R,sh}$ = 356 [W/m^2K]
$i_{R,in,con}$ = 316,6 [kJ/kg]
$i_{R,v,sat}$ = 285,9 [kJ/kg]
L = 0,06 [m]
L_{tube} = 5 [m]
$\dot{m}_{air}$ = 0,1071 [kg/s]
$Nusselt_{R,sh,ev}$ = 32,45 [-]
Pr_{sat} = 1,524 [-]
$\dot{q}_{sat,evap}$ = 1132 [W]
R$ = 'R410a'
$\rho_{air,avg}$ = 1,179 [kg/m^3]
$\rho_{R,g,ev}$ = 15,55 [kg/m^3]
$R_{out,sc}$ = 0,0462 [K/W]
$R_{R,sh}$ = 0,06124 [K/W]
$R_{sh,ev}$ = 0,9003 [K/W]
th_{fin} = 0,000254 [m]
$T_{air,out,sc}$ = 21,47 [C]
$T_{R,in,ev}$ = -18,5 [C]
$UA_{sat,ev}$ = 32,52 [W/K]
U_{sc} = 65,28 [W/m^2K]
$\dot{V}_{air,ev}$ = 0,01 [m^3/s]
$\dot{W}_{comp,act}$ = 211,7 [W]

A_{sh} = 0,4806 [m^2]
$COP_{overall}$ = 2,887 [-]
$\delta_{T,log,sat}$ = 11,85 [C]
DP_{air} = 2322
Fan_{power} = 220,6 [W]
$F_{sh,ev}$ = 0,2 [-]
H = 0,3 [m]
$\bar{h}_{R,sh,ev}$ = 24,85 [W/m^2K]
$i_{R,in,evap}$ = 96,57 [kJ/kg]
k_{copper} = 399,9 [W/m-K]
L_{sat} = 3,5 [m]
μ_{air} = 0,00001855 [kg/m-s]
$\dot{m}_{air,ev}$ = 0,01364 [kg/s]
$N_{t,col}$ = 2 [-]
$Pr_{sat,evap}$ = 0,9974 [-]
$\dot{q}_{sc}$ = 159 [W]
Re_{air} = 1906 [-]
$\rho_{air,ev}$ = 1,364 [kg/m^3]
ρ_{sc} = 1063 [kg/m^3]
$R_{out,sh}$ = 0,0231 [K/W]
$R_{R,sh,ev}$ = 0,8772 [K/W]
σ_{air} = 0,534 [-]
$T_{air,avg}$ = 26,37 [C]
$T_{air,out,sh}$ = 32,73 [C]
$T_{R,in,sh}$ = -10 [C]
UA_{sc} = 15,69 [W/K]
U_{sh} = 24,67 [W/m^2K]
$V_{R,sc}$ = 1,265 [m/s]
$\dot{W}_{comp,act,cal}$ = 189,3 [W]

$A_{sh,ev}$ = 0,4806 [m^2]
Cp_{air} = 1,007 [kJ/kg-K]
$\delta_{T,log,sat,ev}$ = 34,81 [C]
D_{in} = 0,0146 [m]
f_{fin} = 0,6257
f_{tot} = 0,5969
$\bar{h}_{out}$ = 100 [W/m^2K]
$h_{R,sat}$ = 530,9 [W/m^2K]
$i_{R,out}$ = 125,2 [kJ/kg]
$k_{R,g}$ = 0,01875 [W/m-K]
$L_{sat,evap}$ = 4 [m]
$\mu_{R,g}$ = 0,00001565 [kg/m-s]
$\dot{m}_R$ = 0,00634 [kg/s]
$N_{t,row}$ = 10 [-]
p_{fin} = 0,00318 [m]
$\dot{q}_{sh}$ = 194,6 [W]
$Re_{R,sh}$ = 120941 [-]
$\rho_{air,i}$ = 1,204 [kg/m^3]
$r_{fin,eff}$ = 0,01693
$R_{out,sh,ev}$ = 0,0231 [K/W]
R_{sat} = 0,01163 [K/W]
s_f = 315 [m]
$T_{air,in}$ = 20 [C]
$T_{air,out,sh,ev}$ = 76,28 [C]
$T_{R,sat}$ = 39,83 [C]
UA_{sh} = 11,86 [W/K]
$U_{sh,ev}$ = 2,311 [W/m^2K]
$V_{R,sh}$ = 1,561 [m/s]
x = 0,5 [-]

$A_{s,fin,tot}$ = 2,166 [m^2]
$Cp_{air,ev}$ = 1,006 [kJ/kg-K]
$\delta_{T,log,sc}$ = 10,14 [C]
D_{out} = 0,0164 [m]
F_{sat} = 0,7 [-]
f_{tube} = 0,3344
$\bar{h}_{R,sat}$ = 1237 [W/m^2K]
$h_{R,sat,ev}$ = 82,6 [W/m^2K]
$i_{R,out,act}$ = 99,27 [kJ/kg]
$k_{R,g,ev}$ = 0,01118 [W/m-K]
L_{sc} = 0,5 [m]
$\mu_{R,g,ev}$ = 0,00001138 [kg/m-s]
$\dot{m}_{R,calculate}$ = 0,001155 [kg/s]
P = 101,3 [kPa]
P_R = 2400 [kPa]
$\dot{q}_{sh,evap}$ = 51,09 [W]
$Re_{R,sh,ev}$ = 8855 [-]
$\rho_{air,o}$ = 1,154 [kg/m^3]
R_{out} = 0,00462 [K/W]
$R_{R,sat}$ = 0,005034 [K/W]
$R_{sat,ev}$ = 0,03075 [K/W]
s_h = 0,0343 [m]
$T_{air,in,ev}$ = -10 [C]
T_{avg} = 40 [C]
$T_{R,sat,ev}$ = -18,5 [C]
$UA_{sh,ev}$ = 1,111 [W/K]
U_{tot} = 141,1 [W/m^2K]
$V_{R,sh,ev}$ = 0,4438 [m/s]

Appendix A.8. Simulation results of type CF-7.0-5/8J for R410a

CURRICULUM VITAE

Name Surname : Tutku MUTLU

Place and Date of Birth :Tekirdağ- 22.07.1993

Foreign Language :English

E-Mail : tutkumutlu93@gmail.com

EDUCATION

High School	Mehmet Akif Ersoy Anatolian High School -2007
University	Marmara University-Chemical Engineering Department-2011

Presented Announcements

1. Ebru Mançuhan, Sibel Titiz Sargut, Perviz Sayan, Tutku Mutlu, Melih Türkay Beşikçi, Kanatlı Borulu Bir Kondanserin Modellenmesi, Çalışma ve Tasarım Parametrelerinin Isı Transferine Etkileri, 21. Ulusal Isı Bilimi ve Tekniği Kongresi: ULIBTK' 17, Çorum, 2017.
2. Ebru Mançuhan, Sibel Titiz Sargut, Tutku Mutlu, Farklı Soğutucu Akışkanların Kullanıldığı Kanatlı Borulu Bir Evaporatörün Matematiksel Modeli, 30. Ulusal Kimya Kongresi, Gazimağusa, KKTC, 2018, ACCEPTED.